Investigating the Mechanisms Underlying the First Steps of Cancer Metastasis

A Thesis submitted to the University of Sheffield for the Degree of Master of Philosophy (MPhil)

September 2023

Nicholas Nisbet

School of Biological Sciences

List of Abbreviations

AJ	Adherens Junction
AR	APC-Ras
ARS	APC-Ras-Snail
BM	Basement Membrane
CSC	Cancer Stem Cell
CTC	Circulating Tumour Cell
CRC	Colorectal Cancer
C-EMT	Complete Epithelial-to-Mesenchymal Transition
EB	Enteroblast
EC	Enterocrine Cell
EE	Enteroendocrine Cell
EEP	Enteroendocrine Progenitor
EGFR	Epidermal Growth Factor Receptor
EMT	Epithelial-to-Mesenchymal Transition
EMT-TF	Epithelial-to-Mesenchymal Transition Transcription Factor
ECM	Extracellular Matrix
FAP	Familial Adenomatous Polyposis
FGF	Fibroblast Growth Factor
GEMM	Genetically Engineered Mouse Model
GC	Goblet Cell
ISC	Intestinal Stem Cell
JPS	Juvenile Polyposis Syndrome
MPT	Malpighian Tubule
MMP	Matrix Metalloprotease
MET	Mesenchymal-to-Epithelial Transition
NGS	Next Generation Sequencing
PC	Paneth Cell
P-EMT	Partial Epithelial-to-Mesenchymal Transition
PDX	Patient Derived Xenograft
PCI	Post Clone Induction

RTK	Receptor Tyrosine Kinase
RLU	Relative Luminescent Unit
SJ	Septate Junction
TJ	Tight Junction
TA cell	Transient Amplifying Cell
TF	Transcription Factor
TB	Tumour Burden
TME	Tumour Microenvironment
TSG	Tumour Suppressor Gene
VEGF	Vascular Endothelial Growth Factor

Abstract

(250 words)

Metastasis underlies 90% of cancer deaths, nonetheless its mechanisms remain poorly understood. The Epithelial-to-Mesenchymal Transition (EMT) is critical in onsetting metastasis and is therefore a sought-after therapeutic target. Unfortunately, targeting EMT has been difficult, as it is driven by undruggable transcription factors (EMT-TFs). Identifying metastatic effectors downstream of EMT may therefore represent a more efficacious means of targeting metastasis. However, by virtue of genetic redundancy, most metastatic models have failed to identify such drivers. Given, its low redundancy and remarkable similarities to the mammalian gut, the *Drosophila Melanogaster* midgut has emerged a powerful system in dissecting the genetic progression of Colorectal Cancer (CRC). Our lab previously established that activation of the EMT-TF Snail, triggers metastasis when added to a benign model of CRC involving mutations to APC and Ras. Nonetheless, its underlying mechanisms were left undetermined. This thesis sought to identify the mechanisms of Snail mediated metastasis, with the rationale of identifying downstream targets with potential therapeutic relevance. Following histological characterisation of metastatic tumours, three central behaviours could be identified, all occurring concurrently at the tumour invasive edge: destruction of the basement membrane, loss of E-Cadherin, and dysregulation of ADAMTS-A: a protease with strong potential as a drug target. Following experimental knockdown of ADAMTS-A, a loss of metastasis was observed. Although, ADAMTS-A has previously been correlated with metastatic outgrowth, a causal role has rarely been supported in-vivo. Put together, the results presented herein demonstrate that the *Drosophila* midgut is a powerful system for identifying metastatic mechanisms with strong therapeutic implications.

Chapter I

Introduction

The Problem of Metastasis

Cancer may be the biggest threat to human life: 1 in 6 people die from it, another 1 in 2 will develop it in their lifetime [1,2]. As the population continues to age, the frequency is expected to rise. Cancer encompasses two defining features. First, it involves the unremitting proliferation of genetically transformed cells, often—as is the case in solid cancers—into an adherent mass of clones termed benign tumours. However, cancer transcends pathological mitosis: cancer cells engulf neighbouring tissues, infiltrate the circulation, and riddle the body with distant lesions; many of which grow into sizeable tumours of their own. This second step is termed metastasis (Fig.1.1).

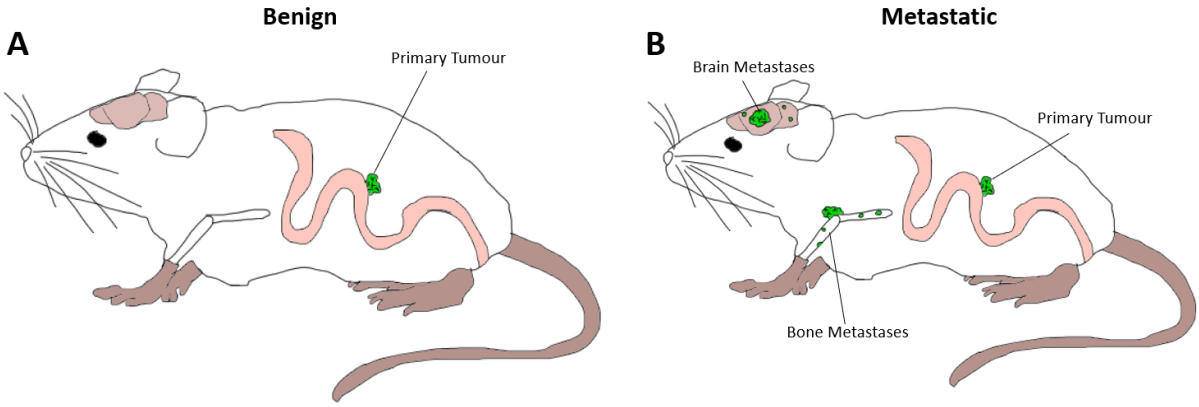

Figure 1.1. Schematic diagram of benign vs metastatic cancer: (A) Depiction of a rat with a benign tumour localized to the large intestine; **(B)** Depiction of a rat with a primary tumour localized to the large intestine, with additional metastatic dissemination to the bone and brain.

Since the molecular biology revolution of the 1980s we have seen an enormous increase in our understanding of the basic biology of primary tumorigenesis. This has translated into new avenues of therapeutic attack with marked, and occasionally curative outcomes, routinely being achieved. Indeed, following the discovery of platinum-based chemotherapy, the cure rate of benign testicular cancer rose from 5 to 90%; childhood acute lymphoblastic leukaemia— which previously invariably resulted in rapid death—now carries a 90% cure rate with appropriate treatment [3,4]. These examples are testament to the utility of cancer research. Nonetheless, mortality is on the rise; many cancers gone into remission recur and become refractory to therapies [1]. This relates to metastasis which associates with 90% of cancer deaths [5]. Unlike primary tumorigenesis, metastasis is often resistant to all established therapies [6] Whereas, management of benign tumours has increased, metastatic outcomes have stagnated. For instance, the 5-year survival rate for benign breast cancer has increased from 63 to 90%

between the years 1963 and 2010; metastatic breast cancer, however, has only increased from 23 to 28% [7].

The poor outcomes surrounding metastasis highlight a need for identifying its underlying molecular mechanisms, which currently remain poorly understood. This thesis seeks to assist in meeting that need by investigating the mechanisms that drive metastasis using a *Drosophila Melanogaster* model of Colorectal Cancer (CRC). Identifying the workings of metastasis is of urgent importance, as the incidence of cancer continues to rise, cancer is at risk of no longer being a possibility, but for most of us an inevitability.

The Nature of Cancer

Cancer is largely a disease of old age: whereas it can develop at any time, roughly 60% of diagnoses occur in individuals over the age of 65 [8]. This relates to cancer being a microevolutionary disease driven by mutation. Most accepted theories of cancer progression posit that cancer begins with mutation to a single cell that seeds clones that acquire more mutations [9]. Through a series of successive expansions, new subpopulations of clones are developed with novel mutations: those with more favourable mutations will outcompete clones less fit for survival (Fig.1.2). In this process of reiterative expansion, the lesion grows more aggressively and eventually, with age, gives rise to full-blown cancer.

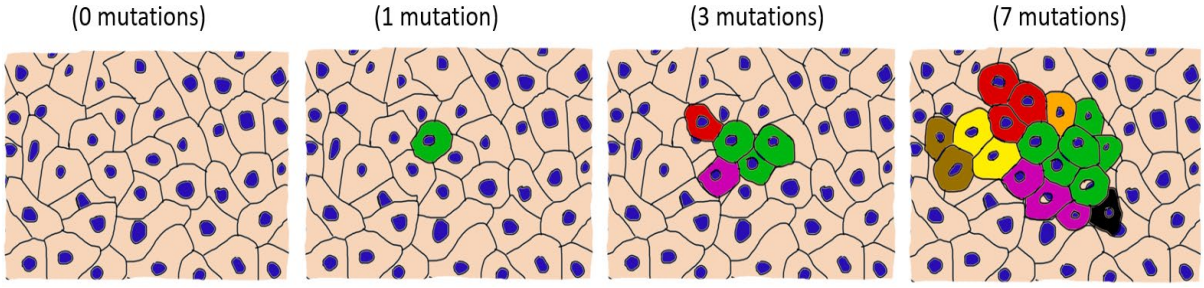

Figure 1.2. Schematic Diagram of Clonal Expansion: A wildtype tissue with no mutations acquires a mutation to a single cell giving it a growth advantage. This cell will then give rise to new subpopulations of cells, which progressively acquire new mutations and diversify the tumour population. New mutations are depicted in green, red, purple, yellow, orange, brown and black.

The subsets of cells that populate tumours can be quite diverse; featuring not only mutated clones, but also recruited stromal and immune cells: which on occasion make up 90% of the tumour mass [10, 11]. Indeed, the term “Tumour Microenvironment” (TME) does justice to the reality that cancer encompasses a broad ecosystem of divergent cell lineages which have been estranged from their normal functioning and exploited for cancer growth. This heterogeneity arms cancer with a menagerie of disposable cell processes that by process of natural selection

become streamlined for growth. As all cellular process relate in some way to the fitness of an organism's cells; an unsurprisingly, almost hopelessly, large catalogue of mechanisms are described in cancer. It is clear that the employment of these diverse mechanisms increases with the quantity of mutations expedited by evolving clones. This raises two questions: how many mutations are required for cancer growth and how do those mutations relate to acquired mechanisms?

The Genetics of Cancer

Genes that drive cancer following activating mutations are termed "oncogenes"; in a non-mutated, currently inactive state, the genes are referred to as "proto-oncogenes". The first firm evidence of a human oncogene arrived in 1981 when the gene *H-Ras* was isolated from a human bladder carcinoma line and transfected into a murine fibroblast line—NIH 3T3—resulting in unrestricted cell proliferation in culture [12]. *H-Ras* was subsequently found to possess a glycine-to-valine substitution on position 12 on a single allele [13]. Later several other oncogenes would be identified, including *Fos*, *AKT*, and *B-Raf*: all transforming cells in culture. Most, like *H-Ras*, encoded cytosolically located proteins and were caused by hypermorphic mutations occurring to single alleles. These experiments represented the first clear evidence that mutations to native genes result in a cancer phenotype: as it was previously established that cancer could be caused by virally transfected genes such as *Src*. However, the results suggested that mutations to single genes are capable of inciting cancer. This could not be true, as the consequences would be catastrophic: estimates, for example, indicate that every cell of the body suffers on average 1000 somatic mutations per/day with cancer typically only developing with age [14].

The fault was later found to lie in the fact that NIH 3T3 cells are a secondary cell line which have been serial passaged for decades. As secondary cell lines are genetically unstable by virtue of the ex-vivo environment and selective pressure of culture conditions; it is likely that these cells have acquired mutations and epigenetic alterations already which poise them to become transformed following a critical mutation. When *H-Ras* was introduced into a primary cell line, cells exhibited finite proliferation [15]. These findings imply that mutation of a single gene is insufficient to trigger cancerous growth.

The Development of Cancer Requires Mutation to Multiple Genes

In a subsequent study, collaboration of the oncogenes *Ras* and *Myc* was found to drive unlimited cell proliferation following transfection into a fibroblast primary cell line [15]. *Myc*,

however, differed from *Ras* in that it carries a nuclear localized protein. This it shares with another set of identified cancer-driving genes, which unlike oncogenes, typically involve loss of heterozygosity resulting in the inactivation of both alleles. These genes are termed "tumour-suppressor genes (TSG)"—because their activated state suppresses tumour growth—and includes genes such as *Rb*, *SMAD4*, and *P53*.

Despite the results observed in culture, the in-vitro environment is unrepresentative of the milieu in which cancer occurs. To relate the mutations of genes to human cancer phenotypes, the site of mutation would have to take place within the body of a living animal. Later on, methods were developed for homologously recombining transgenes into the embryonic stem cells of mice. Using this approach, one seminal study introduced single mutations to *Ras* or *Myc*—or combined mutations to both—into the germline of mice. To prevent embryonic lethality, transgenes were expressed specifically in the breast tissue of the mice using a MMTV promoter. Results demonstrated that single mutations resulted in mostly thickened clonal lesions, with some tumour formation. Whereas mutation to both genes incited more frequent, accelerated, and indeed sizeable tumour growth. However, primary tumour growth is only one facet of cancer; the full range of cancer progression also encompasses the additional condition of metastatic outgrowth: even in the double mutant, progression towards metastasis was minimal and infrequent [16].

If the mutation of two genes is insufficient, how many mutations then are required to capture the full spectrum of cancer growth? Large scale Next-Generation-Sequencing (NGS) has helped provide answers by elucidating the genetic landscape of a broad spectrum of cancers. Through genome-wide sequencing of a wide variety of cancers, with 100+ patient biopsies extracted for each, a pattern emerges where for any given cancer around 33-66 genes exhibit mutation [17]. Some are drivers which play a causal role in carrying out cancer growth. Others are mere passengers that are randomly mutated but provide no growth advantage. However, a set of mutations can be seen to reoccur frequently across patient biopsies: these are likely to be the driver mutations (Fig.1.3).

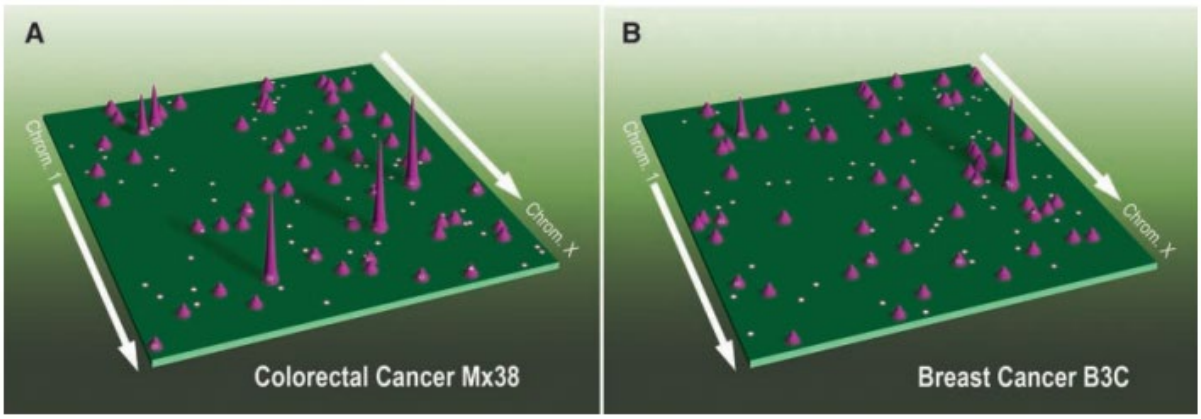

Figure 1.3. Landscape frequency distribution plot of mutations commonly occurring in colon and breast cancer: (A) Colorectal Cancer genetic landscape; **(B)** Breast Cancer genetic landscape. The points on the map represent different mutations with their position on the map corresponding with their chromosomal location. The height of the points represents a measure of the frequency by which the genes are mutated across different tumour biopsies. The very frequently mutated genes—"the mountains"—are considered driver mutations. Some drivers are shared across cancer types: in this case P53 represented on the right is frequently mutated in both colon and breast cancer. Graph taken from [18].

Typically, 3-6 putative drivers can be discerned for any given adult cancer. Put together, these findings imply that a minimum of three drivers are typically required for the full range of cancer progression. However, they raise the question of why multiple mutations are needed? The requirement of multiple disparate mutations suggests that several distinct signalling circuits must be compromised for cancer to develop. This in turn begs the question: what is the nature of these signalling circuits?

The Hallmarks of Cancer

There is a large consensus now that cancer is a multistep process that proceeds by the gradual accumulation of mutations that lend themselves towards progressively more aggressive incarnations of cancer growth. Relating each of these mutations to cancer phenotypes has, however, proven to be a challenging ordeal in large part due to difficulties in defining the cancer phenotype. Involving not only changes in the growth circuitry of cancer clones, but also considerable redeployment of stromal cells such as blood vessels and immune cells. Moreover, the migration of metastasizing cells requires extensive changes to the structure of epithelia and surrounding ECM. Put together, the cancer phenotype can seem awfully complex. The "Hallmarks of Cancer" are a set of defining cancer phenotypes, proposed by Hannahan and Weinberg to be necessary for cancer progression [19]. It represents an attempt to distil the complexity of the cancer phenotype into six obligatory functional capabilities, to which distinct mutations can be mapped and related mechanistically (Fig.1.4). Since its inception in 2000, this conceptual framework has received wide scientific support.

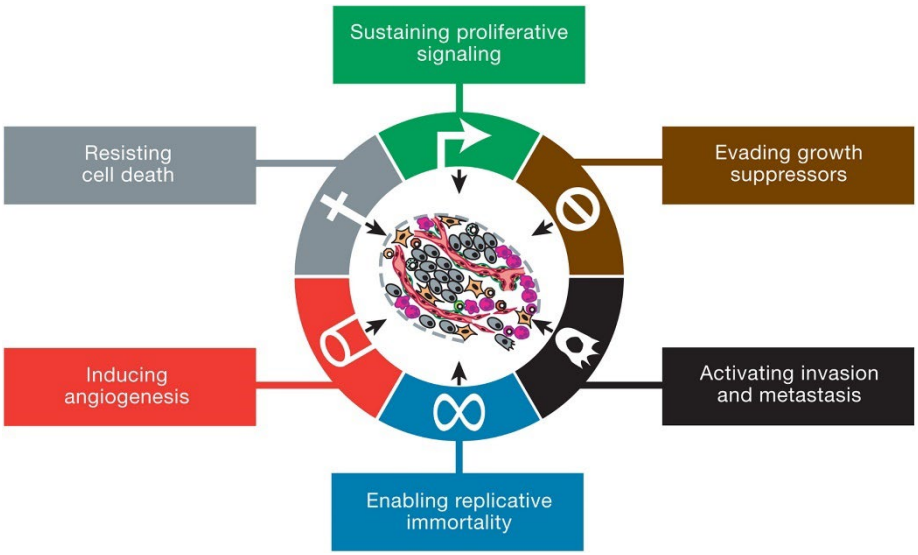

Figure 1.4. The Hallmarks of Cancer: The six hallmarks of cancer, originally proposed by Hannahan and Weinberg to be shared by all cancers. Diagram taken from [19].

1 – Cell Autonomous Proliferation

The most obvious phenotype of cancer is the occurrence of excess proliferation, which is acknowledged in its namesake (neoplasia = "new growth"). Although, far from an insipid platitude, tumour cell proliferation is more than upregulated mitosis; but continued, unrestricted, mitoses that occurs in defiance of the checkpoints that regulate the proliferation of normal cells. Whereas other cells must be licensed to grow under permissive cues, cancer cells have acquired the capacity to proliferate autonomously. This sets cancer aside from other proliferative diseases like psoriasis and inflammatory bowel disease, where increased mitoses are observed but still occur under non-autonomous cues [20, 21]. The environmental inputs that must be received to permit mitoses can be quite diverse. The perhaps most notable requirement, however; is the need to receive extracellular ligands. These proteins bind to cognate transmembrane receptors which relay the signal to intracellular effectors—typically enzymes—which in turn transmit the signal to the nucleus resulting in transcription of proliferative machinery. Many mutated oncogenes provide growth advantages by enabling tumour cells to bypass the need for an extracellular signal: often, by enabling receptor coupled enzymes to signal constitutively and independently of receptor activation [22]. Notably, 20% of cancers involve mutations to Ras GTPases which associate with Receptor-Tyrosine Kinases (RTKs) such as EGFR receptors [23].

2 – Evasion of Growth Suppression

The inability of single mutations to oncogenes like *Ras* to transform primary cell lines in experimental contexts, suggests that cell-autonomous proliferation is insufficient for cancer growth. This relates to the fact that, following mitosis, many cells are instructed to enter a post-mitotic state in which they are non-responsive to growth signalling factors [24]. Mechanistically, this resistance to growth relates to the inhibition of cell-cycle proteins—notably cyclin/CDKs—by nuclear localized master regulatory proteins: these proteins encompass many of the major TSGs, such as *Rb* and *SMAD4*, which become mutated and lost during cancer progression [25, 26]. A second important feature of tumorigenic growth suppression is the loss of proliferative capacity that accompanies the differentiation of cells. The circuity associated with specialization often suppresses the proliferative machinery of cells resulting in quiescence. Cancers are observed to overcome this, as a progressive loss of differentiation is observed with more aggressive cancer growth and can be associated with such TSGs as *Notch* and *APC* [27, 28, 29, 30]

3 – Cell Immortalization

Once cells are given directions to grow and stripped off growth suppression mechanisms, they should be able to multiply more or less freely. However, in culture, cells are typically observed to only undergo a finite number of mitoses before they forcibly senesce: this number—termed the "Hayflick limit" —varies for cell type, but typically falls in the range of 40-60 divisions [31]. This relates to the fact that for each division the ends of DNA become shortened due to the end-replication problem; as a protective mechanism, repetitive non-coding nucleotide sequences termed telomeres cap the DNA end. However, for each division these become eroded, until such a point the coding DNA begins to undergo attrition as well. To hinder the loss of valuable information, cells cease division by undergoing senescence or apoptosis. To overcome this, cancers will most typically upregulate the enzyme telomerase which synthesizes new telomeres at the ends of DNA giving cancer cells the ability to divide indefinitely [32].

4 – Resistance to Apoptosis

Unlimited cell proliferation is a defining feature of cancer. Nonetheless, tumour growth involves not only an increase in cells, but also a reduction in cell death [33]. A cells decision to live or die is mediated by a balance of pro- and anti- apoptotic factors: when the balance tilts in favour of pro-apoptotic factors, downstream caspase signalling will carry out apoptosis [34, 35]. In the context of cancer, resistance to cell death typically relates to acquired mutations to

upstream master regulatory factors which control the expression of pro- and anti-apoptotic factors. Perhaps, most notably is the tumour-suppressor gene *P53* which will often orchestrate cell death following mutation, stress, or other ill-bearings [36]. The critically of this gene is reflected in its inactivating mutation occurring in 50% of cancers [37].

5 – Induction of Angiogenesis

As tumours grow to considerable sizes, nutrition and oxygen becomes increasingly scarce; this represents a barrier to tumour growth. To adapt tumours will often grow, branch out, and recruit new blood vessels to the tumour site [38, 39, 40] In some instances, tumour cells have even been documented to transdifferentiate into endothelial cells demonstrating the innovation by which tumours can overcome their increasing metabolic demands [41, 42]. Cancer angiogenesis strongly relates to hypoxia: lines of evidence demonstrate that when oxygen-starved the Hypoxia Inducible Factor (HIF) transcription factors become activated and drives secretion of angiogenic attractants such as FGF and VEGF [43].

6 – Metastasis

The perhaps most challenging cancer phenotype to understand is the progression of cancer towards metastasis. Despite being the most destructive, and ultimately lethal phenotype of cancer, the molecular biology underlying its progression remains mostly elusive. Nor is it apparent how best to target it [44]. It is clear that the final outcome of metastasis: Colonisation—the formation of detectable macrometastases (>2mm in size)—most strongly associates with mortality through the loss of life-sustaining functions at critical organs. Unfortunately, cancers at that stage are vanishingly difficult to treat with a far greater quantity of micrometastases (<2mm in size) having taken hold at diverse organs, all with the potential of shaping new macrometastases [45, 46]. Combined, with an association with acquired resistance to most established forms of therapy, this stage presents challenges for therapeutic targeting.

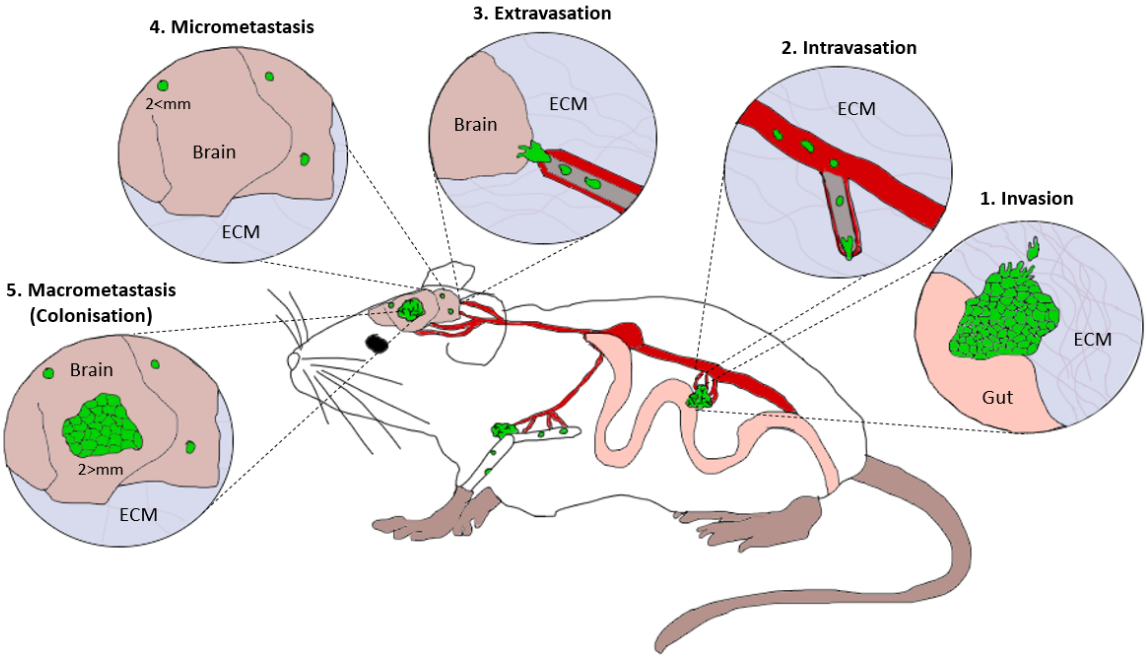

Figure 1.5. The Metastatic Cascade: metastasis encompasses five successive and rate-limiting steps: (1) outgrowth into the local connective tissue and muscle through invasion; (2) entry into local blood or lymphatic vessels through intravasation; (3) extravasation, the arrest and exit of tumour cells from blood vessels at distant sites; (4) the seeding of small (<2mm), and often residual, lesions known as micrometastases; (5) development into sizeable macrometastases (>2mm) through colonisation.

It is known that the seeding of macrometastases depends on the quantity of Circulating Tumour Cells (CTCs) present in the circulatory system. Increasingly higher CTCs per 7.5ml of patient blood associates with significantly higher likelihood of metastatic progression [47, 48]. Inversely, only 15% of patients with benign tumours possess any CTCs [49]. The dissemination of CTCs in turn depends on the primary tumour breaching the outer confines of its organ of origin, paving an exit route. As colonisation can be traced back to these preceding rate-limiting steps—termed the metastatic cascade (Fig.1.5)—the entire process should be preventable by inhibiting the first step: invasion and the subsequent large-scale dissemination of CTCs. A wealth of evidence associates invasion with the process of an Epithelial-to-Mesenchymal Transition (EMT) [50]. Which unlike colonisation, may expose vulnerabilities with potential for therapeutic targeting.

EMT and Invasion

For tumour cells to disseminate they must first separate from the primary tumour. This requires a loss of the restraints that constrain primary tumours to their origin tissues. To this end lines of evidence link the process of EMT [50]. As implied this biological program involves the reversible transdifferentiation of comparably immobile epithelial sheets to more migratory mesenchymal cells: a process conducive to the development and renewal of tissues, but

perversely exploited in cancer. Whereas epithelial cells are constrained by their apico-basal polarity, cell-cell adhesions, and encasement by the ECM; mesenchymal cells migrate through their front-rear polarity, cell-matrix junctions, and localized proteolysis of the ECM. It is in the context of such characteristics that EMTs are intensely researched (Fig.1.6). Nonetheless, many of the details regarding these mechanisms remains unknown.

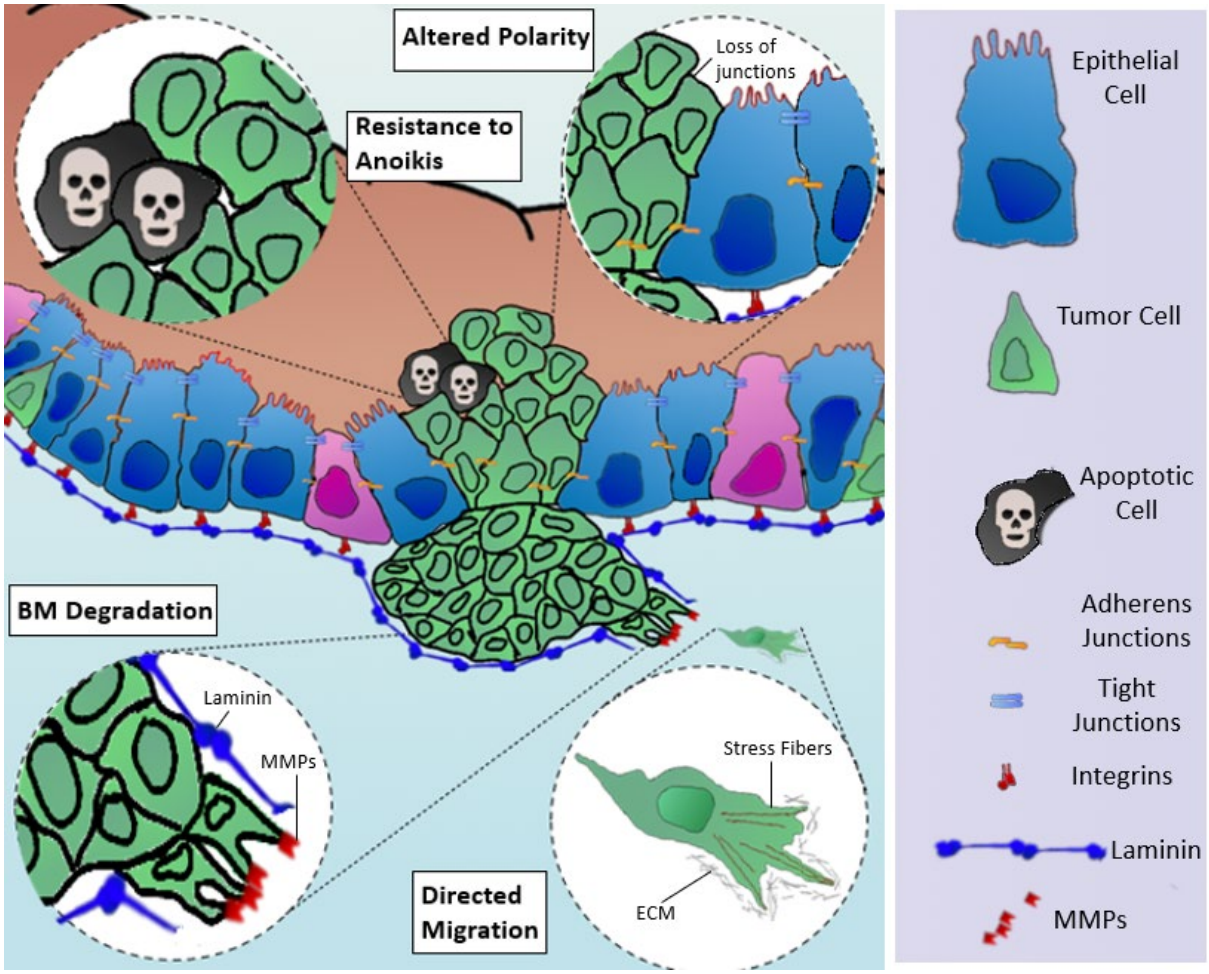

Figure 1.6. Mechanisms of EMT: epithelia are constructed with multiple features that impede invasive outgrowth. Opportunities to overcome these barriers are observed during EMT and commonly exploited for metastatic outgrowth. Such alterations include alterations to cell polarity and cell adhesion, proteolysis of the basement membrane, resistance to cell death mechanisms such as anoikis, and directed migration through the adoption of mesenchymal polarity.

It is known that EMTs are driven by master-regulatory transcription factors which includes such families as Snail, Twist, ZEB, FOXC, E12/E47, and GATA [51]. Upregulation of these TFs strongly associate with metastatic progression, with the degree of expression correlating with worse outcomes [52, 53, 54]. Although, mutations to these TFs are observed in various cancers, they more commonly become dysregulated following aberration to upstream factors, typically growth factor receptors [55, 56, 57] These receptors can be mutated but are often activated by cytokines secreted from recruited immune cells and fibroblasts which pervade the

TME [58]. Indeed, the intersection between EMT and metastasis has often demonstrated to be difficult to analyse upon simply genetic terms.

The strongest and most acknowledged mode of action of these TFs is the direct transcriptional repression of *E-Cadherin*. In some scenarios, experimental downregulation of *E-Cadherin* is sufficient to drive EMT [59, 60]. However, in most circumstances EMT transcends mere repression of *E-Cadherin*. Indeed, EMT-TFs have also been documented to directly bind to genetic regulatory elements of other target genes such as *MMPs*, *N-Cadherin*, and *mIRs* [61, 62, 63]. With an even more diverse gene signature being attained through co-regulation of genes in concert with other TFs [64]. Furthermore, EMT-TFs rarely entirely repress *E-Cadherin,* with many regulating its enhancer motifs to only gradually repress its expression [62]. Finally, other signalling circuits will often be in operation, acting to reverse or compensate for the repression of *E-Cadherin* [65].

EMTs also relate to the development of Cancer Stem Cells (CSCs). A cancer cell type defined by its unique efficiency at seeding secondary tumours at distant sites [66, 67]. Moreover, EMTs have been linked to the development of resistance to cell death: a property which may contribute to metastasis associated resistance to treatment—including many chemo- and radio-therapies—which rely on inducing tumour cell apoptosis [68]. Indeed, the EMT phenotype can be quite complex. A more through account of associated mechanisms and EMTs potential as a clinical target will be discussed below.

Altered Cell Polarity and Adhesion

Cells arrange into tissues through their cell polarity: that is the asymmetric distribution of proteins and lipids along different spatial dimensions of the cell. Notably, the polarized distribution of adhesive molecules binds epithelial cells to each other and the matrix: positioning them in relation to one another and coordinating their assembly into functioning tissues. This defining epithelial feature is accomplished through arrangement into an apico-basal polarity with three domains: a basal domain which anchors the cell to the underlying ECM; a lateral domain which connects cells together; and an apical domain where the cell interfaces the external environment [69]. Gap Junctions, Occluding junctions, Desmosomes, and Adherens junctions localize to the lateral domain; whereas, Integrins and Hemidesmosomes localize to the basal domain (Fig.1.7). Together, these adhesions keep cells together and are all documented to become lost or rearranged during EMT [70].

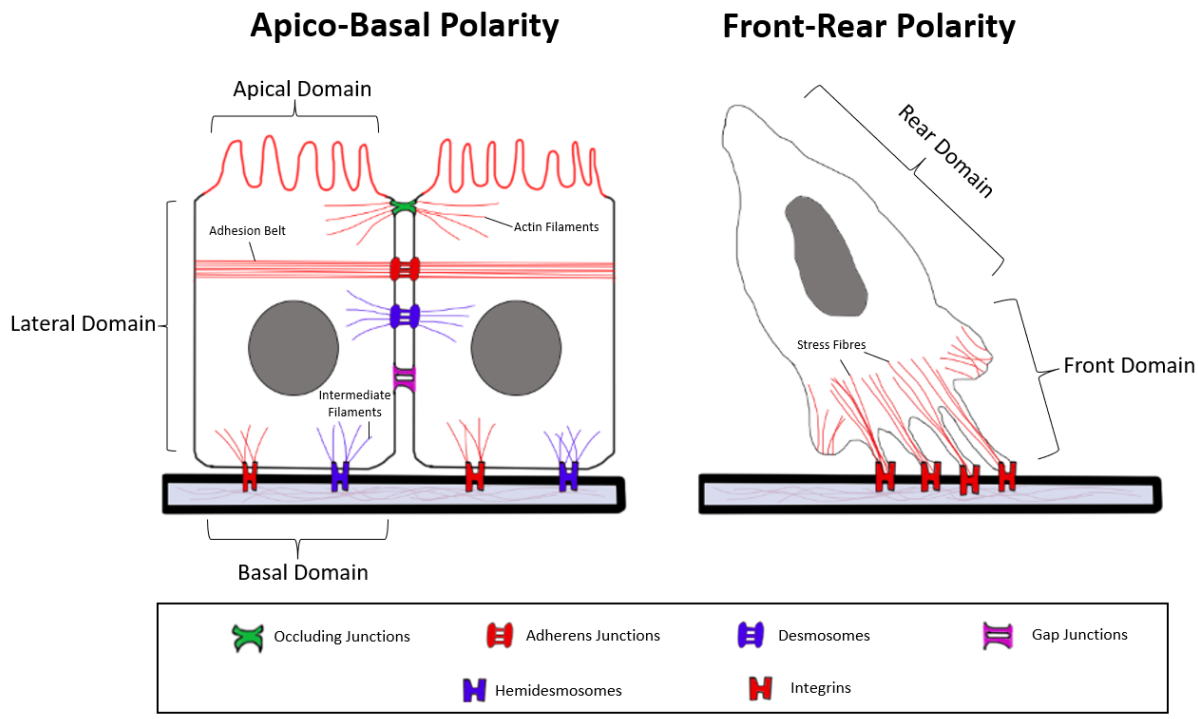

Figure 1.7. Schematic Diagram of Apico-Basal polarity vs Front-Rear polarity: Apico-basal polarity encompasses three domains with adherens junctions, integrins and occluding junctions coupled to actin filaments (depicted in red). Desmosomes and Hemidesmosomes are coupled to intermediate filaments, most typically cytokeratin (depicted in blue). Mesenchymal cells are typified by Front-Rear polarity, which mostly features cell-matrix junctions, coupled to stress fibres, and localized within invasive protrusions at the frontal domain of the cell.

E-Cadherin, which lies at the interstices of opposing adherens junctions, is likely the most studied change during EMT, in no small part due to its repression by EMT-TFs. Indeed, loss of E-Cadherin—completely or partially—is observed in many invasive carcinomas where it almost invariably correlates with progression to metastasis [71]. This relates to the coupling of adherens junctions to the intracellular adhesion belt: a chain of contractile parallel actin bundles which tighten cells together into an epithelial sheet. Through loss of E-Cadherin, the adherens junctions collapse and cells uncouple from the adhesion belt, becoming looser. Although typically other adhesions become altered as well. By in large, cells undergoing EMT exhibit an overturn of cell-cell junctions in favour of cell-matrix junctions [72]. Notably, the integrins tend to remobilize to the front of extended protrusions where they couple to contractile intracellular bundles of anti-parallel actin filaments termed stress fibres [73]. Through this coupling, the protrusions can latch onto the ECM through their integrins and leverage the stress fibres to support forward motion along the ECM.

Moreover, although EMT is often depicted as involving a complete conversion of epithelial to mesenchymal traits, this is actually a rare occurrence. More commonly, partial-EMTs (P-EMT) are observed where some residual cell-cell adhesion, including E-Cadherin, is retained and is

indeed necessary for the migration of collective clusters [74, 75]. In such scenarios some degree of plasticity is required to relax adhesion enough for separation from tissue surfaces, but enough adhesion for clustering of cells ranging anywhere from a dozen to hundreds of cells [76].

Destruction of the Basement Membrane

Epithelia anchor to an underlying layer of extracellular fibrillar proteins termed the basement membrane (BM). The proteins that encompass the BM can be quite diverse, however four core proteins are typically required to construct the BM, as well as retain its structural integrity: Laminin and Collagen IV fibres; stabilized by Perlecan and Nidogen bridges [77, 78]. This layer has the potential of encaging tumours within the boundaries of their organ even if adhesions are lost. Tumours that develop a method of breaching the basement membrane are therefore offered an opportunity of migrating through the paths that are cleared. The significance of this trait is mirrored in patient biopsy data where loss of the BM strongly predicts the incidence of distant metastases occurring within 5-years [79] (Fig.1.8). Indeed, the power of BM degradation as a prognostic marker is reflected in its common use by histopathologists to differentiate benign and invasive biopsy samples [80]. By in large tumours are found to overcome confinement by the BM through the activation of proteolytic enzymes which cleave the components of the BM. The enzymes most commonly associated with cleavage of the BM are the Matrix-Metalloproteases (MMPs) [81].

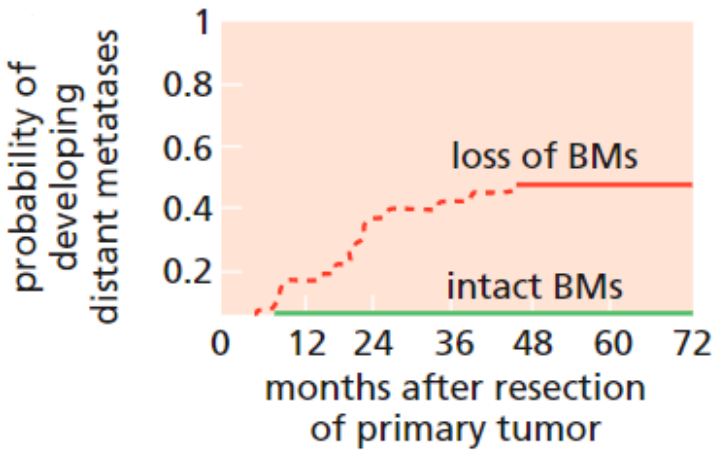

Figure 1.8. Relationship between BM breakage and the development of distant metastases: probability of colon cancer patients developing secondary tumours in the months following resection of a primary tumour with, or without, loss of the BM. Figure retrieved from [210], adapted from [79].

EMT as a Therapeutic Target

Given the critical role of EMT in driving dissemination it can be logically inferred that it should be a valuable target for pharmacological blockade. However, thus far EMT has presented itself as notoriously difficult to treat by virtue of it not meeting the criteria for a good drug target. Biochemical considerations dictate that a good drug target should have a site that is functionally important—and thus vulnerable—while simultaneously structurally amenable to binding by drugs. Typically, enzymes are considered good targets as they meet these criteria: the catalytic clefts are functionally indispensable and bring numerous reactive amino acids within range of a cognate drug [82, 83]. This supports the formation of multiple non-covalent bonds which provides needed affinity. As EMTs are driven by TFs which lack these features, they are deemed poor drug targets. Although, some medicinal chemists argue that TFs have the potential of being druggable [84] However, this is as of yet, largely unrealized and remains to receive wide support.

Even if EMT-TFs could be drugged they are still limited by another consideration. As EMT is a broad transcriptional program involving the altered expression of up to 400 genes—with only a small minority likely to be metastatic drivers—targeting it would likely result in intolerable adverse effects [85]. In particular, the cellular plasticity afforded by EMT is invaluable in homeostatic functions such as tissue-renewal and wound healing [86, 87]. Moreover, whereas EMT participates in invasion and dissemination, the inverse—a mesenchymal-to-epithelial transition (MET)—occurs in later stages of metastasis and is believed to results in re-epithelialization and subsequent secondary tumour formation [88]. Legitimate concerns—which are supported by some experimental evidence—are raised about the possibility that targeting EMT may trigger a switch resulting in MET induced colonisation [89, 90].

An alternate more rational approach is to target the downstream effectors of EMT rather than disturbing the whole signalling network. Identifying downstream drivers merits a more thorough understanding of the EMT phenotype which currently remains unclear. There is an awareness that EMT relates to changes in adhesions, polarity, and ECM remodelling; however how these disparate alterations relate to one another, how they are coordinated in a multistep sequence of events, and a method of assessing their relative contribution towards the dissemination of CTCs remains to be established. Ultimately, if downstream drivers of EMT can be identified and causally related to dissemination this may pave the way for potential therapeutic targets: particularly if the effectors are enzymes which meet the criteria for

selectivity and drugabbility. Identifying targets requires a suitable experimental model whereby candidates can be identified and unambiguously tied to the dissemination of CTCs.

Modelling Metastasis

A good metastatic model should enable all the steps of metastasis to be investigated such that the consequence of early behaviours can be related to later outcomes. Moreover, the model should be genetically tractable and representative such that the role of relevant molecular drivers can be assigned. Finally, considerations such as lifespan, sample size, and mortality should not rise to be significant impediments. Over the years two popular systems have been utilised to study metastasis with both exhibiting significant challenges.

Patient derived cancer cell lines can be plated on ECM components and often form three-dimensional structures reminiscent of tumour epithelia, with some carrying potential as organoids [91]. They have been useful for studying basic invasive behaviours such as migration, protrusions, and cell plasticity [92, 93]. While cheap, accessible, and abundant, they are often secondary cell lines which are unrepresentative of the genetics of bona fide tumour tissue. Moreover, and perhaps more importantly, invasive behaviours do not occur in isolation: metastatic behaviours occur within the context of organs and tissues under the confines of a tumour-bearing individual. For more representative results modelling must take place in an animal.

The traditional, and most popular, in-vivo model of metastasis are mice, of which there are two popular experimental strategies. Patient Derived Xenografts (PDX) involves the transplantation of a patient-derived primary cell line into a mouse. This will often result in colonisation but bypasses earlier steps, such as primary tumour growth and invasion, impeding full analysis of the metastatic cascade [94]. Moreover, as the cells are from a different species than the host, there is a genetic disconnect between the cancer cells and the cells of the TME. This undercuts the critical role of tumour cell interaction with the microenvironment.

Genetically-engineered mouse models (GEMMs) overcome many of these challenges. As orthologous transgenes are homologously recombined into the germline of a mouse, the mice will develop genetically representative tumours—typically homed to specific organs through selective promoters—which capture earlier steps such as invasion. However, they often make for expensive, risky, and time-demanding experiments with substantial difficulties in rearing sufficient sample sizes. Moreover, and more importantly, many GEEM models of cancer are limited by mice dying before colonisation can be studied: yet again denying investigation of

the whole metastatic cascade [95]. The fruit fly, *Drosophila Melanogaster*, although less representative of human cancer, holds the promise of overcoming many of the limitations beset upon other models.

Drosophila Melanogaster as a Model of Metastasis

Drosophila first surfaced as a metastatic model following larval mutagenesis screens in the 1930s, where several genes involved in organizing epithelia were found, after mutation, to disrupt epithelial integrity and result in invasive outgrowth from the imaginal discs [96]. Since then, *Drosophila* grew to become a highly popular system for studying the mechanisms that arrange and hold epithelia together [97]. The genetic redundancy of the fly meant that mutations to single genes—which often have no homologs—would result in a phenotype and readily assignable role. Moreover, the small size of larvae allowed for the whole animal and its tissues to be imaged under the microscope: making the epithelia more accessible than in animals like mice. Additionally, with a 10-day lifespan at $25^{\circ C}$, and females laying up to 100 eggs a day, a large sample size could be quickly analysed and interrogated with drugs and genetics screens [98, 99, 100, 101]. Through these advantages, *Drosophila* would emerge a champion in the identification and early characterisation of many of the most intensely studied cell adhesion and polarity regulators, including *DLG*, *LGL*, and *Scribble* [96, 97, 99].

Leveraging *Drosophila's* strengths in studying epithelial architecture, a wealth of studies have developed investigating the relationship between loss of epithelial integrity and tumour outgrowth [102]. With powerful new advances in *Drosophila* genetics—such as the advent of genetic mosaics—multiple mutations, both oncogenes and TSGs, can be induced in single clones at defined timepoints [102, 103]. This allows for the complex polygenetic and multistep process of cancer to be paralleled in temporally controlled multi-hit models (Fig.1.9). Many of these models capture the entire metastatic cascade from invasion to colonisation at distant organs [100, 104, 105] The combination of tractable genetics and coverage of the entire metastatic process makes larvae an attractive metastatic model. However, the imaginal discs are unrepresentative of human cancer tissues and are therefore limited as accurate disease models.

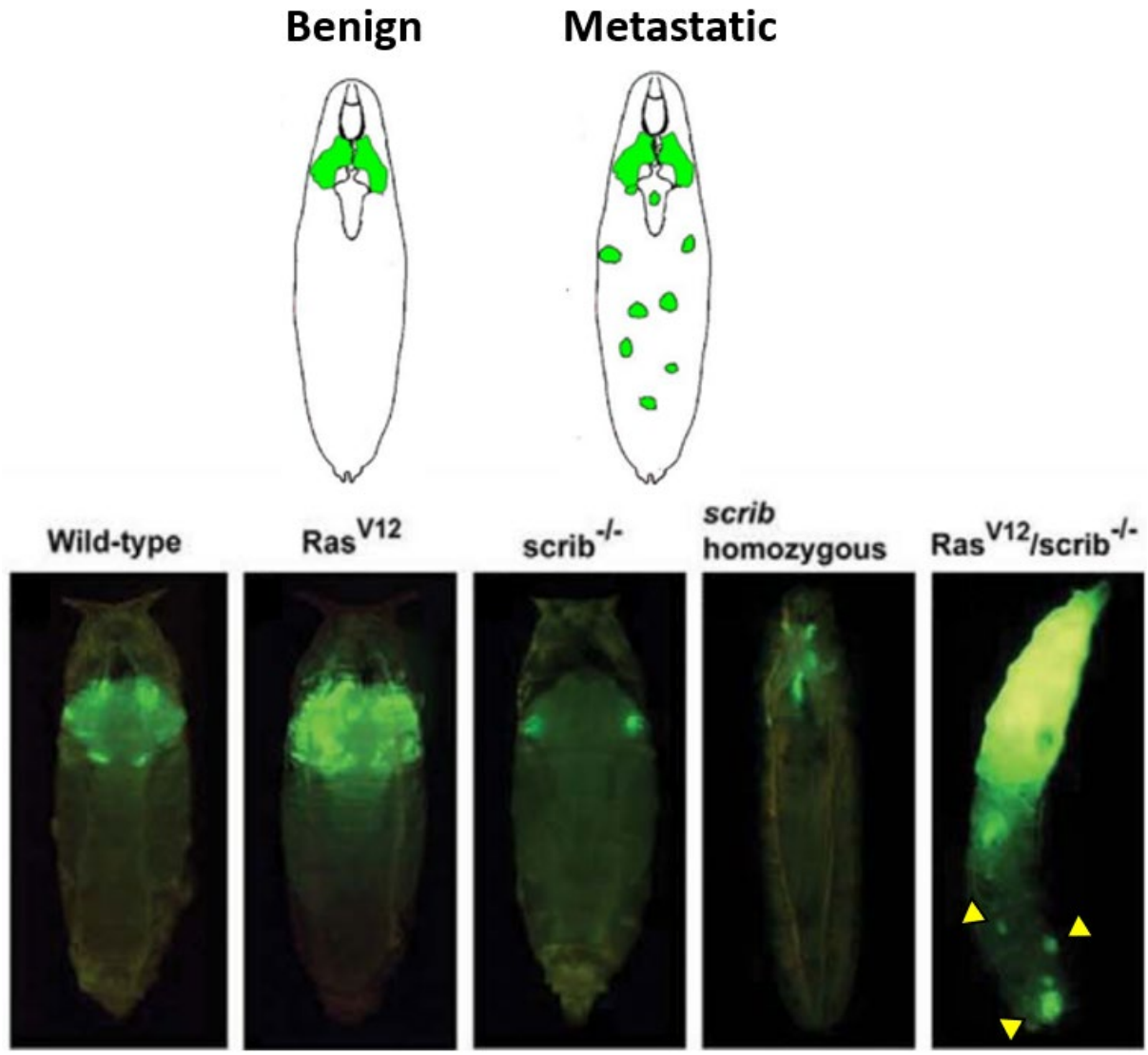

Figure 1.9. The Ras^{V12}; Scribble model of metastasis: the perhaps most popular larval model of metastasis is the Ras^{V12}; Scribble$^{-/-}$ model. Utilising the MARCM system, the oncogene Ras^{V12} and the TSG Scribble are put under the control of Eyeless which becomes selectively expressed in the eye-antennal imaginal discs at the early larval stage. Through to the 3rd instar larvae stage, the developing WT imaginal disc cells undergo fervent proliferation. Scribble$^{-/-}$ disrupts epithelial architecture, but results in extreme apoptosis. Ras^{V12} incurs resistance to apoptosis and enhances proliferation, but epithelial integrity is retained. The combination of Scribble$^{-/-}$ and Ras^{V12}, however, results in aggressive growth with the formation of metastases at distant sites (indicated by yellow arrows). Figure derived from [100].

Given *Drosophila's* powerful genetic toolkit, formidable strength in studying epithelial biology, and growing potential for drug screening; it has the promise of being an extraordinarily powerful metastatic model if presented with an opportunity to exercise these strengths on a tissue which is representative of human cancer. The discovery of self-renewing stem cells in the *Drosophila* adult midgut has set the stage for a wealth of intestinal tumorigenesis models with astounding similarities to human Colorectal Cancer (CRC): a system with promising, and relatively untapped, potential as a metastatic model [106, 107].

The Midgut as a Model of CRC

CRC is the 3rd most common cancer worldwide and the 2nd deadliest, with an approximately equal incidence between females and males [108]. There are familial forms of CRC involving inherited mutations, however 70% of cases are sporadic and involve the acquisition of somatic mutations [109]. CRC strongly relates to age, with 40-45% of individuals developing a benign polyp by the age of 70; 53-58% developing one by the age 80 [110, 111]. Although, due to diet and lifestyle factors younger populations are becoming affected as well. Indeed, a 90% increase in the incidence of CRC is expected to be observed in the age group 20-34 by the year 2030 [112]. As industrializing countries adopt western lifestyles and the global population increases in age, CRC may become the most common, and perhaps, deadliest cancer [112].

The high frequency of CRC relates to the gastrointestinal tract being a highly proliferative tissue undergoing constant renewal. Each minute, 2-5 million cells die and become shed from the colon; 20-50 million are shed from the small intestine [113]. These cells are renewed by fresh cells which upon each iteration of mitosis carry the risk of passing on a mutation and harbouring cancer. With exposure to noxious foods and chemicals the risk of deleterious mutations increases and compounds with age. The gut is also one of the most evolutionarily conserved animal organs with rudimentary gastrointestinal tracts tracing back to early cnidarians [114]. In particular increasing evidence is demonstrating marked similarities in the machinery of the gut between humans and *Drosophila* with strong implications for modelling intestinal behaviour in health and disease [115].

The Structure of the Mammalian and *Drosophila* Gut

The human gut can be divided into the small intestine—which bottoms out of the stomach—and the large intestine, or colon, which follows on from the small intestine and feeds into the rectum and ultimately anus (Fig.1.10A). Around 97% of CRC tumours develop on the colon, which is much shorter than the small intestine (1.5m versus 6m) but is about twice as large in diameter (6-7.5cm versus 2.5-3cm) [116, 117]. However, structurally both are largely the same (Fig.1.11A). Both consist of an inner mucosal layer that encompasses an epithelial layer, an underlaying connective tissue layer termed the lamina propria, and a circular muscle layer termed the mucosal muscle. The epithelia make pockets which descend past the muscle and into a 2nd connective tissue layer termed the submucosa: these pockets harbour the intestinal stem cells (ISCs) and are termed crypts [118]. Additionally, the epithelia of the small intestine occasionally protrude into the lumen as villi and carry out water absorption: a feature the colon

lacks. Finally, the submucosa is surrounded by a thick layer of longitudinal muscle which bounds the gut [118].

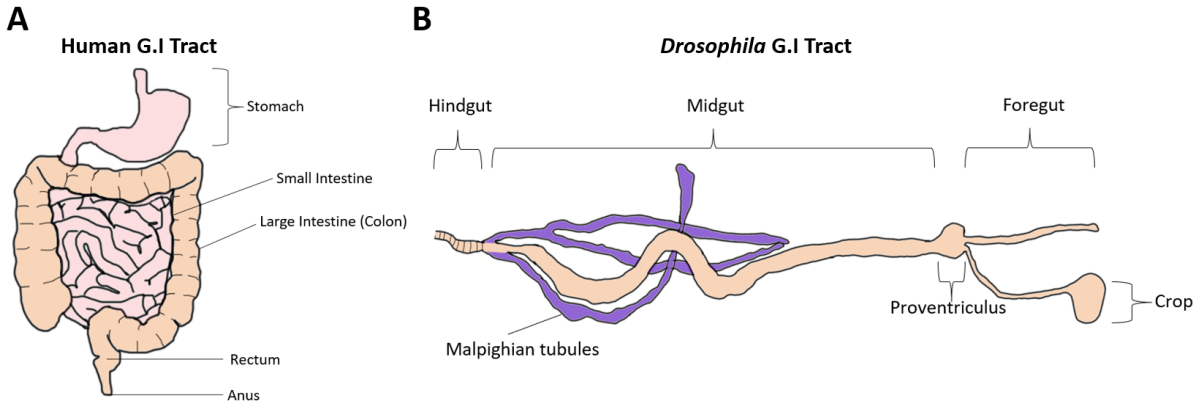

Figure 1.10. Human vs *Drosophila* gastrointestinal tracts: (A) the human gastrointestinal tract, encompassing the stomach, small intestine, large intestine (colon), rectum, and anus; **(B)** the *Drosophila* gastrointestinal tract, encompassing the foregut, crop, proventriculus (cardia), midgut, and hindgut. Additionally, the Malpighian tubules (MpTs) are represented in purple.

The *Drosophila* gastrointestinal tract is on average around 6 millimetres in length and encompasses a foregut, which couples to the probiscis and feeds into the midgut; a hindgut which descends from the midgut, intersects with a network of renal tubules termed the malphigian tubules (MpT), and bottoms out in the rectum (Fig.1.10B). Additionally, the apex of the midgut—the proventriculus (or cardia)—connects to a large storage organ termed the crop [119]. The midgut has been the subject of most research as it is the site of digestion and absorption. Including both walls, it is approximately 150-200um in width and is composed of an epithelial layer anchored to a BM with an underlying circular muscle layer termed the visceral muscle (Fig.1.11B). Furthermore, a layer of chitin and glycoproteins—the peritrophic matrix—embeds into the lumen [119]. Unlike the human intestinal tract, the midgut lacks villi and crypt. However, it is inhabited by similar populations of cells operating under astonishingly reminiscent molecular cues [115].

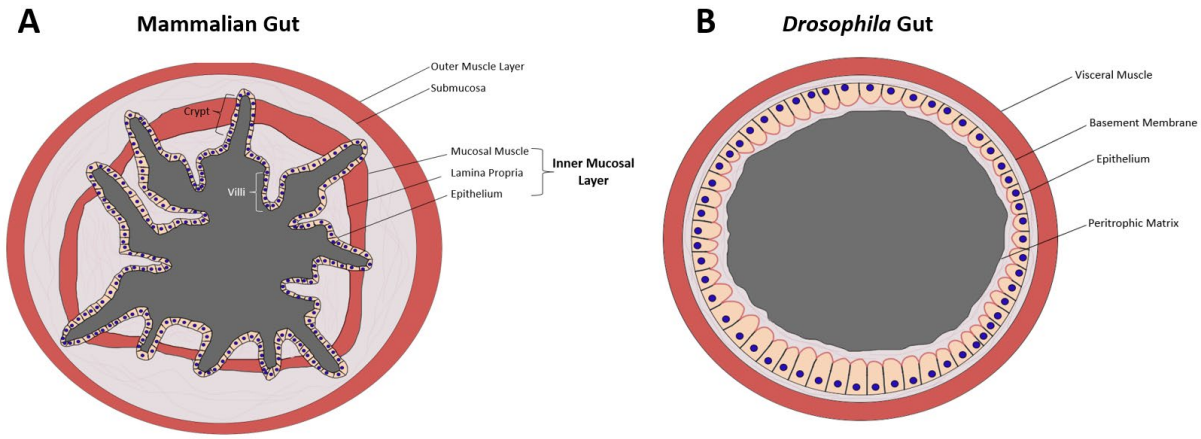

Figure 1.11. Layers of the gut – Mammalian vs *Drosophila*: (A) The mammalian intestines encompass an inner mucosal layer (epithelia, lamina propria, and mucosal muscle) and an outer layer featuring the submucosa and the outer muscle layer. The small intestinal epithelium periodically protrudes into the lumen as villi, whereas the colon does not. The small intestine is depicted here; **(B)** The *Drosophila* gut encompasses the visceral muscle, the BM, the epithelia, and the peritrophic matrix.

The Molecular Basis of Stem Cell Control

"Evolution of form is very much a matter of teaching very old genes new tricks" (Sean B Carroll – Developmental Biologist)

The gut has likely been the subject of more research than any other self-renewing tissue. This can be attributed to it being one of the simplest models of stem cell homeostasis. Unlike renewing epithelia like the epidermis—which comprise multiple layers of widely varied cell types—the intestine consists of a single epithelial layer, with a simple columnar arrangement, and a handful of cell types which can be mirrored closely in the *Drosophila* gut [120, 121, 115, 122] (Fig.1.12).

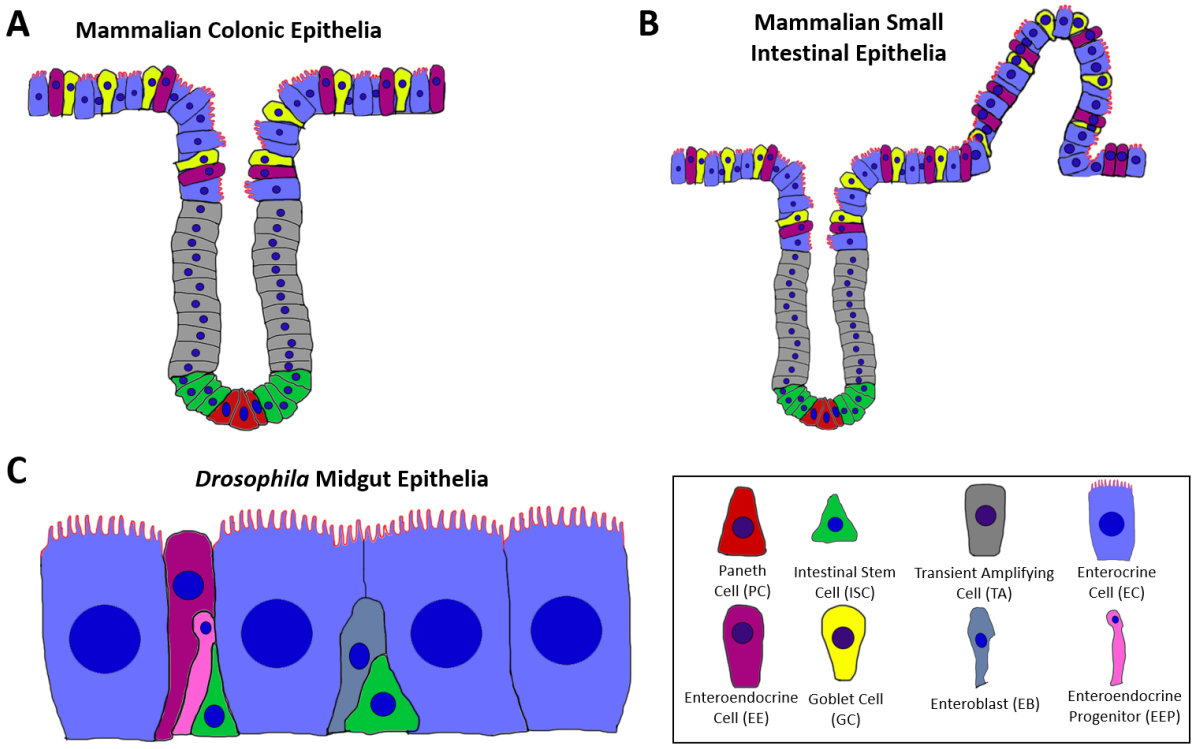

Figure 1.12. The cells of the Mammalian and *Drosophila* guts: (A) The mammalian colon features PCs and ISCs residing in the crypts. Cells become gradually more differentiated as they ascend the crypts, and include TAs, ECs, EEs, and GCs; **(B)** The mammalian small intestine features the same cells, but cells additionally ascend through villi once they reach the surface; **(C)** The *Drosophila* midgut epithelium is a flattened pseudostratified epithelium encompassing differentiated ECs derived from EBs and EEs derived from EEPs. Smaller ISCs are wedged between the differentiated cells and produce the progenitors through asymmetric cell division.

The small intestines harbor ISCs in the crypts which divide asymmetrically to produce another ISC at the base and a progenitor cell—termed transient amplifying cells (TAs)—which continue to undergo 3-4 more rounds of mitosis while simultaneously ascending the villi. There they differentiate into specialized non-dividing cells which carry out purposeful roles before reaching the apex of the villi where they undergo apoptosis and shed off. [123, 124]. The colon, which lacks villi, has cells differentiating as they move up the crypts: resulting in 2/3 of the crypt with ISCs and TAs and 1/3 with differentiated cells which also occupy the overlying flattened epithelium between crypts [125]. The differentiated cells—of both the small and large intestine—encompass two lineages: the absorptive cells and the secretory cells. The absorptive lineage is represented by the Enterocytes (ECs) which extend protrusions into the lumen, termed microvilli, and carry out nutrient absorption. The secretory cells include Goblet Cells (GCs) that secrete protective mucins, Enteroendocrine Cells (EEs) which secrete peptidases and antimicrobials, and Paneth Cells (PCs) which migrate down the villi and flank the ISCs where they aid in their self-renewal [125].

The *Drosophila* midgut instead of utilizing crypts, relies on a pseudostratified columnar epithelial arrangement whereby ISCs are wedged between the lower part of two larger

differentiated cells [126, 115] Through asymmetric cell division one new ISC remains wedged, while a progenitor makes space between two opposing differentiated cells, undergoes differentiation, and adjoins between the two [127]. The progenitor cells can have one of two identities depending on the mode of asymmetric cell division. One mode results in an Enteroblast (EB) progenitor which differentiates into an EC [128, 129]. The other mode gives rise to an Enteroendocrine Progenitor (EEP) which differentiates into an EE [130]. The former mode is more common, resulting in a distribution of 90% ECs and 10% EEs. [128]. The midgut lacks GCs and PCs, however the GCs are compensated for by the Peritrophic Matrix which carries out the same role [131]. The mechanisms by which ISCs generate a continual supply of non-dividing differentiated cells are governed by three central pathways: Wnt, Notch, and BMP, with a fourth – the JAK/STAT pathway – exhibiting importance in *Drosophila* as well (Fig.1.13).

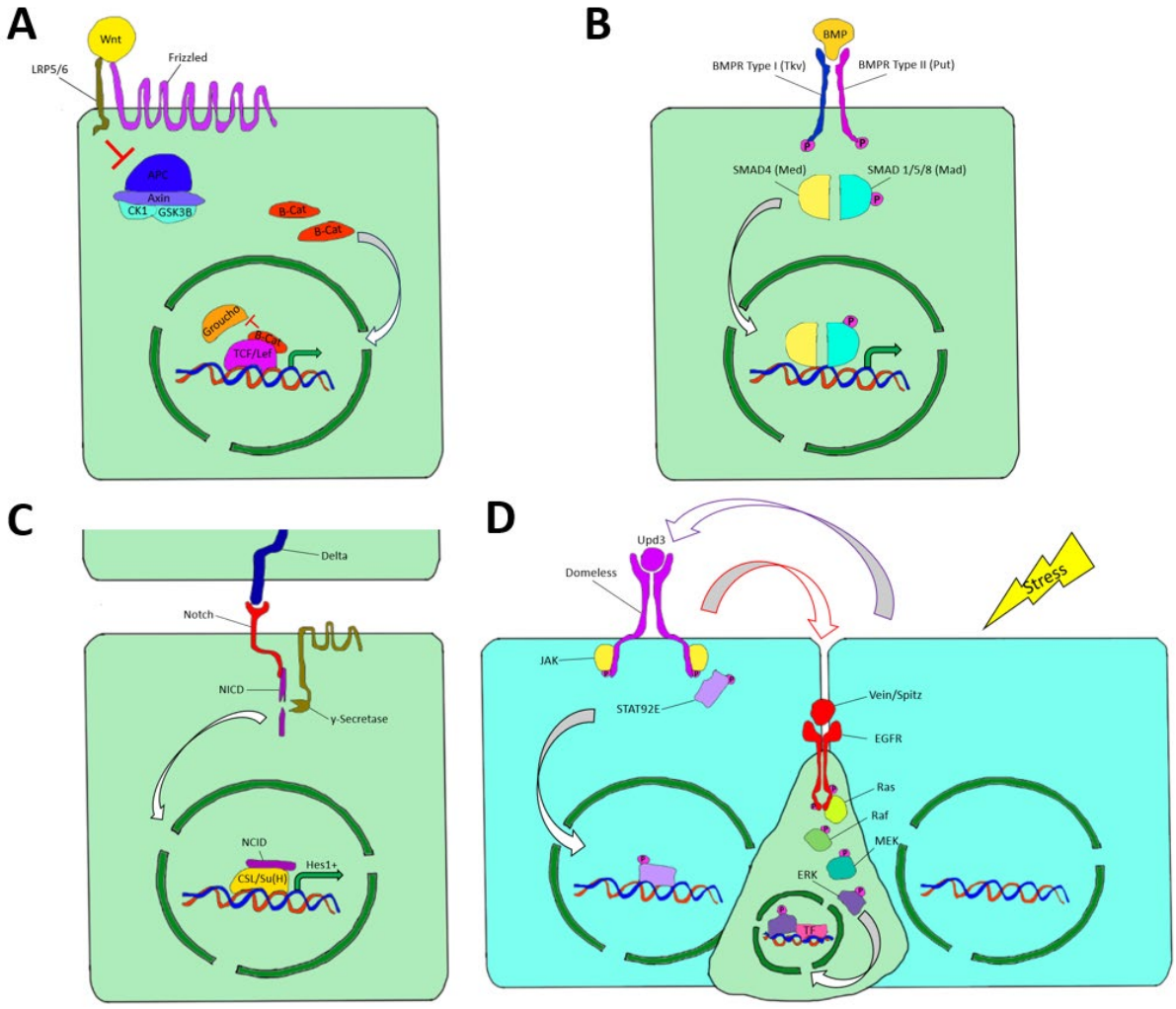

Figure 1.13. The Pathways of the Mammalian and *Drosophila* guts: (A) Wnt signalling. A secreted Wnt ligand binds to the Frizzled receptor and a LRP co-receptor (LRP5 or 6). Subsequent repression of the APC complex (APC, Axin, CK1, and GSK3B) results in liberation of B-Catenin which enter the nucleus, displaces Groucho, and triggers gene expression through TCF/Lef; **(B)** BMP signalling. A BMP ligand binds to a Type I and Type II BMPR (*Drosophila* thickvein and put) resulting in

receptor transphosphorylation. A receptor regulated SMAD (1, 5 or 8, or in *Drosophila:* Mad) becomes recruited and phosphorylated. Heterodimerization with SMAD4 (*Drosophila* Med) occurs, with the subsequent SMAD complex entering the nucleus to influence gene expression; **(C)** Notch signalling. A Delta ligand expressed by one cell, binds to the Notch receptor of a neighbouring cell. Subsequently, an intramembrane y-Secretase becomes activated, liberates the intracellular domain of Notch (NICD), which co-interacts with CSL (*Drosophila* Suppressor-of-Hairless) to express fate-determinant genes such as Hes1; **(D)** JAK/STAT and EGFR signalling. Following stress an EC secretes Upd3 which binds to the Domeless receptor on a neighbouring cell. The receptor becomes phosphorylated by JAK kinases, with further phosphorylation actioned on the recruited STAT92E. STAT92E enter the nucleus and mediates gene expression, with one outcome being the secretion of the EGF ligands Vein and Spitz. Binding of EGF ligands to the EGFR of an ISC results in receptor autophosphorylation. Activated Ras, subsequently triggers the successive phosphorylation of Raf, MEK, and finally ERK. ERK enters the nucleus to influence expression of proliferative genes.

Wnt

The perhaps most critical regulator of intestinal stem cell homeostasis in the mammalian gut is the Wnt pathway, which drives the renewal of ISCs and regulates differentiation into specialized cells [115]. Wnt ligands are believed to be secreted by PCs and myofibroblasts of the mucosal muscle [132]. These ligands comprise a concentration gradient which span from the base of the crypt to the apex of the villi or colon surface. Cells at the base receive higher concentrations and undergo self-renewal while remaining undifferentiated; cells above, acquire lower concentrations, and are incited to undergo a process of differentiation [133, 115]. The core effector of the Wnt pathway is B-Catenin, which reverses Groucho's repression of *Tcf/Lef* which in turn upregulates genes involved in proliferation and stemness [125]. Typically, the protein APC acts in a complex with the scaffold protein Axin, and the kinases GSK3B and CK1, to target B-Catenin for destruction. Through binding to Frizzled receptors, Wnt liberates B-Catenin by blocking APC [134]. The importance of this pathway is reflected in $TCF^{-/-}$ neonatal mice failing to form proliferative crypts [135]; likewise adult mice treated with Wnt inhibitors lose these crypts [136]. In the other direction, individuals with inherited mutations to APC rapidly develop polyps in the colon which invariably become invasive by the age of 40: a disease termed Familial Adenomatous Polyposis (FAP) and typically involving truncation of the C-terminal domain resulting in loss of association with B-Catenin [125, 137].

Like the mammalian gut epithelium, the midgut ISCs receive Wnt ligands from the underlying visceral muscle, as well as EBs, which aid in their subsequent self-renewal [138, 139]. Indeed, ISCs with dominant negative *TCF/Lef* driven by a Flp-out cassette exhibit marked depletion of ISCs [140]; *Wg* mutants exhibit a decreased quantity of ISCs [138]; UAS-*Wg* guts possess elevated quantities [138]. However, these manipulations influence ISC renewal mostly in the anterior of the gut: suggesting that the molecular control of stem-cell renewal follows distinct regionalized cues. Moreover, although Wnt signalling contributes to stem cell renewal in baseline homeostatic conditions, it appears to only be necessary for self-renewal in situations of stress such as infection or damage [139].

Notch

The entry into a differentiated state associated with diminished Wnt signals relates to Notch signalling. ISCs express the Notch receptor, which when bound by Delta ligands expressed by neighbouring PCs, results in an undifferentiated stem cell state. However, TA cells—subject to less Wnt signalling—express both Notch and Delta, although at different levels. TAs with high Delta levels, activate TAs with high Notch levels, but as they themselves lack Notch activation, they differentiate and become GCs and EEs. The other TAs remain undifferentiated under Notch signalling, continue to self-renew and ascend the villi, until they become beyond reach of Wnt signalling, lose Notch and differentiate into ECs and PCs [141]. Mechanistically binding of Delta to Notch results in engagement of an intramembrane y-secretase, which subsequently liberates the intracellular domain of Notch (NICD). NICD localizes with the transcription factor CSL in the nucleus where it activates target genes such as *Hes1* which mediate cell-fate decisions. Notably, genetic ablation of *Hes1* in mice results in secretory cells as opposed to enterocytes in notch engaged cells [125].

In the *Drosophila* midgut, progenitors can be discerned by expression of the Snail family transcription-factor Escargot. ISCs homozygous for an Escargot null allele ($Escargot^{G66B}$) undergo forced differentiation into ECs and EEs marked by the commitment factors PDM1 and Prospero respectively [143]. The loss of Escargot during differentiation relates to Notch signalling, which unlike mammalian Notch signalling, performs an inverse role of driving differentiation as opposed to stemness. Whereas, all the cells of the gut express the Notch receptor, only ISCs express its ligand Delta [115]. Following asymmetric cell division into EBs, Delta becomes lost due to repression by Groucho [129]. The subsequent activation of Notch on EBs by the ISCs drives differentiation into PDM1+ ECs through loss of Escargot. PDM1 appears to be finalizing differentiation by repressing Escargot, as forced expression of PDM1 in ISCs drives differentiation into ECs [143]. Occasionally, ISCs transiently activate Scute and asymmetrically divide into EEPs which after another round of division give rise to EEs [129]. Put together, Escargot expressed by Delta+ ISCs appears to be driving stemness. Whereas activation of Notch+ cells by Delta binding drives differentiation through repression of Escargot. However, the introduction of a $Notch^{RNAi}$ to ISCs—which aren't activated by delta—results in tumour outgrowth, which can be overcome through repression of Escargot [143]. This suggests that besides driving differentiation when interacting with Delta, Notch also carries out tumour-suppression through non-canonical means in the presence of Escargot.

BMP

The tumours seen in FAP are epithelial tumours. Juvenile Polyposis Syndrome (JPS) is a second inherited form of colon cancer, where the tumours are primarily mesenchymal in origin. Deriving from the lamina propria in the posterior end of the colon close to the rectum [144]. However, although initiated in the mesenchyme; a dramatically increased quantity of crypts can be observed [145]. 50% of patients have a mutation in the BMPR1A receptor or its downstream effector SMAD4 [146]. BMP ligands are abundant in the stroma of mice, rising towards the crypts in a gradient. Whereas BMPR1A and SMADs are enriched in the differentiated cells of the villi and colonic surface epithelium [147]. Inactivation of BMPR1A in the crypts of mice using a dominant negative mutation or treatment with the antagonist Noggin, causes an expansion of the stem cell compartment. By contrast, constitutive activation of BMPR1A suppresses ISC renewal through repression of B-Catenin [147]. These findings suggest that Wnt and BMP mutually antagonize one another in opposing gradients with the result of fine-tuning the frequency of self-renewal.

Although the midgut lacks crypts, the BMP ligand Decapentaplegic (DPP) is expressed in the ECs, Trachea, and Visceral muscle [148]. Knockdown of *DPP* in the visceral muscle using an RNAi results in expansion of ISC clones [148]. Likewise, knockdown of the BMP signalling components *Med* and *Shn* in the ISCs results in tumour outgrowth reminiscent of JPS in the posterior midgut [149]. Moreover, the BM has been found to restrict the diffusion of BMP ligands to the ISCs; with mutation to the Collagen IV subunit Viking, resulting in a loss of localization to these cells [150]. These findings suggest that—as in mammalian guts—the BMP pathway acts to negatively regulate ISC renewal, with the outcome of balancing baseline levels of renewal. The formation of BMP mutant tumours in the posterior, is in opposition to Wnt derived tumours which typically occur anteriorly. This suggests that BMP may exert more control on the renewal of posterior ISCs.

JAK/STAT and EGFR – The Stress Response

Despite the similarities in signalling pathways, a key difference can be found in the JAK/STAT pathway, which is critical for ISC renewal following stress in *Drosophila* but appears less significant in mammals [151]. When subjected to stressors such as injury or infection, ECs secrete Upd3 which binds to progenitors, differentiated cells, and the visceral muscle. These cells respond by releasing EGF ligands that drive ISC renewal [152]. The action of EGF is dependent on Ras acting downstream of the EGFR receptor, as inactivation of Ras in ISCs

results in severe deficits in self-renewal following stress [153]. In the other direction, ISCs with a constitutively active Ras^{V12} mutation exhibit aggressive tumour growth [154].

Genetic Landscape of Sporadic CRC

Sporadic CRC is one of the most intensely researched cancers. Not only by virtue of its increasingly alarming frequency, but also because it's one of the most illustrative examples of multistep tumorigenesis: proceeding by gradual and successive mutation to many of the core genes regulating renewal of the gut. Indeed, many of the key signalling pathways involved in intestinal stem cell homeostasis have been identified and understood by inspection of the way they go wrong in CRC [125].

The reason the gut is such a good system of multistep tumorigenesis relates to the accessibility of patient biopsy tissues: a fact which can be tied to an ease of sectioning tissue by colonoscopy, as well as the large quantity of CRC patients to extract tissue from. From such biopsies, multiple lesions of varying severity can be discerned [155]. Hyperplasia's encompass thickened and proliferative lesions, with otherwise normal morphology. Adenomatous polyps are considerably larger, possessing more abnormal morphology, and are typical visible by their outward protrusion into the gut lumen. A final incarnation, the invasive carcinomas, feature aggressive growth with evidence of invasion into the connective tissue and muscle layers. These lesions are often represented as successive stages of tumour growth. The perhaps most striking evidence for this theory, is that more advanced lesions retain mutations present in less severe growths but have also acquired additional mutations suggestive of a succession scheme [155, 156].

The relationship between these lesions and the acquisition of different mutations was first established through the seminal work of Fearon & Vogelstein who sought to map each lesion on to different mutations [155]. Given the heterogeneity of cancer, it is reasonable to expect that each lesion would exhibit widely varying mutations. However, their work found that each lesion was transitioned by a comparatively consistent and stereotype acquisition of defined mutations. APC, which is mutated in 80% of CRC patients [157], was found to coincide with the hyperplasia stage. Besides APC, Adenomas were found to often possess an additional activating mutation to *K-Ras*, which occurs in 50% of patients [158]. More severe adenomas, in 50% of cases, also exhibited loss-of-heterozygosity to an unknown gene on the long arm of chromosome 18 [155]: this gene is believed to be SMAD4 which is mutated in 20% of CRC

cases [159]. The transition into the carcinoma stage was correlated with an added inactivating mutation to *P53*, which becomes mutated in 50% of CRC patients [160].

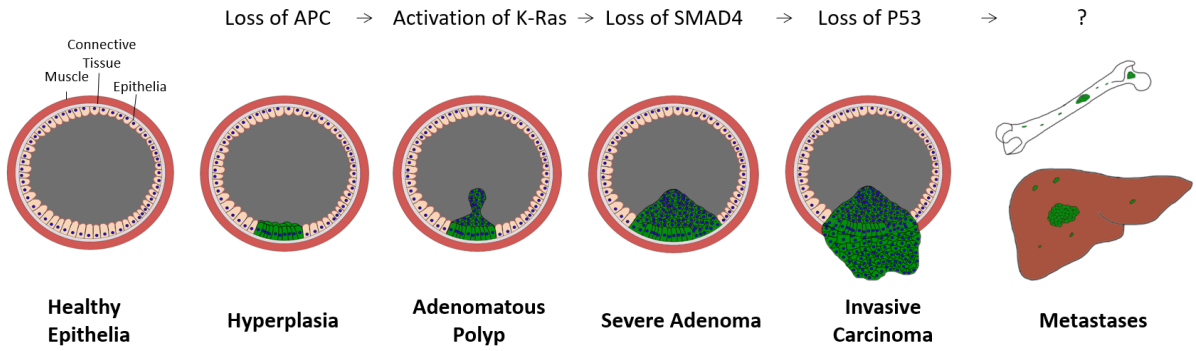

Figure 1.14. Schematic diagram of the genetic progression of CRC: whereas varying stages of primary tumour growth can be mapped to frequently occurring mutations; identification of a genetic determinant underlying progression to metastasis has been unsuccessful.

The results of this landmark study were able to assign genetic correlates to the progressive development of primary tumour growth (Fig.1.14). However, the genetics underlying the next step in cancer development—progression towards metastasis—was left undetermined. Unfortunately, this final step can be said to be the most critical given its association with poor survival and resistance to therapy. Indeed, whereas adenomas and carcinomas correlate with a 90% and 70% 5-year survival rate respectively; metastases—which over 50% of CRC patients acquire at some point in their lifetime—carry a 10% 5-year survival rate [161]. The inability to relate metastatic CRC to a genetic correlate might be tied to the transition being the result of genetic dysregulation rather than mutation. Indeed, given the association between metastasis and EMT—which often results from microenvironmental inputs—it is plausible that the carcinoma transition cannot be clearly traced to a single genetic determinant, but rather occurs from EMT-TF activation following external cues. Lines of evidence link CRC invasion to activation of the EMT-TF Snail1.

Whereas normal colon cells are negative for Snail1 expression; 77% of invasive carcinoma samples are immunoreactive for Snail1 in the stroma: the presence of cells in the stroma suggesting that cells have already detached and begun to migrate out [162]. These cells are E-Cadherin negative and possess mesenchymal morphology. Moreover, transfection of Snail1 into the benign adenoma cell lines HT29 and HCT116 results in an EMT phenotype with diminished E-Cadherin, upregulation of the mesenchymal marker vimentin, adoption of a spindle-shaped morphology, and an up to 20-fold increase in migratory capacity using Boyden migration assays [163]. Additionally, these cells exhibit resistance to oxaliplatin treatment and increase the incidence of secondary tumour formation from 1/10 to 8/10 after transplantation

into mice. Finally, the extraction of budding tumour cells—cells that detach at the invasive front—exhibit marked upregulation of Snail1 [164].

The APC-Ras-Snail Model of Metastatic CRC

With the emergence of the midgut as a representative model of human intestinal biology, a number of labs have sought to model the role of mutated CRC genes by inducing orthologous mutations under the control of *Escargot*. This has yielded interesting insights regarding the pathogenesis arising from mutations to single genes such as *APC*, *Ras*, *Notch*, and *BMP*. In a previous study, the Casali lab sought to model the genetic progression of CRC by developing a multi-hit model of CRC [165]. This model featured null and hypomorph mutations to *APC1* and *APC2* respectively (APC^{Q8} + $APC2^{N175K}$) with APC^{Q8} producing a C-terminal truncation as commonly seen in CRC. Additionally, a valine-to-glycine substitution was incurred to position 12 on Ras resulting in a constitutively active form: Ras^{V12}. This APC-Ras model (AR) resulted in benign tumours with more aggressive growth than single mutations to *APC* or *Ras* with remarkable similarities to human CRC (Fig.1.15).

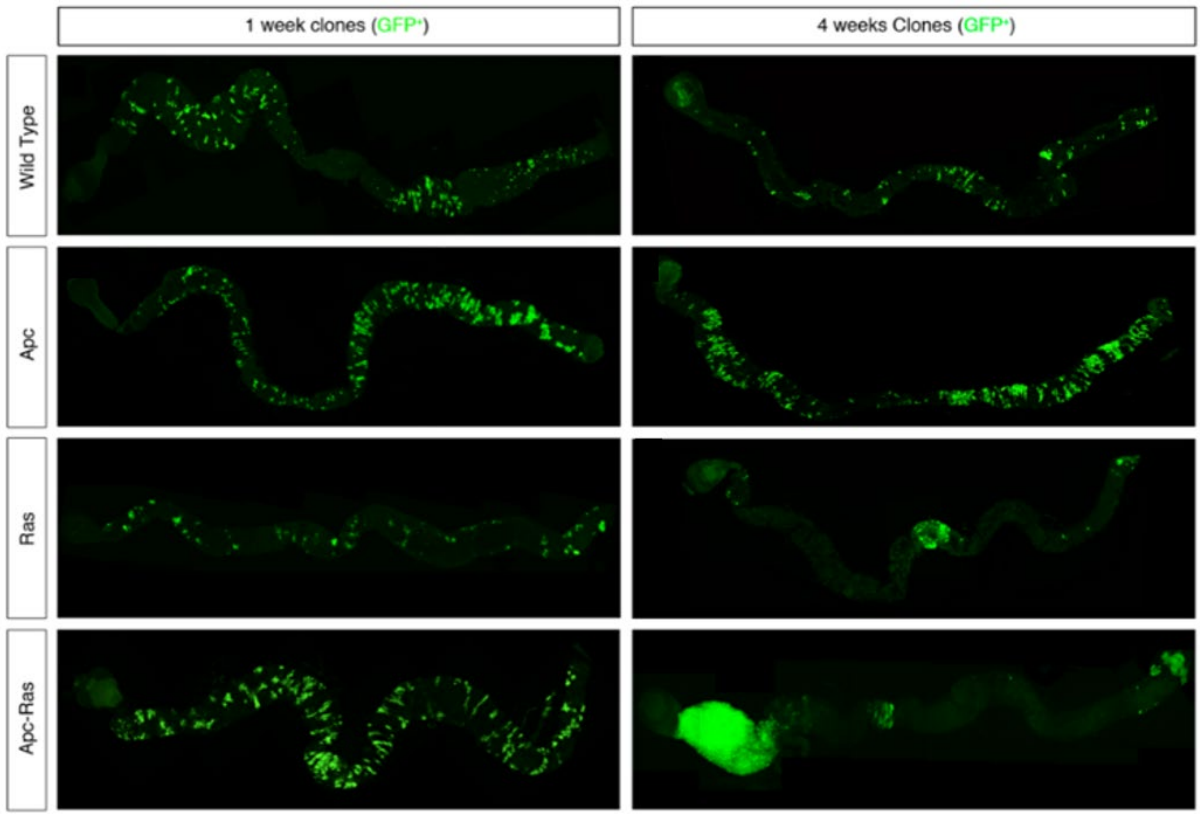

Figure 1.15. Comparison of clonal growth in WT, APC, Ras, and APC-Ras: Representative tile-scans of midguts dissected out and imaged, week 1 and 4 post clone induction. Through staining of Escargot<GFP, the APC-Ras model can be seen to exhibit more aggressive clonal growth than APC or Ras alone. Data derived from [165].

To investigate further progression to metastasis, a collaboration was shored up with our lab, whereby an additional UAS of the *Drosophila* ortholog *Snail* (*Snail1*) was added to the existing model [166]. This APC-Ras-Snail model (ARS) demonstrated aggressive primary tumour growth with a small minority of flies (1.2%) subsequently forming secondary tumours in the head, thorax, and abdomen (Fig.1.16A)

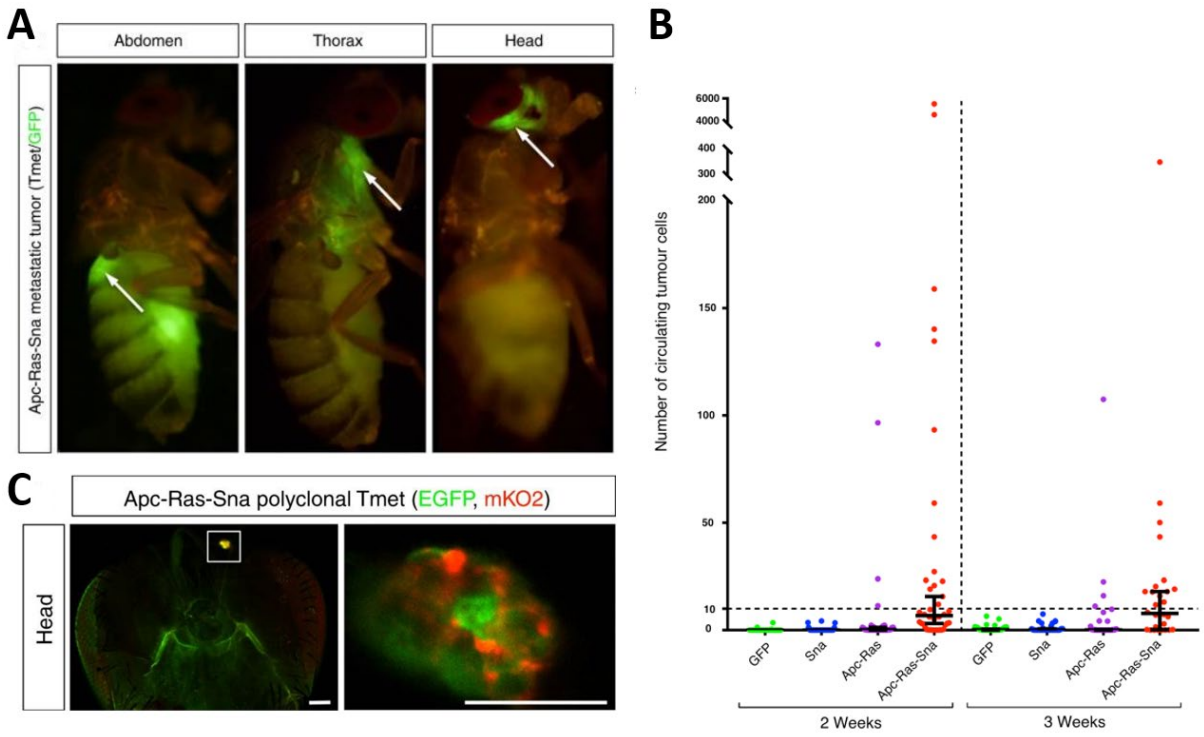

Figure 1.16. The APC-Ras-Snail model: (A) formation of GFP+ secondary tumours in the abdomen, thorax, and head of APC-Ras-Snail flies; **(B)** Comparison of CTCs per/fly of WT (GFP-only), Snail, APC-Ras, and APC-Ras-Snail flies, weeks 2 and 3 post clone induction; **(C)** Using the Brainbow cell-labelling technique [211], an RFP (mKO2) or GFP were stochastically expressed in separate clones following MARCM-mediated recombination. Presence of both RFP+ and GFP+ cells were observed in secondary tumours, suggestive of collective cell migration of polyclonal clusters. Data derived from [166].

Moreover, an UAS-Luciferase was inserted into the genetic cassette to quantify the number of CTCs in the haemolymph. By FACS sorting transformed clones and measuring their luciferase readouts, a strong linear correlation was found between the quantity of cells and the degree of luciferase activity ($r=0.9994$, $p=0.0006$) with a sensitivity down to the 10-cell level. Through this assay ARS flies were demonstrated to have far more CTCs compared to AR, with CTCs inferred to migrate out collectively as polyclonal populations of cells could be discerned in secondary tumours (Fig.16B-C). The sole cell-biological traits found to differentiate ARS from AR tumours were deterioration of the BM and the recruitment of tracheal tubules in ARS: the latter being reminiscent of cancer-induced angiogenesis (Fig.1.17). The encompassment of the entire metastatic cascade, high sample size, and genetic tractability sets ARS aside from the

difficulties faced by murine metastatic models. With the astounding similarities of the midgut to the human gut differentiating it from larval metastatic models.

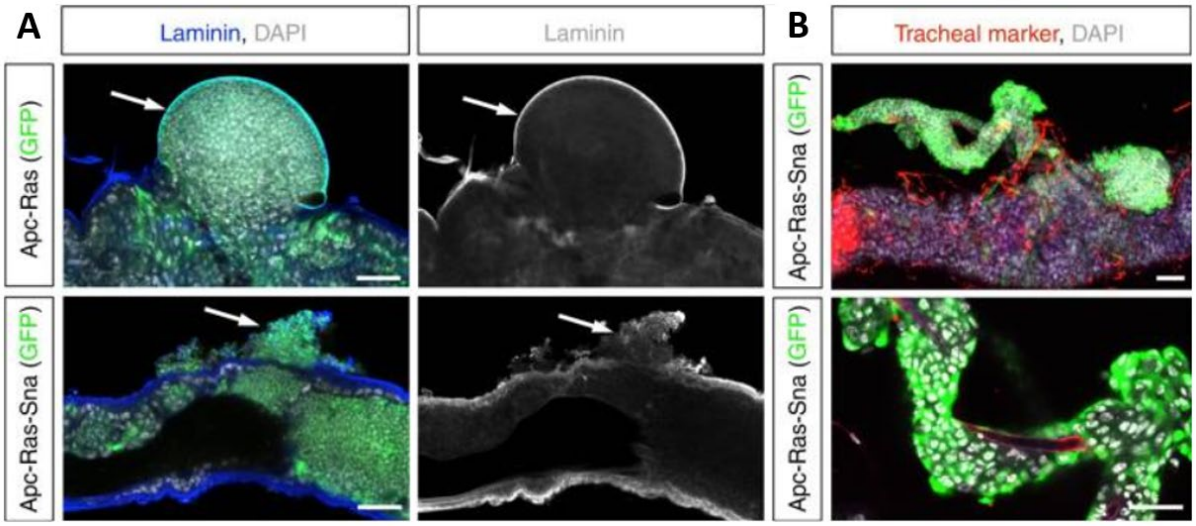

Figure 1.17. Previously identified differences between APC-Ras and APC-Ras-Snail tumours: (A) The BM becomes deteriorated in APC-Ras-Snail, but not APC-Ras, as determined by laminin staining; **(B)** ARS tumour cells invade onto tracheal tubules as determined by co-localization with the tracheal specific marker Chitin-Binding Protein (CBP). Data derived from [166].

Aims and Objectives

Despite the establishment of ARS as a metastatic model, little ground was made on understanding the mechanisms by which it carries out metastasis. ARS was determined to feature multiple metastatic characteristics including secondary tumour formation, dissemination, and destruction of the BM. Nonetheless, the overall metastatic phenotype remained largely a "black box" with little understanding of how these outcomes related to each other or fit in as part of a larger cancer progression scheme. As such the overall character and timing of the metastatic phenotype was unclear and if a mechanism were to be identified at a given time it would be difficult to infer its cause or outcome, and ultimately assign it to an underlying driver. Indeed, as it is the downstream drivers of EMT that have the most therapeutic potential, it is of interest to characterise the lower-order mechanisms by which *Snail* orchestrates metastasis, which in turn merits an ordering of the metastatic phenotype.

To this end I sought out to order the metastatic progression of ARS into a temporal map: delineating its outcomes and relating them to each other, while arranging them into a timeline. By defining the phenotype, I could then rationalize a subsequent characterisation of the behaviour of invasive tumour cells at appropriate timepoints. This would be performed through controlled comparison to AR as a negative control with the object of identifying potentially

casual downstream drivers. These drivers could then be validated by comparison of how the metastatic phenotype—and its previously defined parameters—change following genetic interrogation of said drivers. Given the critical role of cell polarity and ECM remodelling in cancer invasion, I hypothesized that these drivers would relate in some way to one or both of these features; with their loss resulting in diminished dissemination and secondary tumour formation. Should my research succeed, I would have made relevant progress in understanding how EMT drives metastasis: by clarifying its mechanisms and identifying downstream drivers with potential value as therapeutic targets.

My Aims

1. Order the metastatic progression of ARS flies into a timeline.
2. Identify candidate metastatic drivers by characterising the behaviour of invasive tumour cells.
3. Validate candidate metastatic drivers by genetic interrogation.

Chapter II

Materials and Methods

Materials

MATERIAL	SOURCE	IDENTIFIER
Fly Lines		
yw^{122},Hsp70-Flp;Escargot-GAL4,UAS-GFP, UAS-Ras^{V12}/Cyo;UAS-Luc, FRT82B, GAL80/TM6B	Created and supplied by Andreu Casali.	—
yw^{122}, Hsp70-Flp;Sp/CyO;FRT82B, APC^{Q8}, $APC2^{N175K}$/TM6B	Created and supplied by Andreu Casali.	—
yw^{122}, Hsp70-Flp;UAS-Sna^{45}/CyO; FRT82B, APC^{Q8}, $APC2^{N175K}$/TM6B	Created and supplied by Andreu Casali [165].	—
yw^{122}, Hsp70; Escargot-GAL4, UAS-GFP, UAS-Ras^{V12}, UAS-Sna^{45}; UAS-Luc, FRT82B, GAL80/TM6B	Created and supplied by Andreu Casali.	—
yw^{122}, Hsp70-Flp; If/Cyo; FRT82B/TM6B	Created and supplied by Andreu Casali.	—
yw^{122}, Hsp70-Flp; Escargot-GAL4, UAS-GFP/CyO; UAS-Luc, FRT82B, GAL80/TM6B	Created and supplied by Andreu Casali.	—
yw^{122}, Hsp70-Flp; UAS-Shg^{RNAi}/CyO; FRT82B, APC^{Q8}, $APC2^{N175K}$/TM6B	Created and supplied by Andreu Casali.	—
yw^{122}, Hsp70-Flp; UAS-ADAMTS-A^{RNAi}/CyO; FRT82B, APC^{Q8}, $APC2^{N175K}$/TM6B	Created and supplied by Andreu Casali.	—
Oregon-R Wild Type Flies	Supplied by the University of Sheffield Fly Facility	—
***Drosophila* Foodstuffs**		
Medium Cornmeal	Manufactured by Triple Lion Supplied by Lembas/Easton Enterprise	—
Dried Yeast	Manufactured by Kerry Ingredients Supplied by Regina	—
Agar	Supplied by Regina	—
Granulated Sugar	Supplied by Silver Spoon	—

Soya Flour	Supplied by Lembas	—
Malt Extract	Supplied by Rayners Essentials	—
Molasses	Supplied by Rayners Essentials	—
Nipagin (Methyl-4-Hydroxybenzoate)	Thermo Fischer Scientific	CAS: 99-76-3
Propionic Acid	Thermo Fischer Scientific	CAS: 79-09-4
Microscopes		
Zeiss Axio Zoom.V16 Fluorescence Stereo Zoom Microscope	Zeiss	—
Zeiss LSM780 Confocal Microscope	Zeiss	—
Devices		
Varioskan LUX Multimode Plate Reader	Thermo Fischer Scientific	—
Reagents		
Paraformaldehyde Reagent Grade Crystalline	Sigma Aldrich	CAS: 30525-89-4
Triton X-100 Detergent	Biorad	Cat No: 1610407
Bovine Serum Albumin Powder	Merck	Cat No: 810037
Corning Phosphate Buffered Saline, 1x without calcium and magnesium, pH 7.4 ± 0.1	Corning	Cat No: 21-040-CM
Vectashield Antifade Mounting Medium	Vector Labs	Cat No: H-100-10
Poly-L-Lysine 0.01% (w/v) in H_20	Sigma Aldrich	Cat No: P8920
Primary Antibodies/Stains		
Rabbit Polyclonal Anti-GFP	ChromoTek	Cat No: pabg1
Goat Polyclonal Anti-GFP	Abcam	RRID: ab6673
Goat Polyclonal Anti-GFP	Rockland	Cat No: 600-101-215
Invitrogen™ DAPI (4’,6-Diamidino-2-Phenylindole, Dihydrochloride)	Thermo Fischer Scientific	Cat No: D1306
Rabbit Polyclonal Anti-Serpent	Gift from D.Hoshizaki.	[167]
Rabbit Polyclonal Anti-Laminin	Abcam	RRID: ab47651
Rabbit Polyclonal Anti-ADAMTS-A	Gift from D.Andrew	[168]
Rabbit Polyclonal Anti-PDM1	Gift from C.Yu	—
Mouse Monoclonal Anti-Prospero	DSHB	Cat No: MR1A
Mouse Monoclonal Anti-BPS	DSHB	Cat No: CF.6G11
Phalloidin-TRITC	Sigma Aldrich	Cat No: P1951
Mouse Monoclonal Anti-DLG	DSHB	Cat No: 4F3
Mouse Monoclonal Anti-Talin	DSHB	Cat No: A22A
Mouse Monoclonal Anti-Talin	DSHB	Cat No: E16B

Rabbit Polyclonal Anti-Mesh	Gift from M.Furuse	[169]
Rat Monoclonal Anti-E-Cadherin	DSHB	Cat No: DCAD2
Secondary Antibodies		
Donkey Anti-Goat IgG (H+L) Alexa Flour 488	Thermo Fischer Scientific	Cat No: A-11078
Donkey Anti-Rabbit IgG (H+L) Alexa Flour 488	Thermo Fischer Scientific	Cat No: A32790
Donkey Anti-Mouse IgG (H+L) Alexa Flour 555	Thermo Fischer Scientific	Cat No: A-31570
Donkey Anti-Rat IgG (H+L) Alexa Flour 555	Thermo Fischer Scientific	Cat No: A78945
Donkey Anti-Rabbit IgG (H+L) Alexa Flour 647	Thermo Fischer Scientific	Cat No: A-31573
Donkey Anti-Mouse IgG (H+L) Alexa Flour 647	Thermo Fischer Scientific	Cat No: A-31571
Commercial Assay Kits		
Luciferase Assay System	Promega	Cat No: E4530
Software		
Prism 10	GraphPad	https://www.graphpad.com/
Photoshop 2023	Adobe	https://www.adobe.com/products/photoshop.html
Fiji-ImageJ 64bit for Windows	Fiji	https://imagej.net/software/fiji/
Excel 2021	Microsoft	https://www.microsoft.com/en-us/Microsoft-365/excel

Methods

Genetic Crosses

In order to generate appropriate genotypes for experimental study, double-balanced (CyO/TM6B) primary stocks were crossed at a ratio of 20 female virgins to 7 males and kept at 25°C. Progeny of the desired genotype were then selected 17 days later, on the basis of being negative for the CyO/TM6B markers. The specific primary crosses required to generate the following genotypes is provided below:

- **GFP-Labelled Wild Type Control:** Virgins from yw122, Hsp70-Flp; Escargot-GAL4, UAS-GFP/CyO; UAS-Luc, FRT82B, GAL80/TM6B were crossed to males from yw122, Hsp70-Flp; If/Cyo; FRT82B/TM6B.
- **APC-Ras:** Virgins from yw122, Hsp70-Flp; Escargot-GAL4,UAS-GFP, UAS-RasV12/Cyo;UAS-Luc, FRT82B, GAL80/TM6B were crossed to males from yw122, Hsp70-Flp;Sp/CyO;FRT82B, APCQ8, APC2N175K/TM6B.

- **APC-Ras-Snail:** Virgins from yw122, Hsp70-Flp; Escargot-GAL4, UAS-GFP, UAS-RasV12/Cyo;UAS-Luc, FRT82B, GAL80/TM6B were crossed to males from yw122, Hsp70-Flp;Sp/CyO;FRT82B, APCQ8, APC2N175K/TM6B.
- **APC-Ras-Shg^{RNAi}:** Virgins from yw122, Hsp70-Flp; Escargot-GAL4,UAS-GFP, UAS-RasV12/Cyo;UAS-Luc, FRT82B, GAL80/TM6B were crossed to males from yw122, Hsp70-Flp; UAS-ShgRNAi/CyO; FRT82B, APCQ8, APC2N175K/TM6B.
- **APC-Ras-ADAMTS-A^{RNAi}:** Virgins from yw122, Hsp70-Flp; Escargot-GAL4,UAS-GFP, UAS-RasV12/Cyo;UAS-Luc, FRT82B, GAL80/TM6B were crossed to males from yw122, Hsp70-Flp; UAS-ADAMTS-ARNAi/CyO; FRT82B, APCQ8, APC2N175K/TM6B.
- **APC-Ras-Snail-ADAMTS-A^{RNAi}:** Virgins from yw122, Hsp70; Escargot-GAL4, UAS-GFP, UAS-RasV12, UAS-Sna45; UAS-Luc, FRT82B, GAL80/TM6B were crossed to males from yw122, Hsp70-Flp; UAS-ADAMTS-ARNAi/CyO; FRT82B, APCQ8, APC2N175K/TM6B.

Fly Husbandry

Primary fly stocks were kept in a controlled culture room at 25°C and 70% relative humidity with a 12-hour light and dark cycle. These flies were fed standard fly medium provided by the University of Sheffield Fly Facility, that contains: 1liter cold tap water, 80g medium cornmeal, 18g dried yeast, 10g soya flour, 80g malt extract, 40g molasses, 8g agar, 25ml of 10% nipagin in absolute ethanol and 4ml propionic acid. These stocks were maintained by tipping flies into fresh bottles of food every week and discarding old bottles every 21 days.

Experimental genotypes derived from crossed primary stocks were kept in a 25°C incubator and fed a high-protein fly medium composed of: 80g dried yeast, 61.2g medium cornmeal, 129.4g granulated sugar, 9.3g agar, 11.25ml nipagin, and 4ml propionic acid. These raw ingredients were mixed with 1liter of boiling water on a hotplate put on full heat and then dispensed into stock vials at a volume of 25ml per vial. The flies were then tipped onto fresh food every three days to prevent flies succumbing to infection or drowning in their food.

Clone Induction

Temporal control of clone induction relied on MARCM mediated recombination through activation of a temperature sensitive heat shock promoter. To this end female experimental flies were housed in stock vials at a ratio of 20 flies per vial and kept in a 37°C incubator for 1hr to

drive clone induction. Flies were then tipped onto fresh standard fly medium and then after 24hrs tipped onto high-protein fly medium.

Lifespan Assay

For analysis of lifespan, a total of 200 female ARS flies were screened for fly death on a daily basis over a range of 30 days. Females were partitioned into groups of 20 flies per vial and housed with 7 males to ensure mating. They were tipped onto fresh food every two days to rule out death by food infection or drowning in the food. Fly death was assessed based on flies laying immobile, shrivelled, and sunken in the food.

Luciferase Assay for CTC measurements

To quantify CTCs, measurements of Relative Luminisicent Units (RLUs) are made of the haemolymph isolated from flies. Measurements of haemolymph RLUs was initially performed using a centrifuge dependent protocol involving: gently puncturing the surface of the fly cuticle between the abdomen and thoracic cavity, directly underneath the haltere using a tungsten needle. Then transferring individual punctured flies into their own 0.5ml Eppendorf tubes fitted within larger 1.5ml Eppendorf tubes. A hole is pierced into the base of the smaller tube using a tungsten needle, then subjected to centrifugation at 5000g for 5 mins to drain the haemolymph from the fly and filter it into the larger Eppendorf. The haemolymph of individual flies are then loaded onto their own wells in a 96-well microplate, with each well being incubated with 10µl luciferase reporter lysis buffer. Each well is subsequently incubated with 50µl luciferin substrate for 5mins followed by positioning of the microwell plate onto a Varioskan Microplate reader for quantification of RLUs. This method was used to generate the data for Fig.3.4B.

All other experiments involving measurements of CTCs were performed using a second later method. This method is similar to the centrifugal method, only after the thorax is pierced with a tungsten needle, the haemolymph is extracted using a makeshift suction tube composed of a thin capillary needle fixed to the end of a silicon tube; with the other end coupled to a pipette tip. The needle is gently inserted through the surface of the haemocoel; capillary action then suctions the haemolymph into the needle. By blowing out through the pipette tip on the other end, the haemolymph is passaged into the microwell plate. The plate is then prepared and quantified for RLUs using the same parameters as the centrifugal dependent method.

Luciferase Assay for Tumour Burden measurements

To measure the flies tumour burden, quantifications were made of the RLUs from the flies whole-body homogenate. To do this, flies were homogenized using a pipette tip with the resulting homogenate of individual flies then passaged onto their own wells in a 96 micro-well plate. Each plate was then incubated with 20µl of reporter lysis buffer which in turn was incubated with 50µl of luciferin substrate for 5min followed by positioning into a Varioskan Plate Reader for quantification of RLUs.

Extraction of Cells from the Haemolymph and Immunocytochemistry

To extract Escargot+ cells from the haemolymph, the thorax of flies were punctured with a tungsten needle. The haemolymph was then extracted from the haemocoel using a capillary needle and dispensed onto a slide coated with 0.01% (w/v) Poly-L-Lysine in H_20. Cells were then given 5mins to adhere to the Poly-L-Lysine followed by fixation with PFA (4% diluted in PBS) for 5mins. The cells were subsequently permeabilized and blocked by washing the slide with PBST-BSA (4% BSA, 0.1% Triton X-100) four times with a 15min incubation period for each wash. Cells were then stained for GFP (1:500), Serpent (1:200), and DAPI (1:250), kept in PBST-BSA solution at 4°C overnight. The following day the slide was washed three more times at 15min intervals, then stained with appropriate secondary antibodies at a 1:100 concentration and incubated for 2hrs at room temperature on a roller. Finally, the slides were mounted with vectashield mounting medium and imaged under the confocal.

Screening for Secondary Tumours

To screen for secondary tumours, wholebodied flies were anesthetized on a C02 pad and screened for visible GFP+ punctate under a fluorescent stereoscope. As the midgut spans from the lower abdomen to the upper boundary of the thorax, these punctate could be sizeable primary tumours of the gut. Therefore, the guts and cuticle of these flies were dissected out and exposed to determine if the GFP+ signature derives from a primary tumour on the gut or a secondary tumour on the cuticle. GFP+ punctate in the head and appendages of flies were recorded as secondary tumours without dissection.

Histology

Flies were anesthetized on a C02 pad then positioned on a microscope slide coated with PBS. The entire gastrointestinal tract of flies were then dissected out using forceps under a light

microscope. Subsequently, guts were fixed by passaging them into an Eppendorf composed of 8% PFA diluted in 1x PBS, where they were incubated on a rocker for 1hr. Guts were then permeabilized and blocked by washing and incubating the guts in PBST-BSA (4% BSA, 0.1% Triton X-100) four times at 15min intervals. The guts were then stained by incubation with primary antibody in PBST-BSA solution overnight at 4°C. The following day, guts were washed with PBST-BSA three more times at 15min intervals, then stained with secondary antibody in PBST-BSA for 2hrs at room temperature on rocker. Finally, guts were mounted on a slide with Vectashield mounting medium.

All guts were stained with appropriate secondary antibodies at a 1:100 concentration. Primary antibodies and stains were in the following concentration: GFP (1:500), DAPI (1:250), Laminin (1:1000), ADAMTS-A (1:250), PDM1 (1:500), Prospero (1:50), BPS (1:20), Phalloidin (1:500), DLG (1:100), Talin (1:20), Mesh (1:500), and E-Cadherin (1:50).

Quantification of GFP% Coverage of the Gut Area

To perform GFP% coverage quantifications, guts were first dissected out and stained for GFP, as well as the visceral muscle using a Phalloidin stain to delineate the boundaries of the gut. Tile-scans were then taken along the entire anterior-posterior axis of the gut at a 10x objective. Z-Stacks were taken past the far ends of the visceral muscle on both sides of the sagittal axis at a 10µm interval. Subsequent .tiffs were then exported onto ImageJ for analysis. Boundaries were drawn around the midgut specifically and used to clear Malpighian tubules from the image. A previously established script was then run to quantify the GFP% coverage of the remaining area on the image. For more information the script and an accompanying tutorial can be found here: https://github.com/Jadams94/AutomatedGutQuant

Quantification of the Regionalization of GFP+ Areas

To quantify the regionalization of GFP+ areas, .tiffs derived from tile-scanned midguts were duplicated 4 times producing a total of 5 equivalent images. Each image was then assigned its own region of the gut—representing the R1-R5 regions—by drawing a boundary along that region and clearing out the other regions. Quantification of GFP area was then performed using a previously established script and regions were measured for GFP area as a percentage of the net GFP area. For more information the script and an accompanying tutorial can be found here: https://github.com/Jadams94/AutomatedGutQuant

Microarray Gene Expression Analysis

Microarray was performed in a prior study, methods are described in Campbell, 2019 [166].

Statistical Analysis

RLU assay results were compared using Two-Tailed Mann-Whitney and presented as Log2 values with median and interquartile range. GFP+ quantifications were compared using Two Tailed T-Test and presented as Log2 values with mean and interquartile range. Normality was assessed by Q-Q plots and testing using Shapiro Wilks and Kolmogorov-Smirnov. Statistical significance was measured using P values: (ns) represents no significance, (∗) represents < 0.05; (∗∗) represents < 0.01, (∗∗∗) represents <0.001, (∗∗∗) represents < 0.0001. All tests and graphs were performed and created on GraphPad Prism 10.

Chapter III

Ordering the Metastatic Progression of ARS Flies into a Timeline

Introduction

EMT has long been conceived to facilitate metastasis by clearing a path for the dissemination of a large quantity of CTCs, which can only occur when tumours have grown large enough to populate a great number of cells. Indeed, this assumption is upheld in experimental studies with mice where injection of copious quantities of CTC are required for macrometastases to form [170, 171, 172]. However, decades of clinical results demonstrate that considerable quantities of CTCs can be recorded from patient liquid biopsies, even at early stages of tumour development years before any discernible secondary tumour formation [173] Put together these findings suggest that not all CTCs are equal. Emerging research suggests there's a subset of CTCs endowed with unique properties befit for the formation of macrometastases at foreign environments [174]: it is likely these cells develop more frequently at later timepoints, and that very large quantities are therefore required at earlier stages to capture sufficient quantities of this subtype.

The inability of most CTCs to seed secondary tumours likely relates to the circulation being a harsh environment with physical disruption from shear stress and elimination by surveilling immune cells representing formidable challenges [175]. A characterisation of CTCs extracted from patients and animal models reveals both single and collective forms of CTCs. The collective clusters—likely derived from P-EMTs—are much rarer, comprising 1-17% of CTCs [174]. However, they associate more strongly with secondary tumour formation: with injected clusters carrying a 20-500-fold increase in macrometastasis in mouse models of melanoma, breast, and colon cancer [176]. Experimental evidence suggests that these clusters increase survival in transit by forming an outer surface of cells that shield the inner cells from the stressors of the circulation and engender evasion from circulating immune cells [177].

Moreover, collective clusters have been found to be enriched in markers of Cancer Stem Cells (CSCs): a cell type with unique efficiency at seeding secondary tumours [178]. These cells associate with EMT and possibly only become prevalent late in tumour development. Put together these findings underscore an association between later stages of tumour development, CTC dissemination, and subsequent secondary tumour formation. However, this relationship is more complex than just increased tumour growth and proportional dissemination, with the character of late stage disseminating cells likely to play an important role.

When the ARS model was first established, a very cursory suggestion of cancer progression was put forth. Many ARS flies could be seen to survive even after four weeks, with the

percentage of flies exhibiting >10 CTCs in the haemolymph—as well as the quantity of CTCs per/fly—increasing each week (Fig.3.1) However, the full range of cancer progression, including a daily longitudinal analysis of other important parameters such as tumour size and fly survival, was never established. Nor was the quantity or timing of CTCs related to the incidence of secondary tumour formation: which although determined to occur at a low rate of 1.2% was never situated within a timeline.

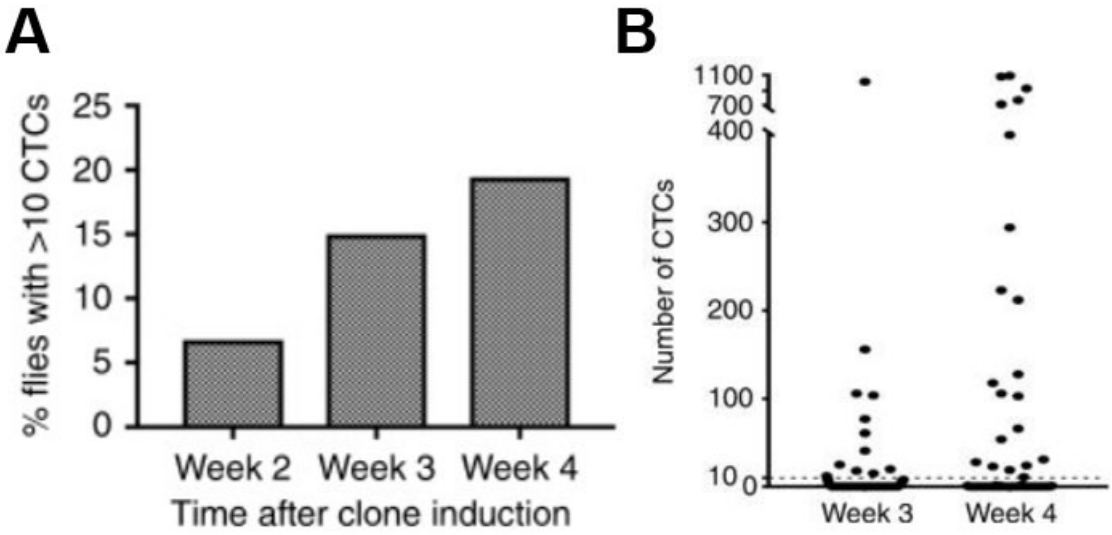

Figure 3.1.Timing of ARS mediated dissemination: (A) percentage of ARS flies with over 10 CTCs recorded from extracted haemolymph, weeks 2, 3 and 4 post clone induction; **(B)** Number of CTCs recorded from the extracted haemolymph of individual flies, weeks 3 and 4 post clone induction. Data derived from [166].

In order to study the biology of primary tumour cells undergoing EMT and identify downstream drivers, it is advantageous to first establish where and when the key outcomes of metastasis occur such as to establish relevant analysis points and a reference frame for relating events. To this end a larger cancer progression scheme should be established, to which metastatic events can be ordered in as points of interest. Recently a new high protein fly food diet has been utilised with the potential of accelerating cancer progression and thus abridging all events into a narrower timespan for study. Therefore, the first objective of this project aimed to arrange key parameters of cancer progression, in particular metastasis, into a sequence of events using this newly developed diet. Moreover, given the suggested potential of late-stage collective clusters in forming secondary tumours; additional care was taken to further investigate the association between metastatic progression and CTC subtypes, while if possible, orienting that within a timeline.

Results

ARS Cancer Progression Occurs Within a Standard Range of 14 Days.

To gain an indication of the range of the cancer progression timeline on the new diet, a lifespan assay was performed on 200 flies kept at 25°C, with recordings of fly death made each day from the point of clone induction. Results reveal that there is an initial steady decrease in fly survival. However, by the second week, a sharp decrease in fly survival is observed with 50% of flies dying by Day 16 and 75% dying by Day 20 (Fig.3.2A). To determine if the drop-off in fly survival associates with tumour size, whole-bodied flies were homogenized and measured for their luciferase readouts—their Relative Luminescent Units (RLU)—to acquire a measure of full-body tumour burden (TB). By analysing multiple individual flies, per day post-clone induction (PCI), for the duration of 14 days, a pattern emerges: the mean TB rises sharply up until Day 10, where it reaches its maximum, then flatlines until Day 13, after which it drops down (Fig.3.2B). Given the exponential decrease in fly survival occurring in the third week PCI, it is likely that the decrease in mean TB is a result of the flies with the most aggressive tumour growth dying. Put together, a standard progression scheme can be conceived whereby for most flies the whole-body tumour burden increases aggressively over the first two weeks ultimately resulting in mortality. The establishment of a 14-day cancer progression timeline, suggests that flies should be screened and studied for metastatic phenotypes within those days.

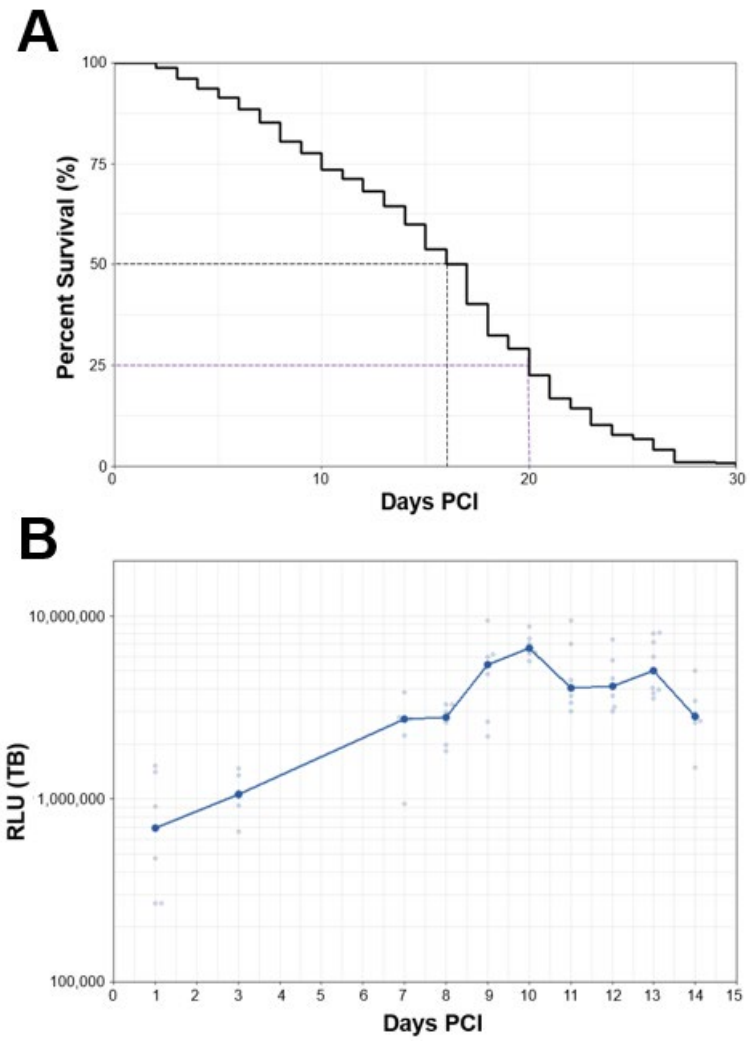

Figure 3.2: (A) Lifespan curve of ARS flies analysed for 30 days PCI, n=200; **(B)** Curve of ARS flies analysed for tumour burden in the days 1-14 PCI, N=60 - Light blue dots indicate individual flies, dark blue dots indicate the means. All flies were kept at 25°C. Experiments performed and shared by permission of Jason Morgan.

The Full Metastatic Process is Completed by Only a Very Small Percentage of Flies Within a Range of 7 Days.

When the ARS model was first developed, 1.2% of flies were documented to develop secondary tumours. To determine if this frequency holds on the new diet, flies were screened for secondary tumours within the established range of 1-14 Days PCI. A slightly higher rate of 2.17% of flies could subsequently be observed to develop tumours in diverse tissues such as the brain, thoracic cuticles, and appendages, with some flies forming multiple simultaneous tumours at different tissues (Fig.3.3B-E). Moreover, as the timing of macrometastasis was never previously determined, flies were also charted for the incidence of secondary tumour formation. Secondary tumour were observed to form even as early as Day 3 PCI, with the highest frequency of secondary tumours centring around Day 6 PCI (Fig.3.3A). This data

implies that tumours typically require just under a week's time to acquire the requisite changes needed to undergo the full process of metastasis. Moreover, this frequency distribution establishes Day 6 PCI as an important reference point for working backwards and establishing the preceding events leading up to macrometastasis.

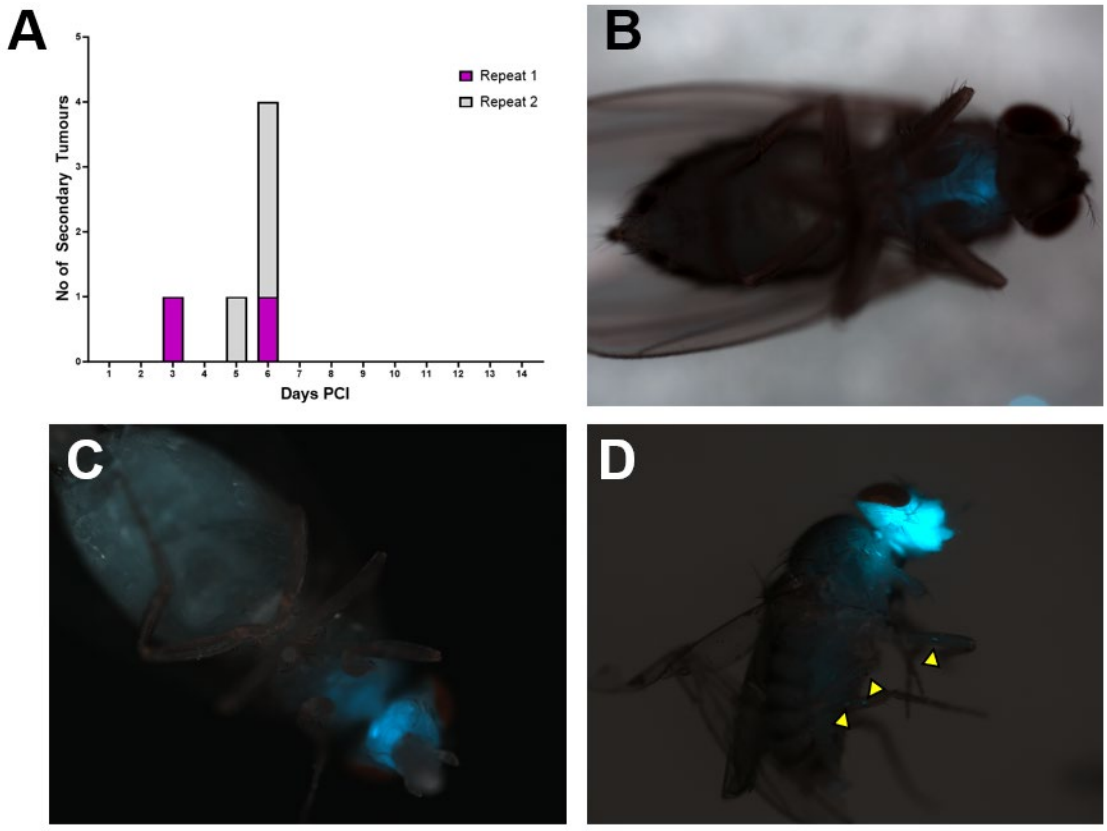

E

Genotype	Flies Screened	No of Mets	%
ARS	230	5	2.17

Figure 3.3: (A) Stacked bar-chart frequency distribution of ARS flies with secondary tumour formation in the days 1-14 PCI. Repeat 1 (n=120), Repeat 2 (n=110); **(B)** Representative image of fly with thoracic metastases; **(C)** Representative image of fly with brain metastases; **(D)** Representative image of fly with multiple metastases (yellow arrows indicates metastatic lesions forming on the appendages); **(E)** Summary table of flies screened, and metastases recorded. All flies were kept at 25°C. Screen performed and shared by permission of Jamie Adams.

ARS Flies Exhibit Increased Dissemination Compared to AR, Although CTC Quantity Can Not Be Correlated to Secondary Tumour Formation.

In order for cancer cells to form secondary tumours they must first exit the gut. As ARS flies metastasize, and AR flies do not, it can be reasoned that this difference derives from a much

greater quantity of tumour cells exiting the gut of ARS flies compared to AR. Although, ARS flies were previously established to harbour more CTCs, a comparison was never made at the time of secondary tumour formation. Therefore, 24 individual AR and ARS flies were compared for CTC quantity, Day 6 PCI, with an additional comparison made to WT (GFP<Escargot) flies as a negative control. AR flies were found to possess a significantly higher concentration of CTCs compared to the WT control, with ARS exhibiting an even more dramatic enrichment compared to AR. Moreover, to assess the possibility of there being Escargot+ cells in the haemolymph of WT flies, independent of endogenous luciferase activity, another comparison was made to OregonR WT flies carrying no UAS-Luciferase, and a much lower quantity of CTCs could be discerned compared to the GFP control (Fig.3.4A).

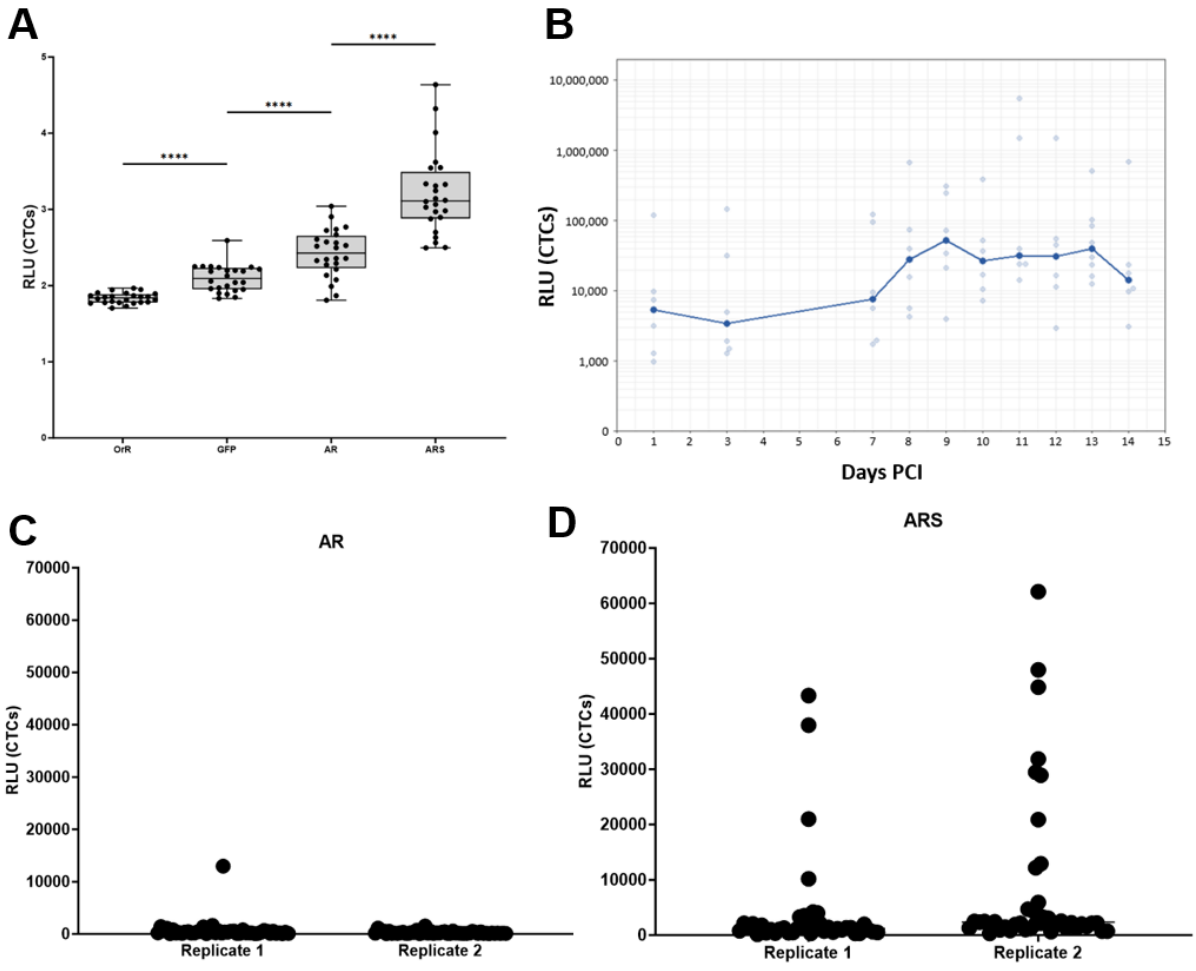

Figure 3.4: (A) Quantifications of CTCs per/fly of the indicated genotypes performed Day 6 PCI, n=24 per genotype, values in Log2 scale; **(B)** Curve of individual ARS flies quantified for CTCs in the days 1-14 PCI, n=62, values in raw units, light blue dots indicate individual fly values, dark blue dots indicate the mean: **(C)** Scatterplot of CTC values derived from individual AR flies, replicate 1 (n=45), replicate 2 (n=48), values in raw units; **(D)** Scatterplot of CTC values derived from individual ARS flies, replicate 1 (n=45), replicate 2 (n=41), values in raw units. Statistical comparison of (A) was made by Two-Tailed Mann-Whitney presented as median with interquartile range. $*p < 0.05$; $**p < 0.01$; $***p < 0.001$, $**** p < 0.0001$. All flies were kept at 25°C. Data for (A) was performed and shared by permission of Jamie Adams; Data for (B) was performed and shared by permission of Jason Morgan.

As only 2.17% of flies form secondary tumours, it is possible that there is a small subpopulation of ARS flies that possess disproportionally high CTCs: such a distribution would unlikely be captured by a sample size of 24 flies. Therefore, an additional comparison was made between 80+ AR and ARS flies. Results reveal that AR flies have a much narrower distribution of CTC values (Fig.3.4C). Whereas 5-10% of ARS flies exhibit far higher quantities of CTCs than the rest of the population: an attribute which can easily be identified by simple visual inspection of raw values (Fig.3.4D). It is plausible that this subset of flies are the ones that have the potential of forming secondary tumours.

With secondary tumours developing no later than Day 6 PCI, it can be hypothesized that mean CTC values rise in the days leading up to macrometastasis, and then decline from there. To assess this, individual ARS flies were measured for CTCs on daily intervals within the Days 1-14 PCI. Unlike the mean TB, which rises sharply from the onset of clone induction, mean CTC quantities remain at a consistent level for the first week. However, from there it follows a comparable trajectory, rising to a maximum upon Day 9 PCI—a day before the mean TB peaks—then similarly proceeding to stagnate until Day 13 PCI, where it undergoes rapid decline (Fig.3.4B). Like the decrease in TB, this is likely attributable to the exponential decrease observed in fly survival: with the death of flies with the most aggressive cancer growth being likely to lower the mean CTC values. Importantly, the finding that mean CTC values are higher after macrometastasis has occurred, contradicts with the theory that secondary tumour formation is a function of increased CTC quantity. If true, there would be no rationale to suspect that the rare subpopulation of flies with higher CTCs underlie secondary tumour formation. Although, given the increasing association of CTC subtypes and metastatic potential, it is possible that only select CTCs with specific properties are capable of seeding macrometastases.

The Haemolymph is Enriched in Single and Collective CTCs at the Time of Macrometastasis.

To assess if macrometastasis associates with different CTC subtypes, cells were isolated from the haemocoel of 30 ARS flies, Day 6 PCI, using a capillary needle and plated on a Poly-L-Lysine coated slide. These cells were then stained with an anti-GFP antibody and DAPI to mark the cells. Additionally, a Serpent stain was included to determine if there are tumour cells that have been phagocytosed by surveilling immune cells. By subsequent imaging through confocal, three cell populations could be discerned: (1) collective clusters containing 20+ cells; (2) single cells; and (3) Serpent+ cells (Fig.3.5). Interestingly, Serpent never colocalized with

collective clusters, suggesting this migration mode may confer resistance to immune surveillance. Put together these results demonstrate that there are single and collective CTCs in the haemolymph at the time of metastasis. To gain a firmer suggestion of whether these collective clusters underlie the incidence of macrometastasis occurring in earlier days, it would be interesting to extract cells from later days when CTCs are higher, but secondary tumours do not form.

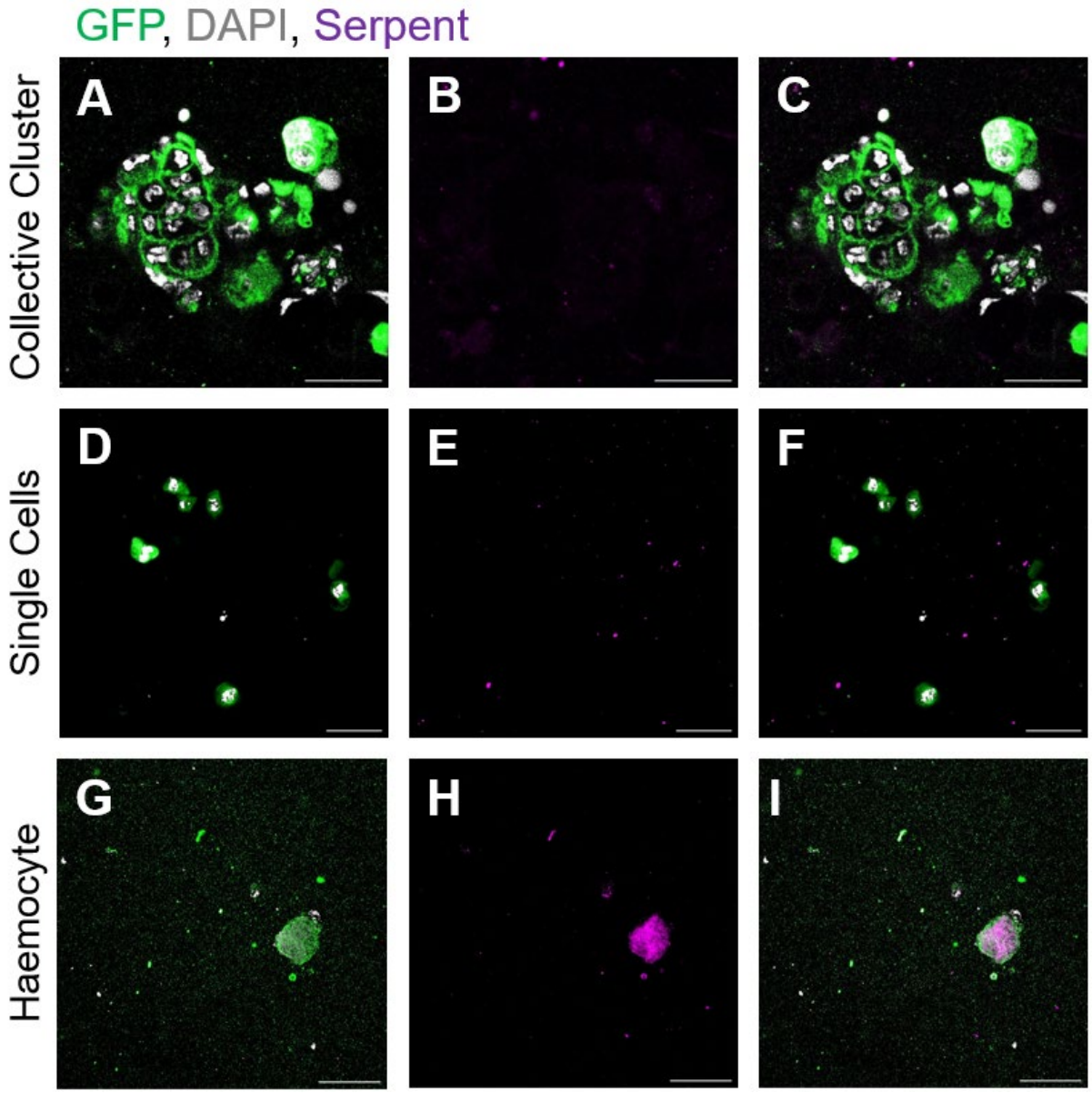

Figure 3.5: (A-C) Representative image of CTC cluster. N=5. Scale bar=20µm; **(D-F)** Representative image of Single CTC. N=5. Scale bar=20µm; **(G-I)** Representative image of Haemocyte. N=5. Scale bar=40µm. Cells are derived from the haemocoel of ARS flies Day 6 PCI, kept at 25°C. Immunostains include GFP (green), nuclei (grey), and Serpent (magenta). Experiments performed and shared by permission of Jamie Adams.

Discussion

The results detailed within this chapter have established a standard 14-day long ARS cancer progression scheme, with TB increasing aggressively over time ultimately coinciding with an exponential decrease in fly survival. Moreover, a very small percentage of flies—2.17%—undergo the full spectrum of metastasis, entirety within six days and no later. Curiously, CTC quantity can be seen to consistently hoover around a low range of values within the first week, only rising to higher levels after macrometastasis has occurred. Combined with the isolation of different CTC subtypes from the haemolymph, this raises the question: is secondary tumour formation a function of CTC quantity or CTC quality?

At face value, the absence of secondary tumours on later days when CTCs are higher would suggests its unrelated to CTC quantity. However, it is possible that as the TB is higher at later days, flies will have died off before secondary tumours can form, even though the higher CTC bearing flies in principle have more potential for forming macrometastases. Moreover, with larger sample sizes, a small subpopulation of flies could be discerned with far higher levels of CTCs: it is conceivable that this subgroup encompasses the flies with the potential of forming secondary tumours, as they may have enough CTCs, but not high enough a TB to die before they can complete metastasis.

This subpopulation—which encompasses 5-10% of flies—is far higher than the 2.17% that from secondary tumours, although this may be explained by: (1) only the most extreme outliers forming secondary tumours; and/or (2) a larger proportion forming micrometastases, unobservable by stereoscope, with only a few transitioning into macrometastases. However, as flies can undergo macrometastasis within 6 days of clone induction, it does raise the question of why flies with far higher CTCs are unable to form macrometastases, when there is over a week before mean CTC values and fly survival begin to undergo exponential decline. This suggests there may be a requirement that CTCs possess particular properties endowing them with the capacity to colonise and grow at distant sites.

Regardless, it is clear that only a select few tumours acquire the necessary changes to disseminate the appropriate CTCs befit for the formation of secondary tumours. This likely occurs through the action of critical drivers occurring uniquely within those invasive tumours. To test this hypothesis, those drivers would need to be identified and targeted. The assays utilised in this chapter can then be repeated using the same parameters to test the metastatic

potential of those drivers. Identifying targets requires a characterisation of the behaviour of invasive tumour cells.

Chapter IV

Dysregulation of E-Cadherin, Laminin, and ADAMTS-A Differentiate Metastatic Tumours from the Benign

Introduction

The midgut has surfaced as a powerful system for studying the molecular control of tissue architecture [179, 180, 181]. Composed of single epithelial, BM, and muscle layers comprised of a few genetically redundant cell types; it makes a good system for dissecting how tissues arrange and maintain specialized cells as functional organ constituents. Moreover, as 90% of cancers derive from solid organs, the midgut holds promise for examining how the boundaries that hold and restrain tissues together become breached during metastatic outgrowth [182].

A prominent regulator of tissue integrity is cell polarity and attendant cell adhesion. The midgut comprises a columnar pseudostratified epithelium with differentiated cells possessing apico-basal polarity (Fig.4.1A). Their basal end is composed of integrins which associate with laminin, to which they require coupling to intracellular actin through the adaptor proteins Rhea (Tallin) and Fit1/2 (Kindlin) [179]. The lateral end features the homotypic interaction of adherens junctions (AJs) and septate junctions (SJs): the invertebrate homolog of tight junctions (TJs). Unlike other *Drosophila* epithelia, the midgut SJs localize superior to the AJs at the subapical domain: demonstrating unique conservation with the arrangement of TJs in mammalian tissues [179]. The apical end is defined by the brush border: a network of intracellular F-Actin harboured within the apical microvilli of ECs. Together, the underlying basement membrane and overlying brush border allow epithelia to encase themselves within a self-contained layer, with the brush border producing a characteristic serrated appearance when stained with F-Actin (Fig.4.1B). Unlike the differentiated cells, the ISCs lack apico-basal polarity possessing a more rudimentary polarity with a cone shaped morphology and a basal-lateral division defined by integrins and AJs, but no SJs or assignable apical domain.

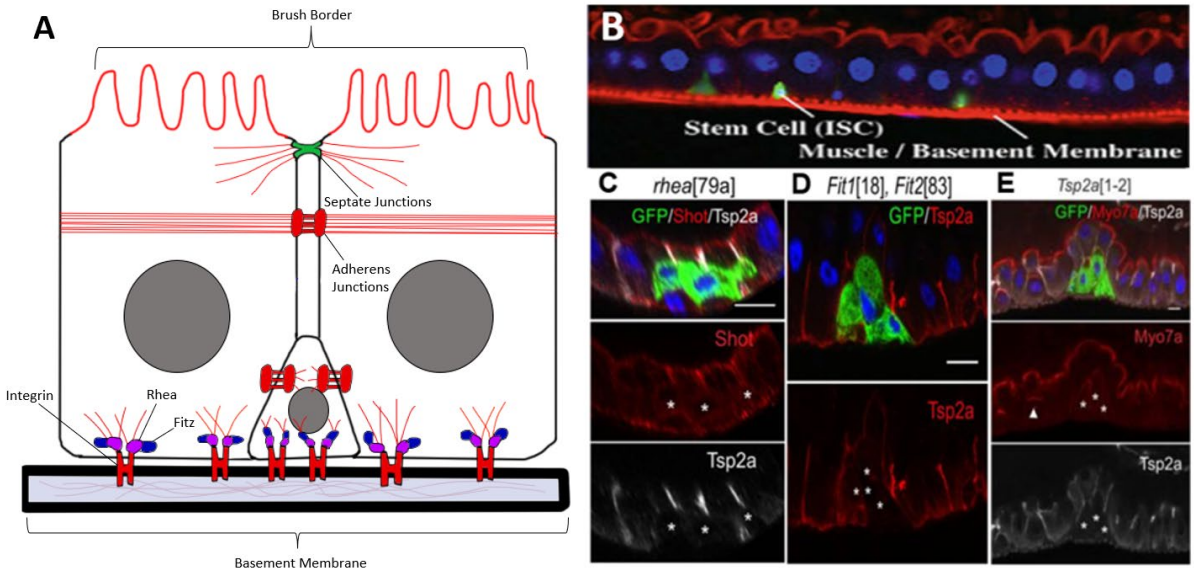

Figure 4.1. Epithelial polarity in the *Drosophila* midgut: (A) Schematic diagram of epithelial polarity in ECs and ISCs. ECs exhibit a columnar shape with apico-basal polarity; possessing AJs, SJs, Integrins, and an apical brush border. ISCs are smaller, cone-shaped, and exhibit less pronounced polarity. AJs and Integrins are expressed, but no SJs or apical domain; **(B)** Representative image of the midgut epithelium. ECs can be discerned by their apical brush border and larger nuclei. ISCs can be identified by their smaller cell and nuclear size; **(C)** Phenotypes observed in *Rhea*, *Fit1/2*, and *Tsp2a* null mutants. *Rhea* and *Fit1/2* can be seen to exhibit abnormal cell shape, BM detachment, and loss of the AJ and SJ markers: E-Cadherin (Shot) and Tsp2a respectively (as indicated by white asterisks). The *Tsp2a* mutant exhibits multilayering and loss of Tsp2a. However, an apical domain is retained as discerned by the brush border marker Myo7a (indicated by white asterisks). Data for (B) derived from [106], data for (C) derived from [179].

Research has been put into determining how polarity is maintained in the adult midgut. In a recent paper it was found that none of the canonical polarity regulators—which include such proteins as LGL, DLG, Scribble, Par-6, aPKC, Crumbs and Stardust—result in a polarity defect following mutation [179]. Rather phenotypes were observed following null mutations to Rhea (Talin) and Fit1/2 (Kindlin), as well as the SJ protein Tsp2a. The Rhea mutant resulted in BM detachment, irregular cell shape, and loss of SJs and an apical domain (Fig.4.1C). This could not be attributed to dedifferentiation as the EC marker PDM1 was still expressed. A similar phenotype was observed with Fit1/2 double mutants (Fig.4.1D). The Tsp2a null resulted in a less severe polarity defect: dysplastic multilayering occurred with a loss of SJs, despite retention of PDM1; however, BM adhesion was retained, and a weak apical domain could be observed through the Myo7a marker (Fig.8E). From these results, a bottom-up polarity mechanism was proposed: with polarity signalling being transduced by basal cues up through SJs.

The apical and basal domains of the epithelia delineate clear boundaries for cell outgrowth, this study shows how loss of polarity can break these boundaries – suggesting a potential role of Rhea, Fitz and SJs in clearing a path for invasive outgrowth should tumorigenic transformation occur. Of note this paper did not address whether Rhea and Fitz produced a phenotype by virtue

of association with the integrins. Moreover, loss of epithelial polarity does not entail adoption of mesenchymal polarity, which more commonly associates with dysregulation of E-Cadherin and carries other important invasive characteristics, such as invasive protrusions and protease activity. This is likely important, as although loss of polarity can sever encroachment by apical and basal boundaries, the BM still segregates liberated cells from the adjacent haemolymph. In this chapter I aimed to characterize the cell biology of invasive tumours cells. Given the association between EMT and altered polarity states, I focused my investigation on the potential contribution of the SJs and basal polarity regulators, with additional caution made not to neglect the role of the Integrins, BM, and E-Cadherin.

Results

Tumours Grow in all the Regions of the Midgut, as well as the Malpighian Tubules.

In order to characterize tumour cells of the midgut, I first set out to identify the sites of tumorigenesis, such as to pinpoint where to direct my analysis. The *Drosophila* midgut can be divided into 5 distinct regions: R1-R5, with R1 being most anterior and R5 being most posterior. The distribution of ARS clones has never been established, although AR was initially established to host 80% of clones within R1 and R2 on Week 4 PCI. To determine if ARS follows a similar pattern at the time of metastasis, guts were dissected out, with tile scans taken across the entire anterior-posterior axis of the midgut. Measurements were then taken of the regionalization of GFP coverage as a percentage of the overall GFP distribution. Results demonstrate that, unlike AR, 4 out of 8 midguts have most of their GFP coverage localized to the R3 region with 2 guts even having more than 50% of their clones within this region (4.2B). Although, excepting R5, considerable coverage could still be seen in the other regions. This pattern could also be borne out by simple visual inspection of the guts, where a more marked coverage of GFP could be discerned in the central region (4.2A). However, in some ARS guts, sizeable tumours could also be observed in the Malpighian Tubules (MpTs) where MpT stem cells express Escargot. This was also true for AR guts, although the MpT tumours were much smaller and less frequent.

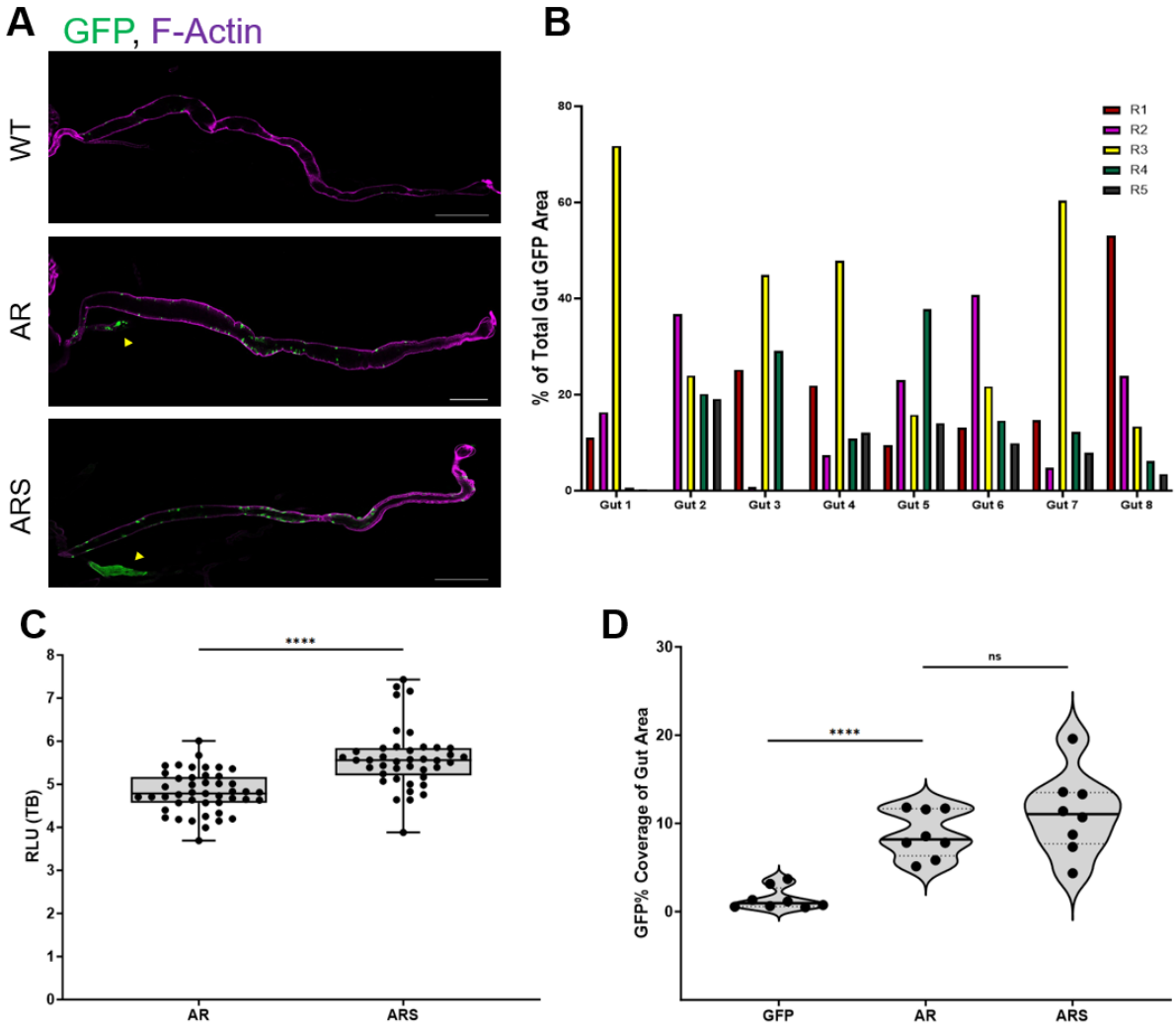

Figure 4.2. (A) Representative images of WT and MpT tumour carrying midguts of the indicated genotypes. Yellow arrows indicate the site of MpT tumours. n=8 for each genotype. Scale bar = 500µm for each genotype; **(B)** Regionalization of GFP% coverage per gut represented as grouped bar chart frequency distribution. n=8; **(C)** Quantification of TB per fly of the indicated genotypes. AR (n=45), ARS (n=41); **(D)** Quantification of GFP% coverage of gut area per fly of the indicated genotypes. n=8 for each genotype. Statistical comparison of (C) was made by Two-Tailed Mann-Whitney presented as median with interquartile range. Statistical comparison of (D) was made by Two-Tailed T-Test presented as mean with interquartile range. $*p < 0.05$; $**p < 0.01$; $***p < 0.001$, $****$ $p < 0.0001$. All flies were analysed Day 6 PCI kept at 25°C. Tissues are stained for GFP (green) and F-Actin (magenta). RLUs are in Log2 scale.

By performing measurements of TB, ARS can be seen to possess a significantly higher quantity of whole-body tumour cells compared to AR (4.2C). To assess if this difference may be a result of increased MpT tumour growth, quantifications were made of the GFP coverage as a percentage of the overall gut area. Results reveal, that although both AR and ARS have significantly higher coverage than WT, the difference between one another is insignificant (4.2D). Put together these results suggest that invasive outgrowth is most likely to occur in the R3 region, followed by the R1, R2 and R4 regions, with the posterior most R5 region being the most unlikely. However, given the occasional and considerable tumour sizes of the MpTs, it is possible that invasive outgrowth may occur form them as well. With these results in mind,

tumour cells were assessed for phenotypes in all regions of the gut, with caution made not to ignore potential changes occurring within the cells of the MpTs as well.

Cancer Cells Undergo Divergent Methods of Invasion at Stereotype Sites

In order for tumour cells to make their way into the haemolymph, they must first make their way past the BM. Although, ARS guts were previously reported to exhibit loss of the BM marker laminin, the frequency by which this change occurs was never established. Therefore, 392 flies were dissected throughout the full range of the established cancer progression timeline—Days 1-14 PCI—stained for laminin, then screened for invasive events. Results reveal two states of BM deterioration: some tumours exhibit breaks localized to the outer edge of tumours with some cells having breached the BM (Fig.4.3A-C); other tumours appear to have already expanded out into the haemocoel (Fig.4.3D-F). It is plausible that the two states represent two successive stages.

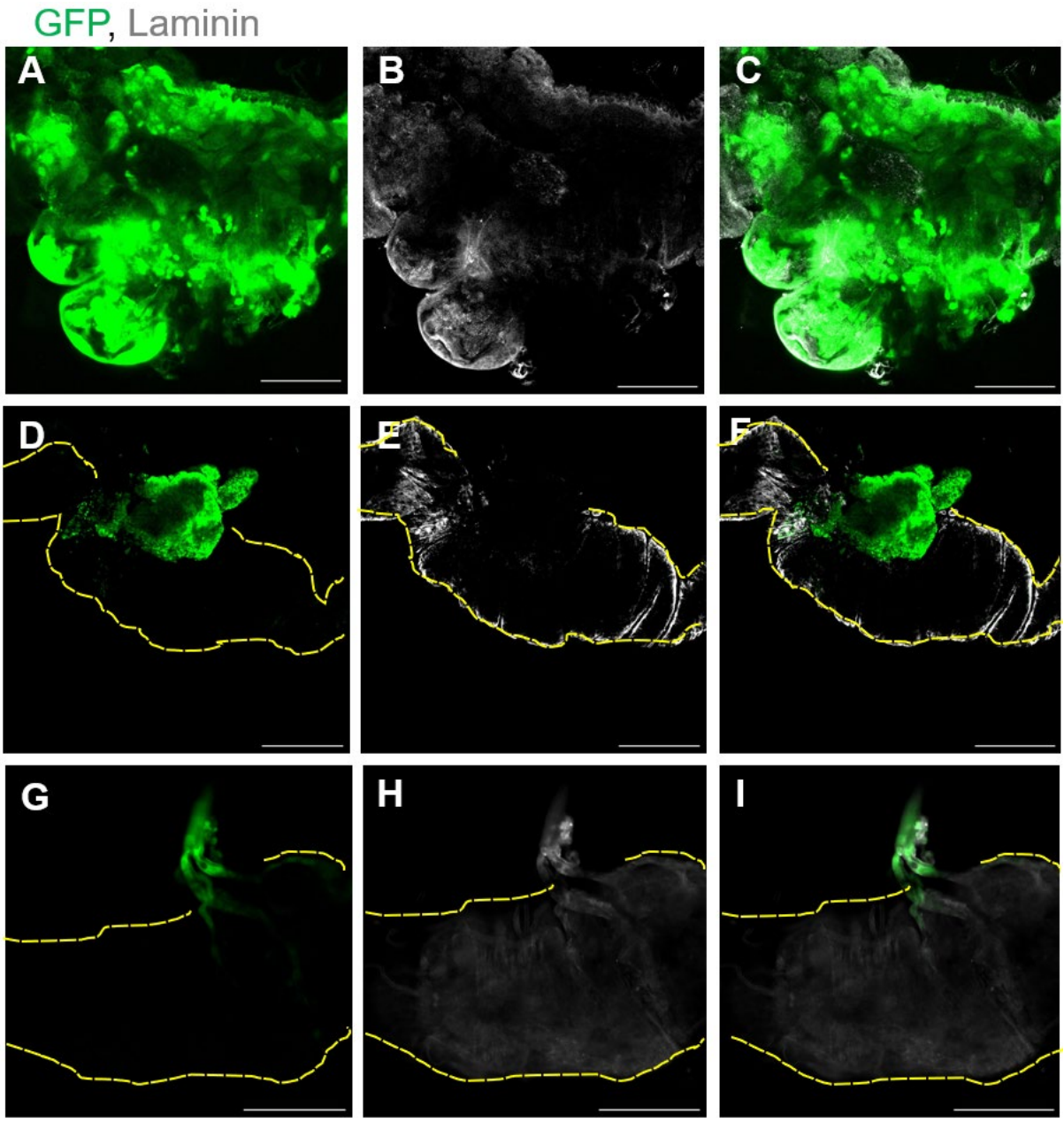

Figure 4.3: (A-C) Representative image of tumour invasive edge. n=9 tumours from 9 guts. Scale bar = 100µm; **(D-F)** Representative image of tumour expansion into the haemocoel. n=1 tumour from 1 gut. Scale bar = 200µm; **(G-I)** Representative image of tumour cell invasion onto tracheal tubules. n=3 tumours from 3 guts. Scale bar = 100µm Tissues are stained for GFP (green) and Laminin (grey). Yellow dashed lines outline the boundaries of the gut.

Cumulatively, the combination of these two events were recorded to comprise 2.55% of the overall sample size (Fig.4.4A). At some sites GFP+ cells could also be seen to colocalize with tracheal tubules on the outside of the gut, even though no visible deterioration of the BM could be observed (Fig.4.3G-I). It is possible that tumour cells may be able to latch onto these tubes without having to destroy the BM: this would represent a 2nd strategy of dissemination. By contrast this invasive form comprised a lesser 0.77% of the total sample size (Fig.4.4A). In total the net incidence of invasion, including both BM breaks and tracheal-mediated invasion,

was found to encompass 3.32% of analysed guts, with 77% of invasive events being BM breaks and 23% being tracheal mediated (Fig.4.4B). The cumulative rate of invasion lines up with the percentage of flies which undergo macrometastasis, although it is disproportionate to the percentage of flies which yield very large quantities of CTCs.

A

Invasive Phenotype	Flies Screened	Observations Made	% of Sample Size
BM	392	10	2.55
Tracheal	392	3	0.77
BM or Tracheal	392	13	3.32
Colonisation	230	5	2.17
Large-Scale Dissemination	86	4-9	5-10

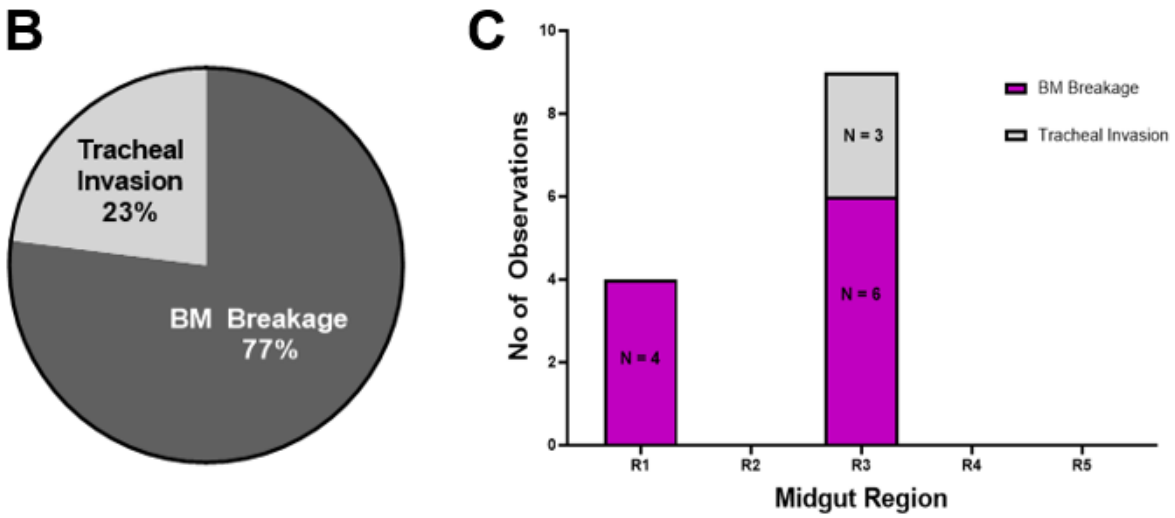

Figure 4.4: (A) Summary table of flies screened and record of invasive phenotypes; **(B)** Pie chart frequency distribution of invasive phenotypes; **(C)** Regionalization of invasive modes along midgut regions, represented by stacked bar-chart frequency distribution.

As most tumours can be found in the R3 region, the guts were also screened for the site of invasive outgrowth. As expected most invasive events were found to localize to the R3 region, however just under 1/3 of invasive events were recorded from the R1 region (Fig.4.4C). It is possible that there are larger R1 tumours specifically in invasive guts, a phenomenon that would not be captured by the quantifications of clone regionalization which were performed on non-invasive ARS guts.

Put together these findings demonstrate that invasion out of the midgut, like macrometastasis, is a rare event proceeding by BM deterioration or tracheal mediated invasion. Although, it cannot be ruled out that cells invading onto tracheal tubules move out by forming microtears not visible through confocal.

The Protease ADAMTS-A Becomes Upregulated in ARS Tumours and Exhibits Indications of Secretion at the Invasive Edge.

The deterioration of the BM suggests there is likely a protease that becomes employed to proteolyze the BM constituents. To identify potential proteases that may be proteolyzing the BM, I revisited results from a genome-wide microarray screen performed on WT, AR, and ARS gut tumours. In particular, I searched for proteases that are upregulated in ARS where metastasis occurs, and not in AR, where metastasis does not occur (Fig.4.5A). By inspection of the mean fold change from WT, both MMP1 and MMP2 are upregulated in ARS. However, they are more strongly upregulated in AR where BM breaks do not occur, suggesting that they are not responsible for destroying the BM. By contrast, ADAMTS-A, a secreted protease, is upregulated in AR, with an even stronger increase observed in ARS, implying it may be responsible for breaching the BM.

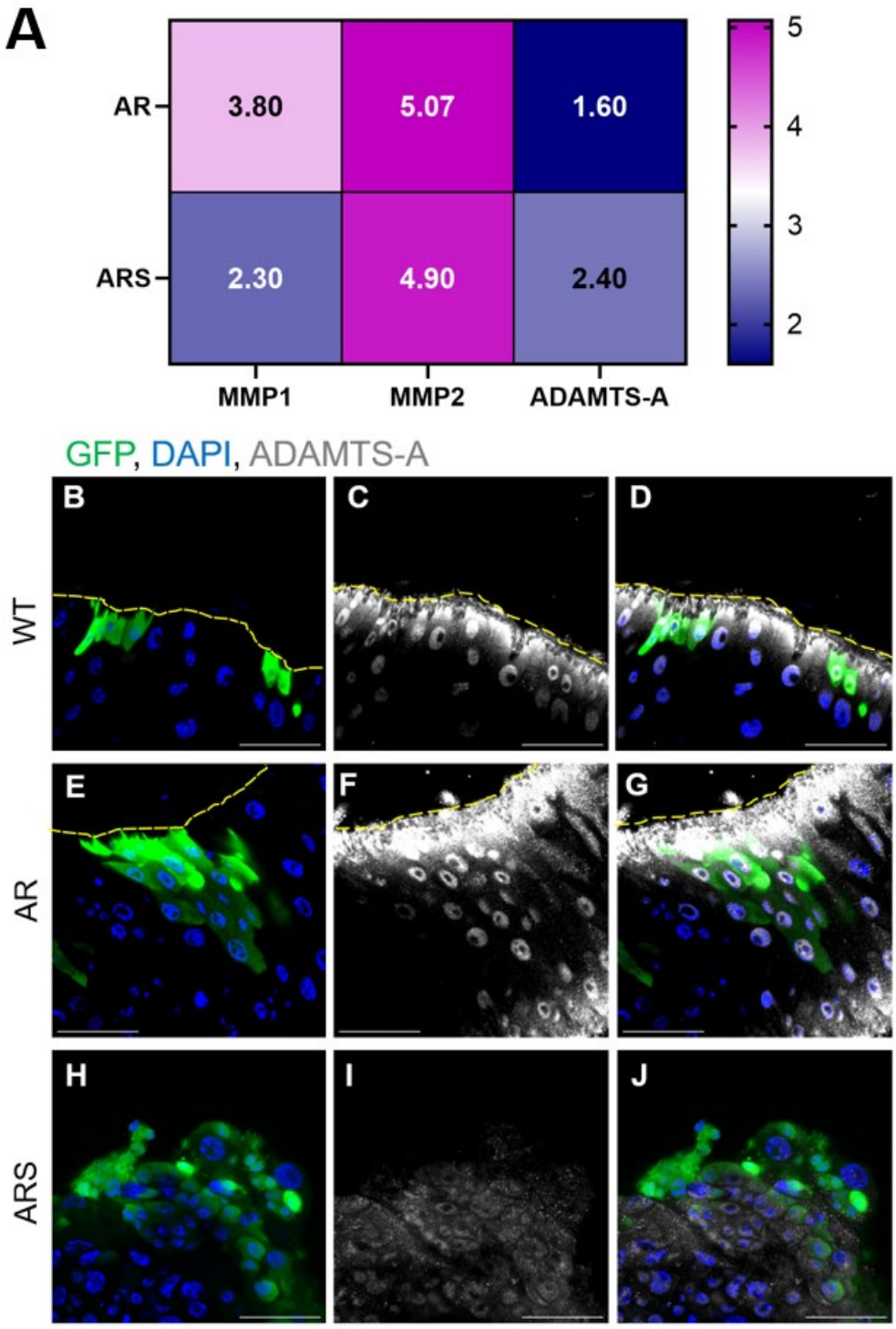

Figure 4.5: (A) Heatmap depicting the expression of protease genes as quantified by log2 mean fold change expression from WT control; **(B-D)** Representative image of ADAMTS-A behaviour in WT tissues. n=6 tissues from 6 guts; (E-G) Representative image of ADAMTS-A behaviour in AR tumours n=6 tumours from 6 guts; **(H-J)** ADAMTS-A behaviour in an invasive tumour dissected from a fly suffering from a brain metastases. n=1 tumour from 1 gut. Scale bar = 40µm (B-J). Tissues are stained for GFP (green), ADAMTS-A (grey) and nuclei (blue). Yellow dashed lines outline the boundaries of the gut.

To investigate this further, guts were stained for ADAMTS-A. In WT flies, ADAMTS-A can be seen to exhibit a perinuclear pattern of expression in not only Escargot+ cells, but also the other cells of the gut (Fig.4.5B-D). In AR tumours, cells retain this pattern of expression even

as they grow into tumours (Fig.4.5E-G) This phenotype holds for most ARS tumours as well, with the exception of an invasive tumour extracted from a metastatic fly where decreased ADAMTS-A staining can be observed at the invasive edge (Fig.4.5H-J). This is at the same site where laminin is typically lost, suggesting that both changes may be occurring concurrently in time and space in the same subpopulation of flies.

Given that ADAMTS-A is a secreted protease, it is possible that the diminished staining pattern relates to the protein being secreted. With more time it would be interesting to generate an HCR probe for ADAMTS-A to determine if the gene is still being expressed in those cells with diminished staining: this would be suggestive of it being potentially secreted. Nonetheless, these findings draw attention to ADAMTS-A as a potential downstream driver of Snail, likely operating with outcome of clearing space for tumour cells to move out. However, clearing space for cells to move into the haemolymph is likely to be insufficient for invasive outgrowth if cells are still adhered to the inside of the gut. The migration of single or collective CTCs likely requires the disassembly of cell-adhesions which constrain migration.

Tumours Consist of a Heterogeneous Population of Cells Dominated by Undifferentiated Cells.

To investigate changes to cell polarity, care must first be taken to situate these changes within the context of cellular subtypes. Whereas progenitors carry a rudimentary form of polarity with basal and lateral domains, only the differentiated cells possess full apico-basal polarity. Importantly, if a cell is found to lack apico-basal polarity this could be because progenitors fail to differentiate. Or, alternatively, it could be because differentiated cells lose polarity after undergoing an EMT. To begin to assess this, the identity of cells harboured by ARS tumours must first be established. By staining for the EC marker PDM1, and the EE marker Prospero—Day 6 PCI—cells could be found to consist mostly of cells negative for both differentiation marker (Fig.4.6A-D). However, some PDM1+ could be discerned with nuclear and cell sizes consistent with an EC identity. Prospero+ cells were also identified, but at a much lower frequency than the PDM1+ cells. As 90% of differentiated cells assume an EC fate in wild-type tissues, this does not come as a surprise.

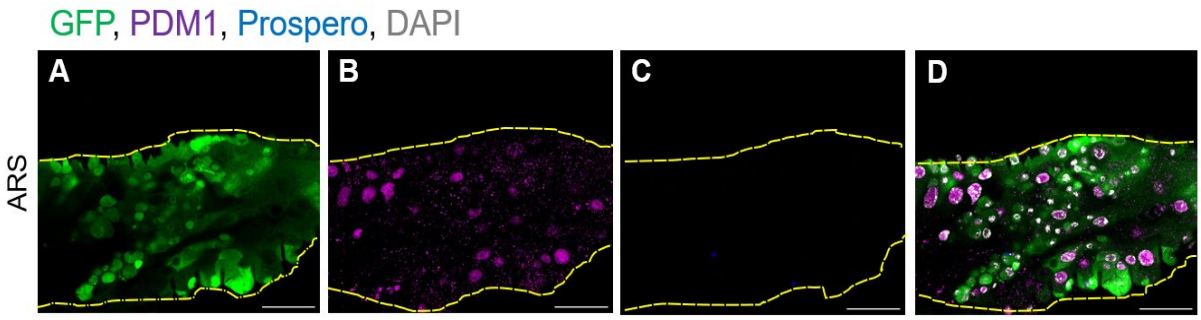

Figure 4.6: (A-D) Representative image of the differentiation status of an ARS tumour. n=10 tumours from 10 guts. Scale bar = 40µm Tissues are stained for GFP (green), PDM1 (magenta), Prospero (blue) and nuclei (grey). Yellow dashed lines outline the boundaries of the gut.

Put together, these findings suggest that tumours consist mostly of undifferentiated cells, however the presence of PDM1 and Prosepro demonstrates that there are some differentiated cells as well. Furthermore, as the vast majority of differentiated cells are comprised of PDM1+ cells, it means differentiated cells can be identified based on cell and nuclear size without consistently utilising a PDM1 stain. Importantly, this means that if a cell meets these criteria and lacks apico-basal polarity, it is likely to be due to a loss of polarity regulators and not a failure to differentiate. Although, it is important to note: progenitor cells remain adherent even in their less developed polarity state. As such my investigation into polarity will pay consideration to alterations occurring to both cell types.

Loss of Polarity Coincides with Loss of Adhesion to the Basal Substrate

The perhaps most prominent indicator of apico-basal polarity is the brush border, whose serrated pattern makes up the apical domain of ECs and exposes the periodic arrangement of adjoining cells. Using a Phalloidin stain—which labels F-Actin of the microvilli—the epithelia of WT guts can be observed to possess normal tissue architecture with a visible monolayer and intact apical domain (Fig.4.7A-D). By contrast, AR and ARS clones undergo dramatic multilayering as they develop into tumours; pushing aside their apical boundary with an observable loss of cellular periodicity and irregular arrangement of actin filaments, with some cells exhibiting expansion of F-Actin from the apical to the lateral domains, suggestive of a loss of apico-basal polarity (Fig.4.7E-L)

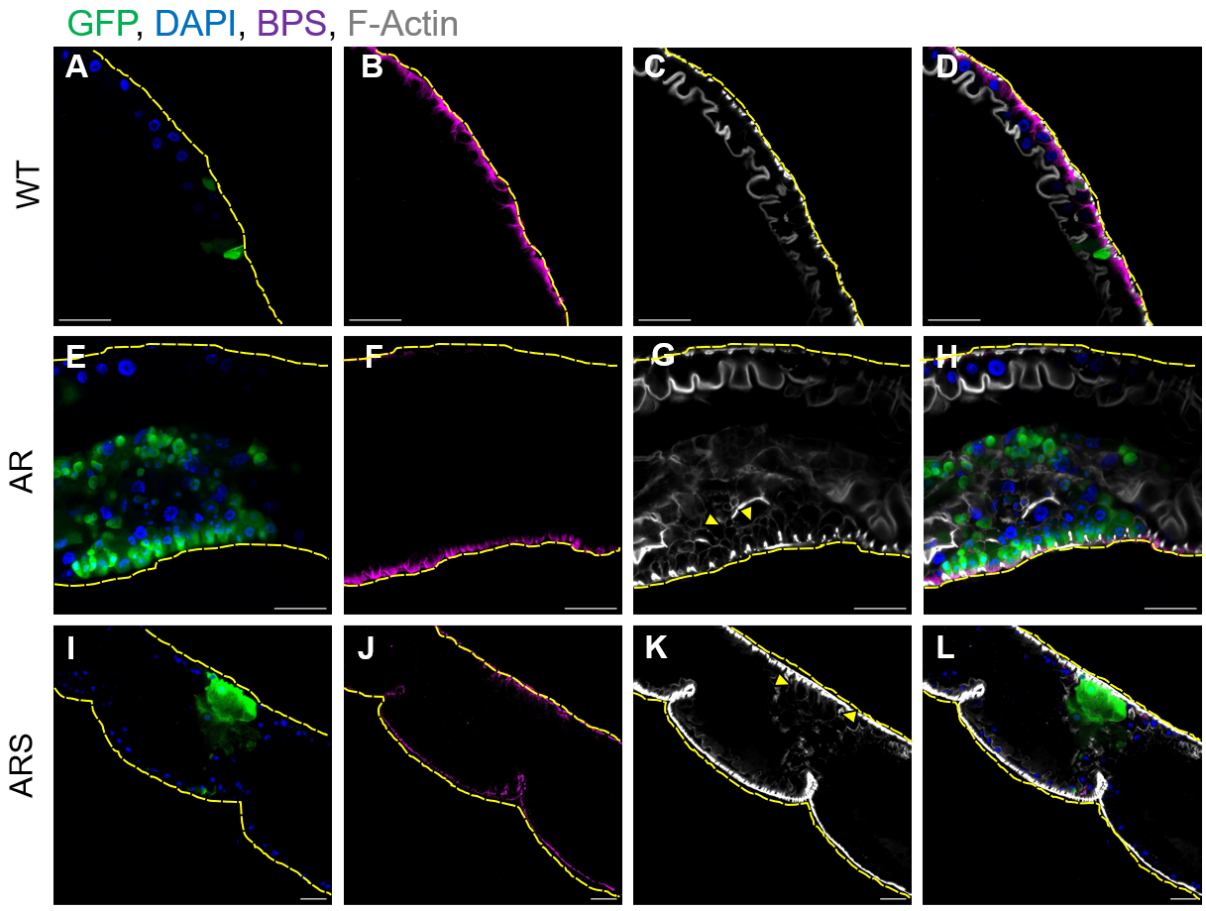

Figure 4.7: (A-D) Representative image of tissue architecture in wild-type tissues. n=7 clones from 7 guts; **(E-H)** Representative image of tissue integrity collapse in AR tumours, cells with delocalization of F-Actin to the lateral domains is indicated by the yellow arrows. n=8 tumours from 7 guts; **(I-L)** Representative image of tissue integrity collapse in ARS tumours. n=10 tumours from 10 guts. Scale bar = 40μm (A-L). Tissues are stained for GFP (green), BPS integrin subunit (magenta), F-Actin (grey) and nuclei (blue). Yellow dashed lines outline the boundaries of the gut.

Previous studies link the maintenance of midgut apico-basal polarity to the disruption of basal polarity regulators [179, 181]. To investigate if this holds true during tumorigenic outgrowth, guts were also stained for their integrins. *Drosophila* integrins are heterodimers composed of one of five alpha subunits (aPS1-5), and one of two beta subunits (BPS and Bv). BPS dimerizes with all alpha subunits and is more predominant in the midgut [183]. Therefore, to image a larger quantity of integrins, the BPS subunit was stained. As expected, BPS can be seen to localize to the basal domain of WT epithelia. However, in both AR and ARS, tumours are observed to lose expression of BPS as they undergo multilayering. It is likely that by losing their integrins, tumours can overcome confinement to the ECM and grow out into the lumen collapsing tissue architecture in the process.

To gain a stronger indication of the polarity status of tumours, cells were stained for DLG: a polarity marker, which in WT epithelia is not expressed by progenitor cells but localizes subapically in differentiated cells [179]. As expected, staining of WT guts demonstrates that

DLG is not expressed by progenitors (Fig.4.8A-D), but becomes localized subapically as cells mature (Fig.4.8E-H). However, in AR tumours, DLG appears to be universally lost: by both progenitors, but also more mature cells as discerned by larger nuclear size (Fig.4.8I-L). Strikingly, the addition of Snail to the AR background appears to reverse this as DLG becomes ubiquitously expressed in all tumour cells, including presumptive progenitors with smaller nuclei (Fig.4.8M-P). An isolated ISC can also be seen to express it cytosolically suggesting that DLG becomes switched on early, likely following initial recombination and activation of Snail. Combined with the rearrangement of the apical actin network, these results demonstrate that AR and ARS tumours lose epithelial polarity.

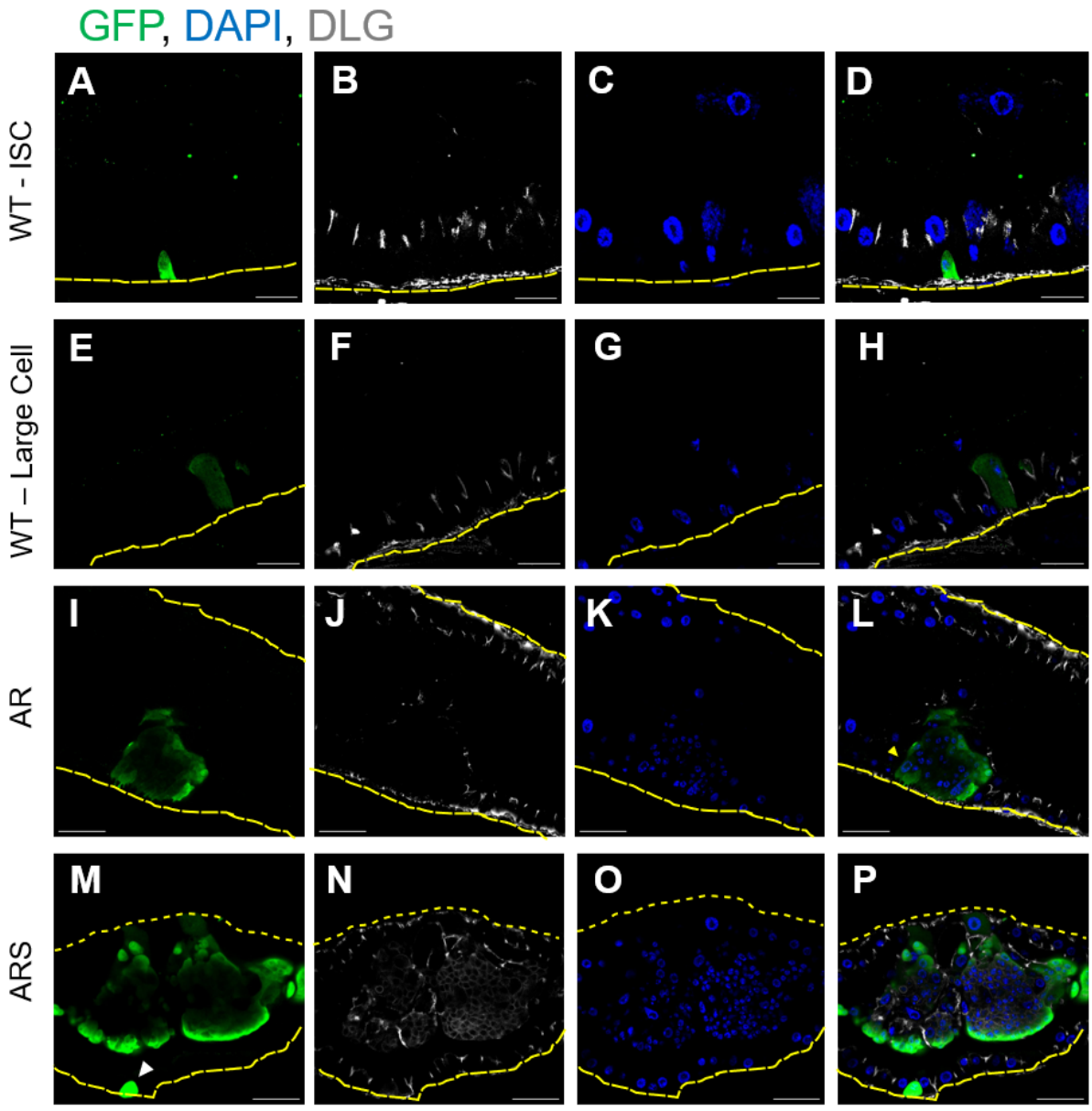

Figure 4.8: (A-D) Representative image of missing DLG expression in wild type ISCs. n=6 clones from 6 guts; **(E-H)** Representative image of subapical DLG expression in a mature cell. n=1 clone from 1 gut; **(I-L)** Representative image of missing DLG expression in AR tumours, yellow arrow points to a mature cell that has lost DLG expression. n=4 tumours from

4 guts; **(M-P)** Representative image of ARS tumours with upregulated and delocalized DLG expression, white arrow indicates a solitary ISC. n=8 tumours from 8 guts. Scale bar = 20μm (A-H), 40μm (I-P). Tissues are stained for GFP (green), DLG (grey), and nuclei (blue). Yellow dashed lines outline the boundaries of the gut.

Tumours Retain Expression of the Integrin Adaptor Talin

Integrins are coupled to internal actin filaments through the adaptor proteins Talin and Kindlin: loss of either of these proteins is sufficient to collapse apico-basal polarity in the midgut [179]. Therefore, Talin was stained to investigate if the aberration of cell polarity and integrins might relate to it being dysregulated. Given Talin's canonical role as an integrin adaptor, it can be reasoned that it would localize exclusively to the basal domain of WT epithelia. Strikingly, Talin can be seen to localize to all three domains of the WT epithelia (Fig.4.9A-C). Moreover, even though tumours lose expression of their integrins, Talin is still expressed in this same pattern in both AR and ARS tumours (Fig.4.9D-I). These findings suggest that the loss of polarity phenotype which coincides with integrin loss occurs independent of dysregulation of Talin. Although, this data does not rule out the potential dysregulation of Kindlin. Unfortunately, no antibody is available for this protein. However, with time it would be interesting to generate a probe against Kindlin for in situ-HCR.

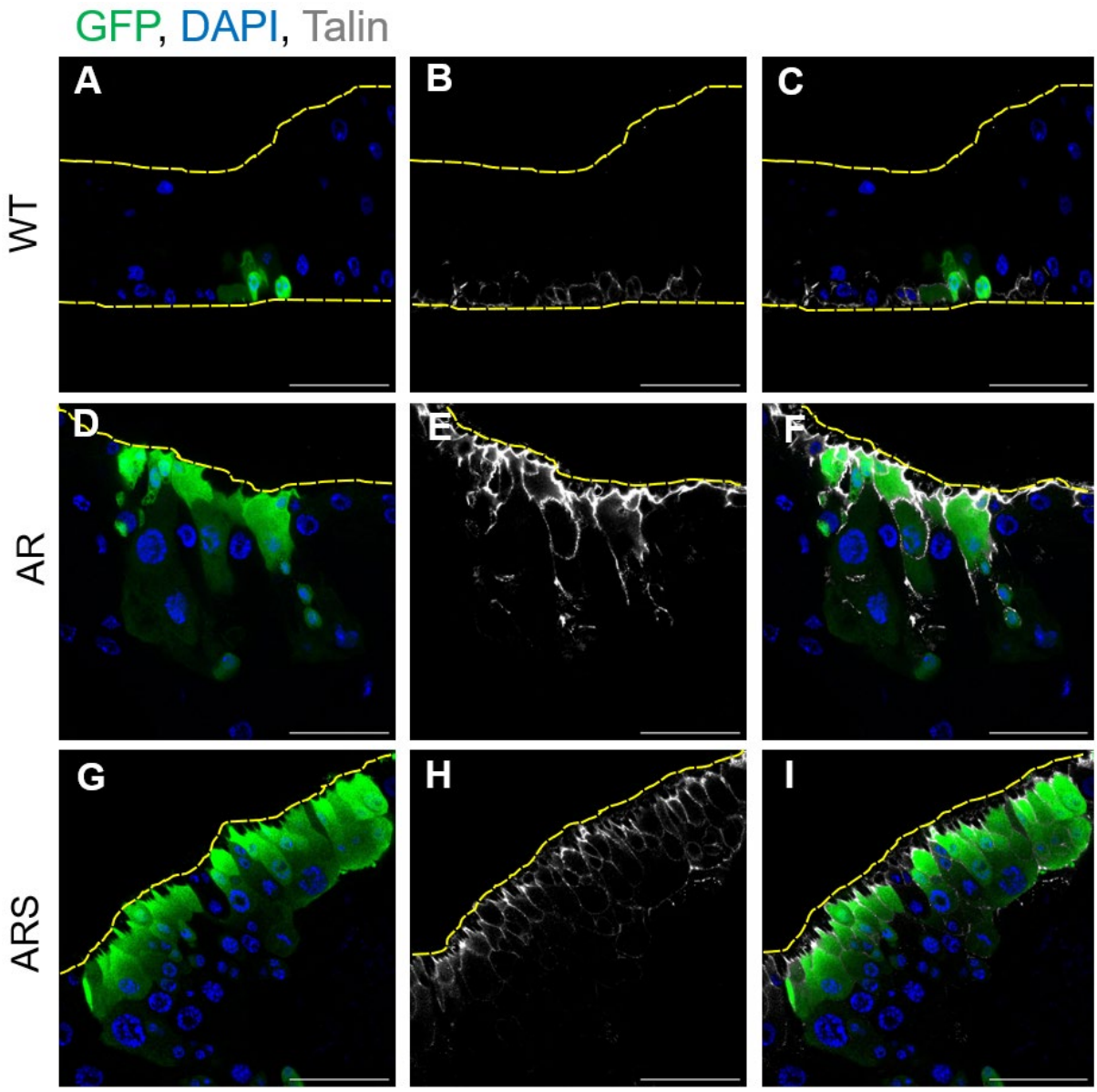

Figure 4.9: (A-C) Representative image of Talin expression in wild-type tissues. n=8 clones from 8 guts **(D-F)** Representative image of Talin expression in AR tumours. n=5 tumours from 3 guts; **(G-I)** Representative image of Talin expression in ARS tumours. n=8 tumours from 8 guts. Scale bar = 40µm (A-I). Tissues are stained for GFP (green), Talin (grey), nuclei (blue). Yellow dashed lines outline the boundaries of the gut.

ARS Tumours Lack Septate Junctions

Evidence suggests that the loss of polarity phenotype observed from loss of Talin and Kindlin is compounded by aberration of the SJs. The SJs are composed of three proteins: Snakeskin, Tsp2a, and Mesh. All 3 are mutually dependent on each other with Mesh being the intercellular molecule mediating homotypic interaction between adjacent SJ [184]. To assess a potential role of SJ dysregulation in tumour outgrowth, guts were stained for Mesh with results revealing that ARS tumours have a complete lack of SJ expression (Fig.4.10A-D). As progenitors do not contain SJs anyway, it would be interesting to co-stain Mesh with PDM1 to definitively

determine that SJs are lost in cells where they are otherwise expressed. However, due to PDM1 and SJ antibodies being of the same species, and difficulties associated with SJ staining, this could not be performed. However, as PDM1 associates with larger nuclei, both tumours with small and larger nuclei were stained. Results reveal that even cells with larger nuclei are negative for Mesh (Fig.4.10E-H). Combined with previous data establishing the presence of differentiated cells in tumours, it would appear that the absence of SJs is not attributable to a loss of differentiation. However, whether SJs become lost or fail to express in differentiated cells cannot be determined from this data.

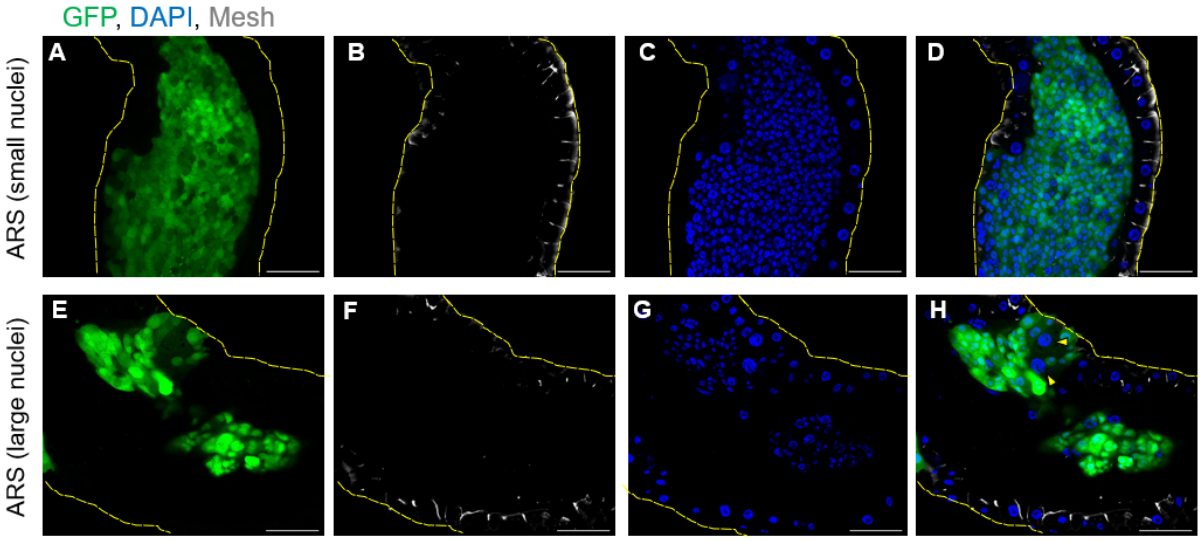

Figure 4.10: (A-D) Representative image of ARS tumours with small nucleated cells; **(E-H)** Representative image of ARS tumours with large nucleated cells indicated by yellow arrows. n=7 tumours from 7 guts. Scale bar = 40µm (A-H). Tissues are stained for GFP (green), Mesh (grey) and nuclei (blue). Yellow dashed lines outline the boundaries of the gut.

Unfortunately, due to the issues with SJ staining, this experiment could not be repeated in AR and WT controls. Attempts were made with probes with no success. Future work will be required to determine if the absence of SJs is exclusive to ARS. Although, given that invasion only occurs in 3.32% of ARS guts—and a far lesser quantity of tumours—loss of the SJs cannot be sufficient for invasion to occur as the consequent would be invasion occurring from all tumours. Although, this does not rule out SJ loss being a necessary feature. With time, the insertion of an UAS-Mesh construct in ARS could be an interesting experiment to determine if it can inhibit metastasis: potentially, by forcing epithelial polarity.

Loss of the AJ Component E-Cadherin Colocalizes with BM Degradation and is an Exclusive Feature of Metastatic ARS Tumours.

With Integrins and SJs being lost in all tumours—including the many that don't metastasize—there is only one cell-adhesion molecule left that can differentiate those rare ones that do: the Adherens Junctions. By staining guts for the AJ marker E-Cadherin, AR tumours can be seen to retain expression even as they grow to considerable sizes: although dispersion across the membranes can be seen, suggestive of altered polarity (Fig.4.11A-D). With ARS the same pattern can be observed in most tumours, except for tumours-bearing guts extracted from flies that have metastasized, where it becomes lost specifically on the invasive edge and co-localizes with deterioration of laminin (Fig.4.11E-I). This phenotype is not unique to invasive tumours of the gut, as the same can be observed in MpT tumours suggesting they also may have invasive capacity (Fig.4.11J-N).

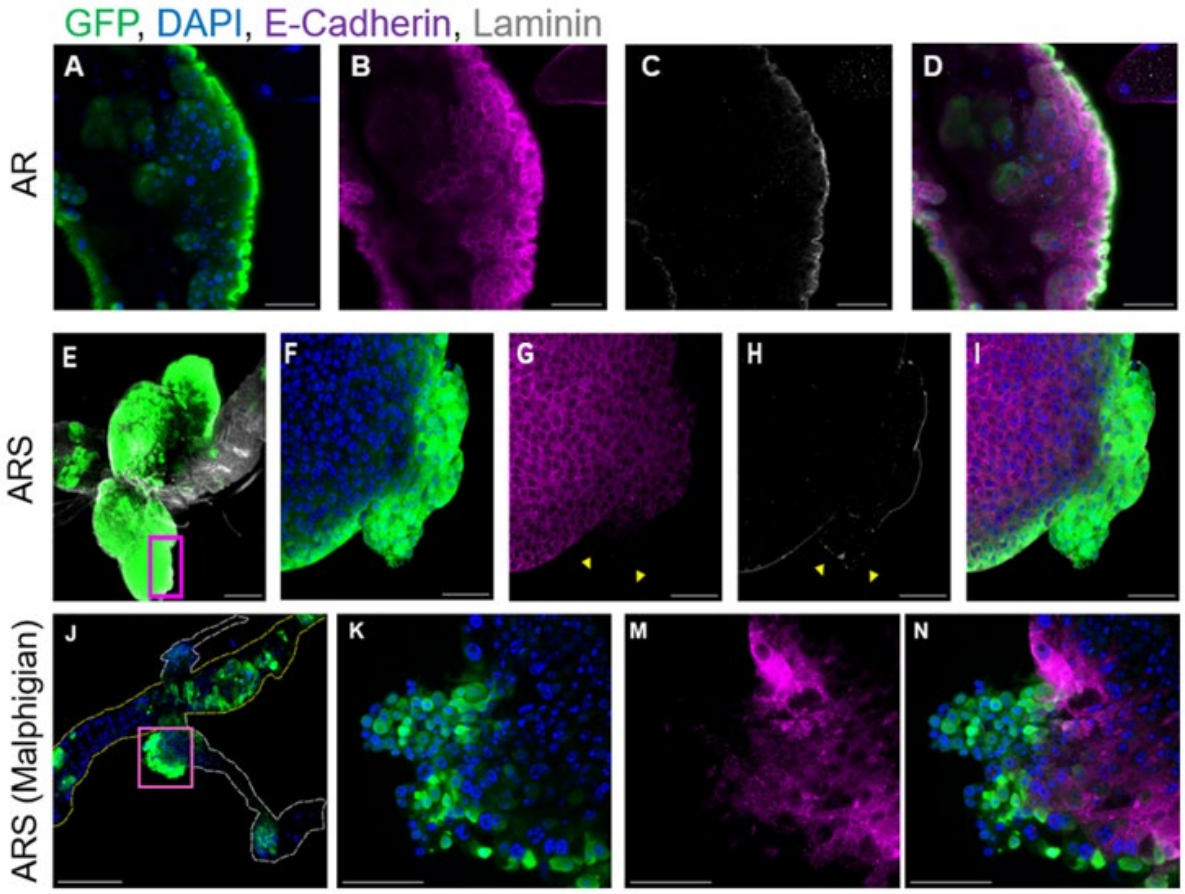

Figure 4.11: (A-D) Representative image of E-Cadherin and Laminin expression in AR tumours. n=9 tumours from 8 guts; **(E-I)** Representative image of colocalization of E-Cadherin and Laminin loss at the invasive edge of metastatic ARS tumours. Magenta box indicates the site of the invasive edge; yellow arrows indicates where E-Cadherin and Laminin become downregulated and deteriorated respectively. n=5 tumours from 5 guts; **(J-N)** Representative image of E-Cadherin

downregulation at the invasive edge of a malphigian tubule tumour. Magenta box indicates the site of the invasive edge; yellow dashed lines indicate the boundaries of the gut; white dashed lines indicate the outlines of the malphigian tubules. n=1 tumour from 1 malphigian tubule. Scale bar = 40µm (A-D), 150µm (E), 30µm (F-I), 200µm (J), and 40µm (K-N). Tissues are stained for GFP (green), Nuclei (blue), E-Cadherin (magenta), and Laminin (grey).

Discussion

The results within this chapter have established that ARS tumours are composed of primarily undifferentiated cells which lose polarity, as evidenced by delocalization of DLG. Differentiated cells positive for PDM1 and Prospero were also present, which additionally appear to lose apico-basal polarity as F-Actin, which is specific to ECs, becomes delocalized from the apical end to all three domains of the cells. Given prior findings, this may be attributable to loss of the SJs and integrins which are not expressed by the tumours. However, even though most flies lose their adhesion molecules and exhibit altered polarity, only a small percentage of guts (3.35%) actually invade out of the gut. Results demonstrate that specifically in those guts that do metastasize, three central changes can be seen to occur at the invasive edge of tumours at the same frequency: loss of Laminin, loss of E-Cadherin, and dysregulation of the secreted protease ADAMTS-A. As the frequency by which these changes occur line up with the number of flies that form metastases, it can be reasonably inferred that these are the critical changes that initiate metastasis.

These findings raise some interesting questions. Firstly, although all three changes can be seen to occur, I have not been able to establish a sequence of events. It is possible that E-Cadherin becomes lost, triggers an EMT, with one of the consequences being upregulation of ADAMTS-A which destroys the BM. However, it is also possible that ADAMTS-A is upregulated first, destroys the BM, allowing cells to receive cytokines from the haemolymph which trigger a loss of E-Cadherin. To determine the sequence of events, I would need to co-stain markers and identify tumours where the one changes has occurred and not the other. As metastatic flies are rare this would necessitate a very large sample size, which would represent a challenging ordeal, but with more time, a doable one.

Secondly, it is interesting that E-Cadherin becomes completely repressed at the invasive front: unlike partial repression, a complete repression of E-Cadherin is rarely observed during EMT and raises the question of how ARS flies can support collective migration. It is possible that there are two populations of invasive cells: one that completely represses E-Cadherin and migrates as single CTCs, and a second population that partially represses E-Cadherin and migrates collectively. With more time it would be interesting to analyse a larger sample size to try and determine if there are cells that only partially repress E-Cadherin.

A final, and most pressing question relates to whether the three aforementioned changes are causally responsible for driving metastasis. The fact that these three changes coincide in space and occur at the same frequency as macrometastasis strongly suggests they are metastatic effectors. However, determining this requires that the candidates be interrogated genetically, then assessed by how the previously established metastatic outcomes change, including: secondary tumour formation, CTC dissemination, and BM destruction.

Chapter V

ADAMTS-A is Required for the Metastatic Dissemination of ARS Flies.

Introduction

Comparison of ARS to AR tumours identified numerous changes occurring to cell polarity. However, only loss of the BM and E-Cadherin, as well as dysregulation of ADAMTS-A were found to be unique to ARS and occurring at the same frequency as macrometastasis; suggesting they may be causally responsible for initiating metastasis. This hypothesis is given additionally strength by ADAMTS proteins being extracellular proteases with established roles in cleaving extracellular matrix proteins, lending credence to the suggestion that ADAMTS-A may be responsible for destroying the BM and permitting invasive outgrowth. Therefore, this chapter aimed to determine if dysregulation of E-Cadherin and ADAMTS-A are sufficient and/or necessary for metastatic outgrowth through appropriate loss-of-function analysis. In particular, as E-Cadherin is lost in ARS, an UAS:E-Cadherin^{RNAi} was put in the AR background to assess if this may phenocopy ARS. As ADAMTS-A becomes upregulated in ARS, an UAS:ADAMTS^{RNAi} was put in the ARS background to determine if this may eliminate metastasis.

Dysregulation of E-Cadherin at the invasive front came as no surprise given the transcriptional repression of *E-Cadherin* by Snail and its established association with EMT and metastatic progression. However, the role of E-Cadherin in *Drosophila* midgut tumorigenesis has in previous studies been established to be quite complex. In an *APC1/2* $^{(-/-)}$ midgut tumour model, multiple varieties of *E-Cadherin* mutations were introduced to the progenitor cells and assessed for phenotypes [185]. An *E-Cad*^{CR4h} mutant disrupting cell-cell adhesion through loss of the extracellular adhesion motifs, almost eliminated tumorigenesis. By contrast, an *E-Cad*^{JM} mutant which truncates the p120 catenin association motif, resulted in marked tumour growth, as liberated p120 went on to activate EGFR signalling. Moreover, in one line of research, *Ras*^{V12} was introduced into all the cells of the midgut resulting in aggressive tumour growth, BM deterioration, and the formation of metastatic foci on the gut visceral muscle [154, 186]. This appeared to occur through MMP1 activity at the site of invasive protrusions, proceeding in a manner dependent on delocalization of E-Cadherin to these sites. Expression of various E-Cad^{RNAi}'s under the control of *Escargot* eliminated invasive outgrowth. Put together, these findings demonstrate a role for *E-Cadherin* as both a tumour suppressor and an oncogene.

ADAMTS encompasses a broad family of secreted extracellular proteases involved in diverse cellular processes [187]. Like MMPs they are Zinc-metalloproteases, but differ by contrasting structural domains [188]. There are 19 human ADAMTS proteins, which can be divided into

four groups (A, B, C, and D) based on their substrates and domains [168, 189]. ADAMTS-A belongs to the A-group—from which it derives its name—and is most closely related to human ADAMTS9 and ADAMTS20, which possess a GON-1 domain and cleave glycoproteins such as aggrecan, versican, and brevican. Although, *Drosophila* do not possess these proteins, nor has an alternative substrate been identified. Like MMPs, ADAMTS proteins have been associated with EMT and metastatic progression in a variety of cancers, including CRC [190]. Moreover, experimental approaches in-vitro relate ADAMTS to invasive behaviours [191]. However, unlike MMPs, there are very few experimental scenarios where a causal role has been established for ADAMTs proteins in driving metastasis in-vivo [192]. Given the high potential of enzymes as drug targets, if causality could be supported for ADAMTS in invasive outgrowth, this could expose a vulnerability by which metastatic cancer can be targeted with strong therapeutic implications.

Results

Genetic Ablation of E-Cadherin Is Insufficient to Drive Metastatic Outgrowth

Characterisation of midgut tumours identified loss of E-Cadherin at the invasive front as being a potential mechanism of metastatic outgrowth. As Snail transcriptionally represses E-Cadherin, and experimental ablation of E-Cadherin has, in some circumstances, been sufficient to trigger EMT: I sought to determine if genetic ablation of E-Cadherin in AR is sufficient to phenocopy activation of Snail. Therefore, an established and validated UAS-E-Cadherin^{RNAi} line (#103962, Vienna *Drosophila* RNAi Centre) was introduced into the AR background. Relying on previously established metastatic outcomes, flies were first screened for secondary tumours within the earlier determined cancer progression timeline: Days 1-14 PCI. With a sample size of 200, no secondary tumours could be discerned (Fig. 5.1A). However, it is possible that earlier steps of metastasis could still be occurring. As such, flies were also quantified for CTCs, Day 6 PCI, and compared to AR and ARS to determine if CTCs may increase and approximate ARS levels. Consequently, no significant increase from AR could be observed, although a narrower distribution of values could be observed (Fig.5.1B).

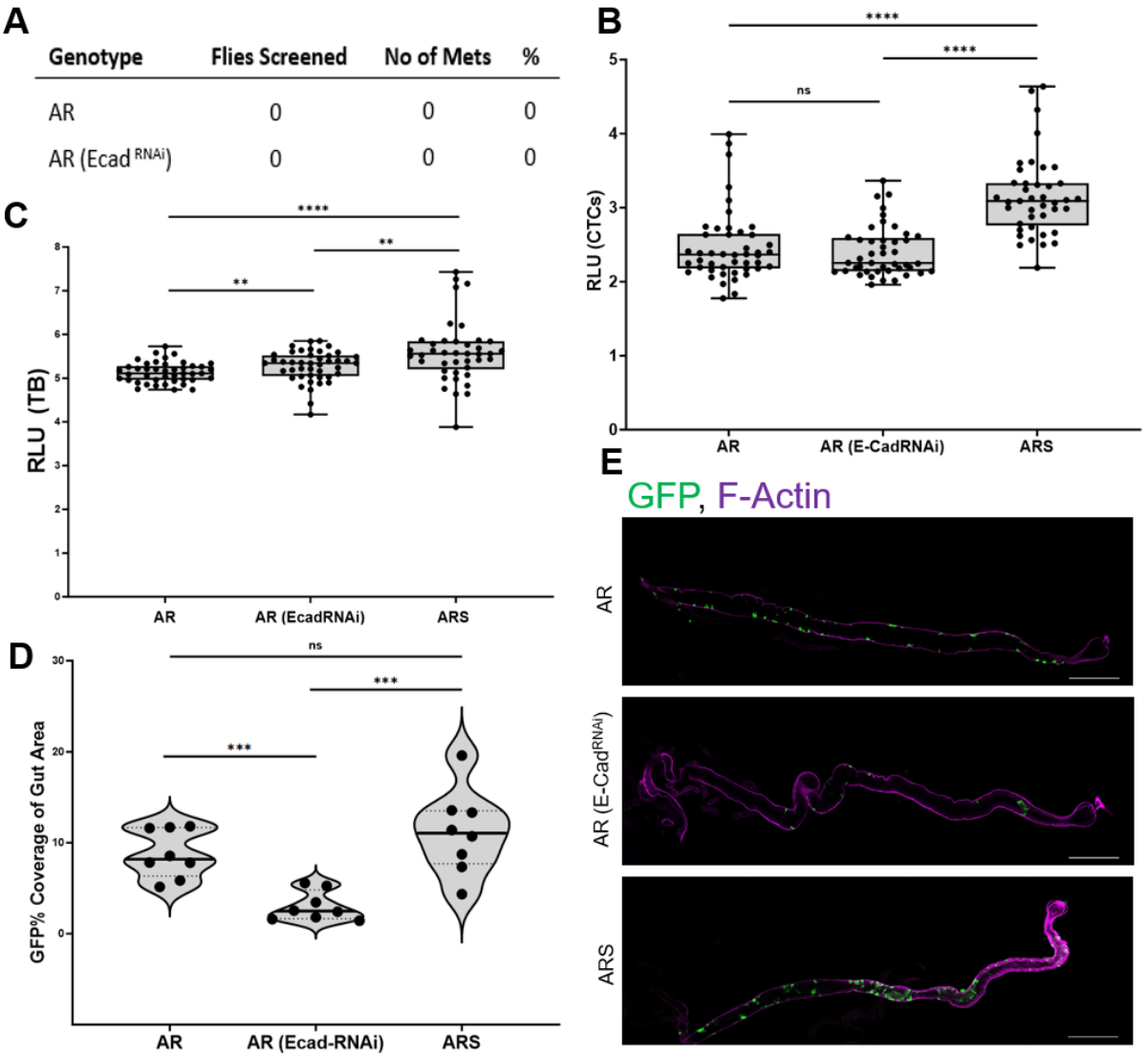

Figure 5.1: (A) Summary table of flies screened and record of secondary tumour formation; **(B)** Quantification of CTC per/fly of the indicated genotypes. AR (n=46), AR-E-Cad^{RNAi} (n=44), ARS (n=41); **(C)** Quantification of TB per/fly of the indicated genotypes. AR (n=43), AR-E-Cad^{RNAi} (n=44), ARS (n=41); **(D)** Quantification of GFP% coverage of gut area per/fly of the indicated genotypes. n=8 for each genotype; **(E)** Representative images of midguts of the indicated genotypes. n=8 for each genotype. Scale bar = 500µm for each genotype. Tissues are stained for GFP (green) and F-Actin (magenta). Statistical comparison of (B-C) was made by Two-Tailed Mann-Whitney presented as median with interquartile range. Statistical comparison of (D) was made by Two-Tailed T-Test presented as mean with interquartile range. $*p < 0.05$; $**p < 0.01$; $***p < 0.001$, $**** p < 0.0001$. All flies were analysed Day 6 PCI, kept at 25°C. RLUs are in Log2 scale.

As repression of E-Cadherin has been shown to almost eliminate midgut tumour growth in an *APC* $^{(-/-)}$ model, I speculated the possibility that the failure to disseminate a large quantity of CTCs may be attributable to decreased tumour size. Therefore, the same individual flies assessed for CTCs were also quantified for TB. Results demonstrated that there is a moderately significant increase from AR in TB. However, not quite at the level of ARS (Fig.5.1C). Paradoxically, when performing quantifications of the GFP+ area of AR$^{E\text{-}Cadherin(RNAi)}$ guts a strong decrease can be compared to AR (Fig.5.1D). It could be theorized that the TB is much larger by virtue of more sizeable MpT tumours, however upon visual inspection of dissected

out guts and MpTs this does not appear to be the case (Fig.5.1E). It could be a result of prevalent micrometastases, unobservable by stereoscope, but this seems implausible given the low CTC count. Given E-Cadherins documented potential as both an oncogene and a tumour-suppressor, it would be worthwhile to perform repeats of these experiments to ascertain if a firmer answer can be attained, or if the current results still hold.

Loss of ADAMTS-A Abolishes Secondary Tumour Formation

Besides loss of E-Cadherin, my prior characterisation also made suggestion of a potential role for ADAMTS-A in destroying the basement membrane, with the outcome being invasive outgrowth. Using an UAS-ADAMTS^{RNAi} put in the ARS background, flies were assessed for impairment of metastasis. Firstly, 200 ARS$^{ADAMTS\text{-}A(RNAi)}$ flies were screened for secondary tumours using a stereoscope throughout the standard ARS cancer progression timeline of 1-14 Days PCI. Resultingly, no secondary tumours could be observed (Fig.5.2). This contrasts with ARS, where a similar sample size yielded 5 flies suffering secondary tumours (2.17%). These findings suggest that loss of ADAMTS, at minimum, eliminates the final step of metastasis.

Genotype	Flies Screened	No of Mets	%
ARS	230	5	2.17
ARS (ADAMTS-RNAi)	200	0	0

Figure 5.2: Summary table of screened flies and record of secondary tumour formation

ADAMTS-A Knockdown in ARS, not AR, Dramatically Reduces Dissemination of CTCs

ADAMTS-A is believed to permit metastasis to occur by creating a gap in the gut, allowing tumour cells to escape and disseminate as CTCs. To determine if ADAMTS-A may be driving metastasis by enabling dissemination of CTCs, a comparison of CTC levels in ARS$^{ADAMTS\text{-}A(RNAi)}$ was made to AR, where CTCs are insufficient to drive metastasis and ARS where metastases do form. Comparison was made Day 6 PCI, where CTC levels coincide with secondary tumour formation and thus are likely to be most relevant. Results reveal that loss of ADAMTS-A results in a dramatic decrease in CTCs compared to ARS, although a strong increase can still be observed compared to AR (Fig.5.3A). It was established in the first chapter that ARS harbour a subpopulation of flies (5-10%) that exhibit far higher CTCs compared to

the rest of the population. The possibility that these are the flies that form metastases was considered. Comparison of results reveal that an almost complete elimination of this minority can be observed following loss of ADAMTS-A, with only 2 flies in the lower range of these extreme values remaining (Fig.5.3B).

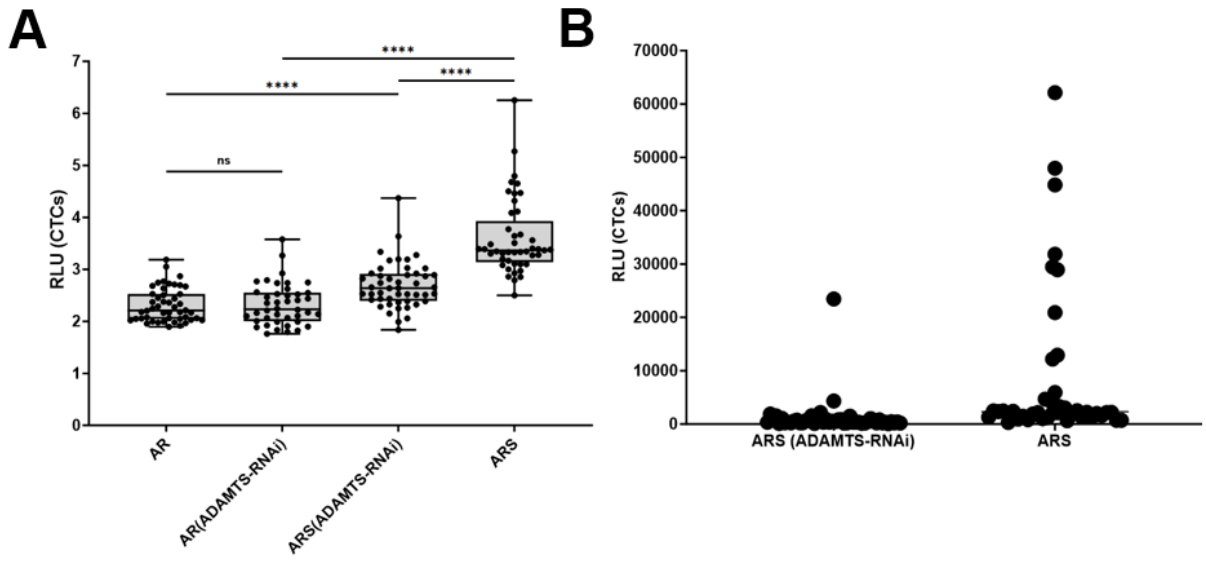

Figure 5.3: (A) Quantification of CTCs per/fly of the indicated genotypes. AR (n=48), $AR^{ADAMTS(RNAi)}$ (n=42), $ARS^{ADAMTS(RNAi)}$ (n=48), ARS (n=45). **(B)** Scatterplot comparison of CTCs per/fly of the indicated genotypes. ARS (n=45), $ARS^{ADAMTS(RNAi)}$ (n=48). RLUs in (A) are in Log2 scale; RLUs in (B) are in raw values. Statistical comparison was made by Two-Tailed Mann-Whitney presented as median with interquartile range. $*p < 0.05$; $**p < 0.01$; $***p < 0.001$, $**** p < 0.0001$. All flies were analysed Day 6 PCI, kept at 25°C.

ADAMTS-A is also expressed in AR tumour cells. However, unlike ARS where ADAMTS-A appears to become secreted, AR tumours possess a nuclear pattern of expression equivalent to WT guts. To gain an indication if it is specifically ADAMTS-As localization and mode of action in ARS that is relevant to dissemination, an additional comparison was made to AR with an $ADAMTS^{RNAi}$ insertion. Results demonstrate that, although loss of ADAMTS-A decreases dissemination in ARS, its impairment in AR guts causes no significant difference in dissemination compared to AR guts where it is intact (Fig.5.3A).

When Regulated by Snail, ADAMTS-A Acts to Increase Tumour Load.

It is possible that loss of ADAMTS-A lowers dissemination by decreasing tumour size, thus resulting in a lesser quantity of cells to be disseminated. To investigate this, a comparison of TB was performed on the same individual flies that were assessed for CTCs. Results reveal that an accompanying dramatic decrease in TB can be seen in $ARS^{ADAMTS(RNAi)}$ compared to ARS (Fig.5.4A). Although, the TB still remains at a much higher level compared to AR.

However, by assessing the mean fold change in CTC and TB values from ARS$^{ADAMTS\text{-}A(RNAi)}$ to ARS, a more dramatic CTCs fold change increase can be discerned compared to the TB fold change increase (Fig.5.5B). This demonstrates that, although loss of ADAMTS-A causes a decrease in both CTC and TB, the decrease in CTCs is far more considerable and unlikely just a function of decreased tumour size.

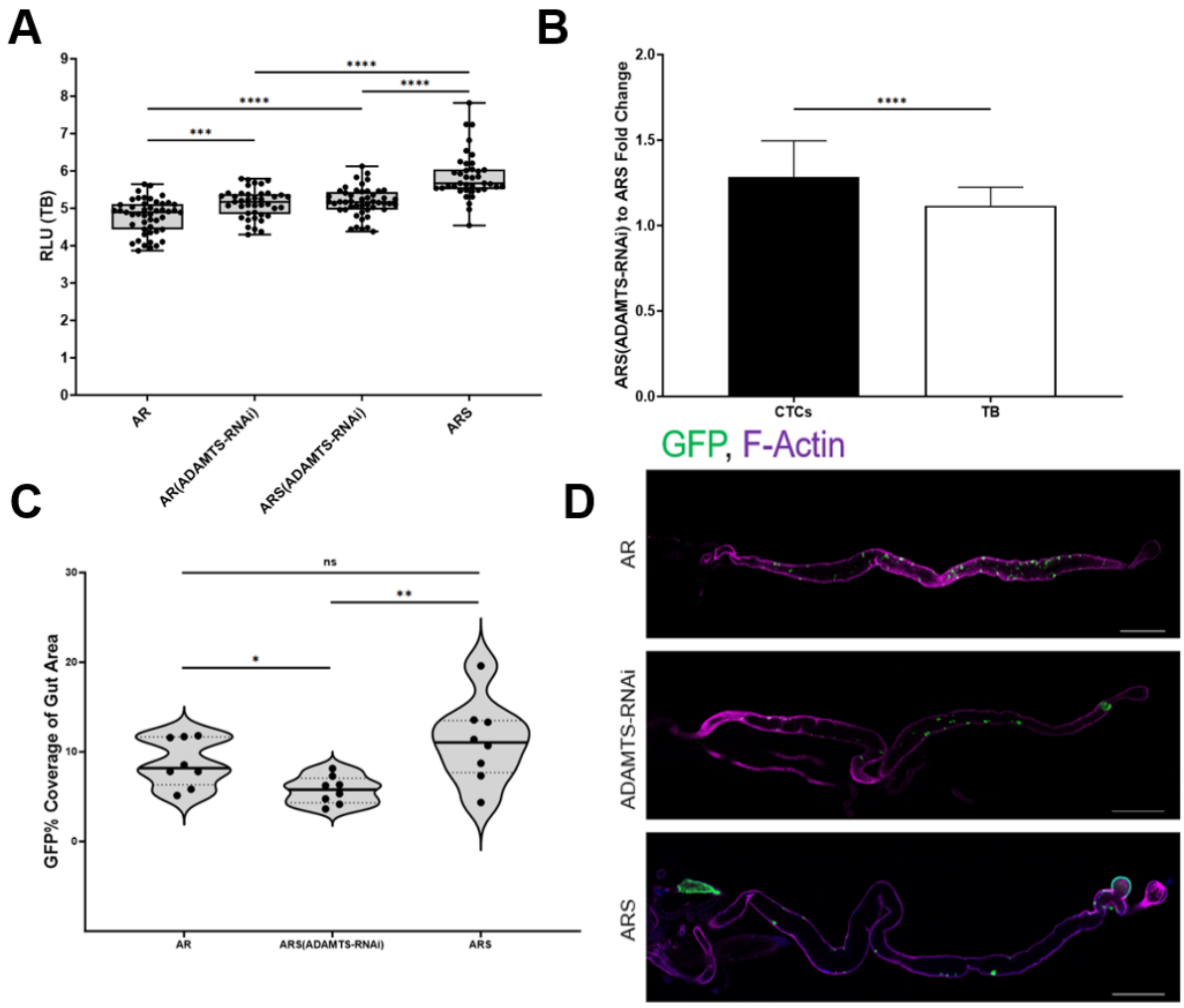

Figure 5.5: (A) Quantifications of TB per/fly of the indicated genotypes. AR (n=48), AR$^{ADAMTS\text{-}A(RNAi)}$ (n=41), ARS$^{ADAMTS\text{-}A(RNAi)}$ (n=48), ARS (n=39); **(B)** Quantifications of CTC and TB Mean Fold Changes (Log2) from AR to ARS. CTCs (n=45), TB (n=39); **(C)** Quantification of GFP% coverage of gut area per fly of the indicated genotypes. n=8 for each genotype; **(D)** Representative images of midguts of the indicated genotypes. Scale bar = 500µm for each genotype. Tissues are stained for GFP (green) and F-Actin (magenta). Statistical comparisons of (A-B) were made by Two-Tailed Mann-Whitney and presented as median with interquartile range. Statistical comparisons of (C) were made by Two-Tailed T-Test and presented as mean with interquartile range. $*p < 0.05$; $**p < 0.01$; $***p < 0.001$, $****$ $p < 0.0001$. All flies were analysed Day 6 PCI and kept at 25°C. RLUs are in Log2 scale.

To determine if the decrease in TB relates to a decrease in the size of gut tumours, an additional comparison was made of GFP coverage of the gut. Results demonstrate that, ARS$^{ADAMTS(RNAi)}$ guts not only exhibit significantly decreased GFP coverage compared to ARS, but also AR where the overall TB was lower (Fig.5.5C). It is conceivable that ARS$^{ADAMTS(RNAi)}$ guts could

have a lower gut tumour load compared to AR, but nonetheless have an overall higher TB by virtue of increased MpT tumour size. However, by visual inspection of $ARS^{ADAMTS(RNAi)}$ guts this does not appear to be the case as MpT tumours could not be observed (Fig.5.5D). This paradox may be attributable to the sample size of 8 being insufficient to capture the full range of values. Curiously, although loss of ADAMTS-A in AR has no significant bearing on dissemination, a powerful increase in TB can be observed in the same flies. Put together, these findings suggest that ADAMTS typically represses tumour growth, except when influenced by Snail where the opposite can be observed.

Knockdown of ADAMTS-A Results in A Loss of Invasion Out of the Midgut.

The decrease observed in dissemination following knockdown of ADAMTS-A raises the question of how ADAMTS-A is acting mechanistically to promote dissemination. As of yet, ADAMTS-A has no established substrate. However, as ADAMTS-A becomes dysregulated at the same site that laminin is lost, it can be inferred that it either proteolyzes laminin directly, or some other BM protein that supports laminin and indirectly causes its collapse. To investigate this, 200 $ARS^{ADAMTS(RNAi)}$ guts were screened for laminin breaks within the Days 1-14 PCI. Resultingly, no breaks could be observed (Fig.5.6A-B). By contrast, when ARS guts were screened within the same timeline, 2.55% (n=10) guts with breaks could be observed. It was previously established that some tumour cells invade out onto tracheal tubules. Therefore, the same flies were also screened for this phenotype. Unlike ARS, where 0.77% of flies exhibited this phenotype (n=3), this was completely unobserved in $ARS^{ADAMTS(RNAi)}$.

A

Genotype	Flies Screened After Invasive Phenotype		No of Observations By Invasive Phenotype		% By Invasive Phenotype	
	BM Break	Tracheal Invasion	BM Break	Tracheal Invasion	BM Break	Tracheal Invasion
ARS	392	392	10	3	2.55	0.77
ARS(ADAMTS-RNAi)	200	200	0	0	0	0

B GFP, Laminin

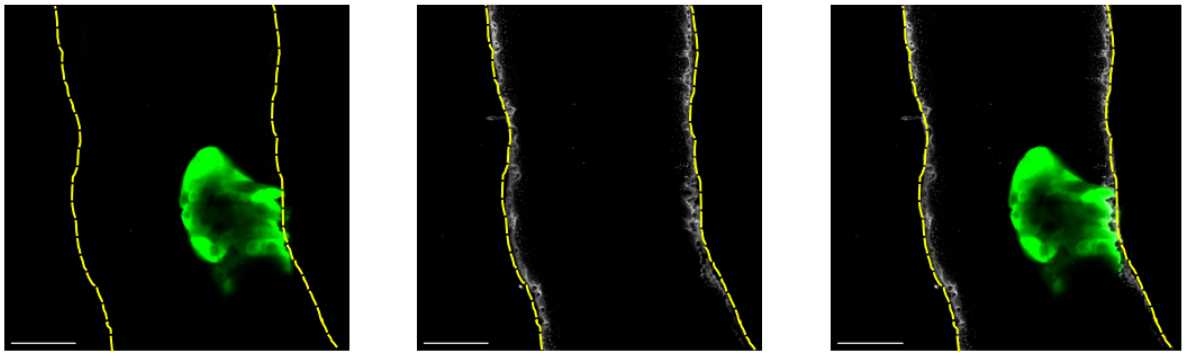

Figure 5.6: (A) Summary table of screened flies and record of invasive phenotypes; **(B)** Representative image of intact basement membrane in ARS-ADAMTS-A^{RNAi}. n=6 tumours from 6 guts. Scale bar = 40µm. Tissues were stained for GFP (green) and Laminin (grey). Yellow dashed outlines indicate the boundaries of the gut.

Discussion

Working on from the previously established association between metastatic outgrowth and dysregulation of E-Cadherin and ADAMTS-A, this chapter set out to assess if the aberration observed to these proteins are causally responsible for initiating metastatic dissemination. E-Cadherin was targeted with an RNAi in the AR background to determine if it could phenocopy the metastatic outcomes observed in ARS. Resultingly, this manipulation failed to increase dissemination, but rather resulted in conflicting results regarding tumour size. These findings demonstrate that despite EMT-TFs primary action being the transcriptional repression of E-Cadherin, they cannot be reduced to a simple insular repression of protein expression. Nontheless, E-Cadherin could still be a critical—and indeed necessary—change needed for dissemination to occur. Given the role of BM degradation in metastatic progression, it is likely that both loss of E-Cadherin and proteolysis of the BM constituents are needed.

It is conceivable that complete repression of E-Cadherin is actually counterproductive for metastasis. As alluded to before, when a Ras^{V12} mutant is introduced to all the cells of the midgut, metastatic progression necessitates delocalization of E-Cadherin, not repression, in order to support the employment of MMP1 at invasive protrusions [154, 186]. In lieu of these findings, complete repression may prevent protease activity from occurring at the invasive front of metastatic ARS flies. Moreover, with a complete loss of adhesion it could become impossible

to support the migration of collective CTCs, which may be the most potent in terms of metastatic potential.

Although, E-Cadherin failed to promote metastasis in AR, $ARS^{ADAMTS(RNAi)}$ gave more promising results. The complete loss of macrometastasis and invasion—as well as the powerful loss of dissemination—following loss of ADAMTS-A, support its possible role as a metastatic effector. Moreover, as flies were negative for secondary tumours over a longer timeline—Days 1-14 PCI—a more durable revocation of the final step of metastasis, macrometastasis, could be inferred. As macrometastasis likely depends on preceding invasion and dissemination, it is likely that a robust loss of these phenotypes occurs within this range as well. However, this cannot be said with certainty. Moreover, given the attendant decrease in TB, it is plausible that the standard progression observed in ARS is pushed back following loss of ADAMTS-A. This would imply that screening for metastatic behaviours such as BM breaks and secondary tumour formation within that timeline, may have failed to capture a potential delayed onset of metastasis. With more time, a set of urgent experiments would be to establish a timeline for $ARS^{ADAMTS(RNAi)}$ then screen for metastatic phenotypes, including CTCs, within that range. In particular, if CTCs remain low, while the TB rises, this would imply there is a durable repression of metastasis that is independent of tumour size.

It is also interesting how loss of ADAMTS-A in AR causes an increase in tumour burden. Particularly, as ADAMTS proteases have been linked to anti-tumour and pro-tumour capabilities depending on context and cancer type [190]. Metalloproteases are typically conceived of as ECM regulators; however, increasing evidence also support a role for these proteases in regulating gene expression [193]. As ADAMTS-A is expressed in the nuclei of all cells, including WT cells, it is conceivable that ADAMTS-A may be partaking in stem cell homeostasis through growth suppression when not delegated to the ECM. Indeed, the ubiquitous expression of ADAMTS-A in WT guts raises the question of what the physiological role of ADAMTS-A is in baseline conditions.

Put together, ADAMTS-A and E-Cadherin appear to play important roles in tumour growth and metastatic outgrowth. ADAMTS-A especially, appears to be a promising potential driver initiating metastasis. More work needs to be done to assess if ADAMTS can be firmly grounded as a metastatic driver. Nontheless, the results presented herein, establish that loss of ADAMTS-A, at minimum, temporarily eliminates metastasis. This represents one of the few instances establishing a causal role for an ADAMTS protein in driving metastasis in-vivo.

Chapter VI

General Discussion

Introduction

The aims of this project were to order metastatic events into a timeline; use that timeline to inform a subsequent characterisation of invasive behaviours leading up to those events; then finally utilise the characterisation to identify candidate metastatic drivers that can be assessed by genetic interrogation. An overall endpoint was ambitioned, being the validation of a metastatic driver downstream of EMT that meets the criterion for a relevant drug target in the treatment of metastasis. I hypothesized that such a driver would relate to regulation of cell polarity and/or ECM remodelling.

Through my efforts, I was able to establish a standard metastatic progression scheme with alterations to cell polarity and the ECM coinciding with invasion out of the midgut. In particular, three central changes were found to be unique to invasive tumours and coincide at the site of the invasive edge: (1) Loss of the cell adhesion molecule E-Cadherin; (2) Loss of the BM component Laminin; (3) and dysregulation of the secreted protease ADAMTS-A. With the latter resulting in a temporary—potentially durable—elimination of metastasis following knockdown. These findings affirm my hypothesis that downstream drivers of EMT would relate to changes to cell polarity and/or ECM remodelling. Moreover, from these findings a working model of EMT can be proposed, whereby: E-Cadherin is lost, ADAMTS-A becomes relocated from the nucleus to the membrane, where it then becomes secreted and subsequently acts to proteolyze a critical BM component (Fig.6.1).

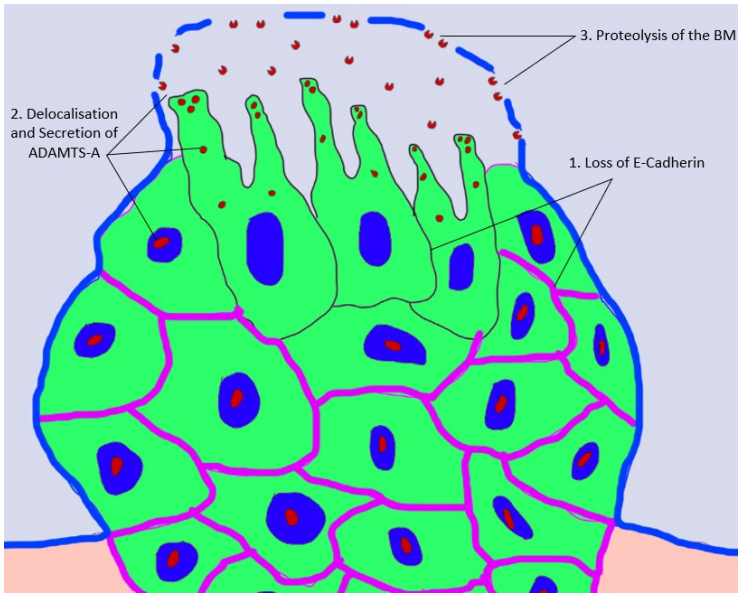

Figure 6.1. Working model of ARS mediated EMT: In an undefined order: E-Cadherin (represented in purple) becomes lost. ADAMTS-A (represented in red) becomes relocated from the nucleus, carried by the secretory pathway, and ultimately deposited to perform proteolysis on a critical BM component.

Despite resulting in some important findings, the current data raises some pressing questions relating to the disproportionate frequency of different metastatic events, as well as the role of disseminating CTCs. Moreover, investigation into E-Cadherin and ADAMTS-A revealed some interesting findings deserving of further research. Finally, the execution of the project exposed some shortcomings in experimental procedure that need to be addressed. Below, I will discuss, in more detail, some of the interesting themes and unresolved questions that emerged from this project: the strengths and weaknesses of my experimental strategy; as well as important future directions to resolve the uncertainties that have emerged. Moreover, these topics will be discussed with an ongoing contextualization of how my work has contributed to the field.

Arranging Metastatic Events into a Timeline

I set as my first aim to define the timeline of the ARS phenotype by arranging previously established metastatic phenotypes into a sequence of events. Through these efforts a cancer progression scheme was established with increasingly higher CTCs and TB rates occurring within a range of Days 1-10 PCI. From there these rates would decline with an exponential decrease in fly survival. The occurrence of secondary tumour formation could be seen to centre around Day 6 PCI, occurring at a low rate of 2.17%, and coinciding with increased dissemination of a population of CTCs which include collective and single cell entities. The rate of secondary tumour formation could then be found to track with a nearly equivalent rate of 3.35% of flies that undergo invasion: with the two therefore being likely to relate. However, what lies in between—the dissemination of CTCs—raises interesting questions: in particular, whether macrometastasis is a result of CTC quantity or CTC quality.

Is Macrometastasis a Function of CTC Quantity or CTC Quality?

As macrometastases derive from CTCs, it can be reasoned that secondary tumour formation is more probable with increased quantities of CTCs. However, if this is true, this raises the question of why secondary tumour formation centres around Day 6 PCI when CTCs continue to increase up until Day 9 PCI? If macrometastasis is a function of CTC quantity one would expect the high point of secondary tumour formation to occur in the period following Day 9 PCI. It is possible that as such a large fraction of flies have high TBs at that timepoint, most flies with higher level CTCs will have died off by the time secondary tumours have time to form. By contrast, the 5-10% of flies identified with higher level CTCs at earlier time periods, by virtue of having lower TBs, are given time for those CTCs to take hold at distant sites and grow to visible macrometastases. To challenge this assumption, an interesting future

experiment would be to screen for flies that have suffered metastasis and quantify their CTCs specifically. If their CTCs lie at a far higher level than most flies, it would suggest CTC quantity may be relevant for macrometastasis. Moreover, haemolymph can be extracted from flies Day 9 PCI and become injected into wild-type flies: if the formation of secondary tumours is a result of CTC quantity, these flies should form secondary tumours as fly death from primary tumour growth is no longer a barrier. If however, secondary tumours are not observed, secondary tumour formation is unlikely to be solely a function of CTC quantity.

Isolation of CTCs on Day 6 PCI demonstrates the presence single and collective cell clusters, with some single cells phagocytosed by haemocytes. It is possible that the formation of secondary tumours, around Day 6 PCI, relates to a relative enrichment of collective clusters which have greater metastatic potential. Co-localisation of Serpent to single cells, and not collective clusters, suggests these cells evade immune surveillance. However, it is possible other pro-invasive traits may be acquired as well such as resistance to apoptosis or CSC characteristics.

To determine if the occurrence of macrometastasis around Day 6 relates to an enrichment of collective clusters, the haemolymph of a large quantity of flies should be extracted at daily intervals and screened for the ratio of different CTC subtypes. If there is a correlation between collective clusters and secondary tumour formation, these cells can then be characterised by staining for pro-invasive behaviours such as apoptosis resistance with a Caspase-3 stain or examined by RT-qPCR for CSC genes such as Nanog or CD44+ [194, 195]. If a CSC gene is identified, an UAS construct of that gene can be created and put in the ARS background to see if it results in increased secondary tumour formation. Finally, to more definitively relate collective clusters to macrometastasis, the haemolymph of flies at earlier dates can be injected into wild-type flies and assessed for improved metastatic potential compared to later day haemolymphs.

Another outstanding question is how the different CTC subtypes relate to loss of E-Cadherin and Laminin. E-Cadherin was observed to be completely lost in the flies that were analysed, but it is probable that there are also invasive tumours that have only partially repressed E-Cadherin. Moreover, whereas large BM breaks could be seen to occur at a low rate of 2.55%, it is possible there may also be microtears unvisible by confocal. It is possible that collective clusters may migrate through large breaks and partial repression; whereas, single cells additionally can migrate through microtears and complete repression. An interesting future

endeavour would be to live image dissemination in alive flies to relate the dissemination of single and collective CTCs to BM breaks. Multiple live-imaging platforms have been developed for the adult midgut, with some having the capacity to image alive flies for as long as 16hrs at a single cell level [196, 197, 198]. I can envision an experiment where flies are screened under a fluorescent stereoscope in the days leading up to Day 6 PCI, with the flies with the most aggressive growth being selected for live imaging. Sites with single or collective cell migration will then be recorded, with guts from the same flies subsequently being dissected out and stained for laminin to assess for BM breaks at the same site.

Identification of Downstream Drivers of Snail Induced Metastasis

As my second aim, I set forth to perform a cell-biological characterisation of the tumours of the gut, with the object of identifying candidate proteins that, as a third aim, can be assessed as metastatic effectors by genetic interrogation. Through my efforts I identified two proteins that, as hypothesized, relate to cell polarity and ECM remodelling: E-Cadherin and ADAMTS-A respectively. Both raise interesting questions.

E-Cadherin

Aberration of E-Cadherin is likely the most studied change associated with metastatic outgrowth, with its dysregulation occurring in most, almost all, instances of EMT [199]. Indeed, Snail binds to the E-Cadherin enhancer region through its Zinc-Finger domains to repress its transcription [200]. However, Snail exhibits wider transcriptional control than just E-Cadherin. Likewise, given the diverse input of other regulators, E-Cadherin is rarely entirely and homogenously repressed in all cells. These findings are reflected in the addition of Snail to the AR background only being observed to cause loss of E-Cadherin to the cells at the invasive front of a very small subset of tumours. Moreover, when an RNAi is raised again E-Cadherin in the AR background, tumours fail to phenocopy ARS, and no increase in dissemination is observed. These findings are in keeping with the operation of Snail not being reduced to a simple global repression of E-Cadherin.

Given E-Cadherins well documented role in retaining cytoskeletal stability and cell-cell adhesion, it is no surprise that E-Cadherin is lost during ARS mediated metastatic outgrowth. However, interestingly knockdown of E-Cadherin in AR resulted in an increase in the whole fly tumour burden. These findings imply that the tumour suppressor role of E-Cadherin is not

limited to metastasis, but also regulation of primary tumour growth. From these cumulative findings, two outstanding questions merit further discussion: (1) What is E-Cadherins role in regulating primary tumour growth? (2) Why does loss of E-Cadherin only occur in a small subset of tumours.

E-Cadherin as a Suppressor of Tumour Growth

As previously discussed, the role of E-Cadherin in midgut tumorigenesis is diverse and has been associated with both repression of metastasis and regulation of primary tumour growth [185]. The control of primary tumour growth can go in both directions: in an APC1/2 $^{(-/-)}$ midgut tumour model, loss of the extracellular adhesion motifs dramatically reduces tumour load; conversely, mutation of the association motif which binds p120 catenin drives tumour growth [185]. E-Cadherins paradoxical role as both a negative and positive regulator of primary tumour growth is not unique to *Drosophila.* Indeed, in mammalian systems E-Cadherin mediated extracellular adhesion has been found to mediate pro-survival signalling that confers tumour resistance to apoptosis [212]. However, loss of E-Cadherin has also in other circumstances been found to drive cell proliferation by dissociating B-Catenin from its association with E-Cadherin. With B-Catenin subsequently proceeding to enter the nucleus and upregulate proliferation [213].

It is possible that the increase in tumour burden observed following E-Cadherin knockdown may be due to dissociation of B-Catenin. Therefore, it would be interesting to stain for B-Catenin and assess if increased nuclear staining can be discerned. It is also conceivable that Ras^{V12} may be conferring resistance to apoptosis: a Ras^{V12} induced feature which has been observed in numerous *Drosophila* models of tumorigenesis [100, 214]. This induced resistance to apoptosis may explain why there is no big decrease in tumour burden following loss of extracellular adhesion, as is the case in the APC1/2 model.

Why is E-Cadherin Only Lost in a Small Subset of Tumours?

As Snail is a transcriptional repressor of E-Cadherin, it begs the question of why constitutive activation of Snail only downregulates E-Cadherin in small subset of tumours, and specifically the cells of the invasive front. It is possible that with the exception of invasive tumour cells, Snail fails to bind to the E-Cad enhancer due to repression by other regulators. To rule out such a possibility, a method of assessing DNA-Protein interaction may be required such as Chromatin Immunoprecipitation to validate that Snail is binding to its enhancer. However, this would not provide a mechanism for why invasive tumour cells overcome such repression.

Moreover, it would not rule out other factors regulating E-Cadherin expression other than by repression of the transcriptional control of Snail. Unfortunately, gaining a complete picture of the regulatory network of such a critical gene as E-Cadherin, and its relation to Snail, would represent an unfeasible challenge, far outside the scope of this project.

ADAMTS-A

Proteases feature a large catalogue of pleiotropic molecules, encompassing an extensive network of substrates, inhibitors, and homologues. Although, lines of experimental data have established a role for MMPs in driving metastatic outgrowth, an equivalent causal role has rarely been supported for an ADAMTS protease [81, 201]. The finding that genetic ablation of ADAMTS-A, at minimum, causes a transient loss of metastasis, represents one of the few instances evidencing a causal role for an ADAMs in inciting metastasis in-vivo [192]. This is of interest, as given ADAMTS-As status as an enzyme, it may present itself as a promising target for the therapeutic treatment of EMT-induced metastasis.

Despite genetic evidence for ADAMTS-As contribution, there are four outstanding questions: (1) Does loss of ADAMTS-A eliminate metastasis, or only delay it? (2) What is the mechanism by which ADAMTS-A may be driving metastatic outgrowth? (3) Does ADAMTS-A become secreted and if so, how does it become moved from the nucleus? (4) What is the physiological role of ADAMTS-A in wild type guts? As the first point was already discussed in the preceding chapter—with suggested future experiments—a more focused discussion of the other three points will be elaborated below. The relationship of ADAMTS proteins to EMT and their potential as a drug target will also be discussed.

What is the Mechanism of ADAMTS-A in Driving Metastasis?

As of yet no validated substrate has been established for ADAMTS-A. Therefore, it is difficult to speculate on the mechanism of action by which it may be driving metastatic outgrowth. Although, as ADAMTS-A becomes dysregulated at the same site where laminin is lost—and ADAMTS-A knockdown results in a loss of laminin deterioration—it can be inferred that laminin is its substrate. However, in one study ADAMTS-A was knocked down in the perineural cells of third instar larval CNS. Following this manipulation, the BM that couples to the perineural cells was observed to be enriched in Collagen IV as assessed by an GFP reporter and western blotting [215]. By contrast, upregulating ADAMTS-A with an UAS resulted in a marked decrease in Collagen IV.

Although, differences in the quantity of laminin and perlecan could not be observed, staining revealed that these proteins exhibited a more punctate and irregular appearance following ADAMTS-A knockdown. This contrasted with the WT control, where laminin and perlecan had a more smooth and layered appearance. Although, this study did not establish Collagen IV as a direct substrate of ADAMTS-A, it nonetheless sets Collagen IV aside as a strong candidate. Interestingly, the disruption observed to laminin and perlecan is suggestive of the possibility that loss of Collagen IV may destabilize other BM proteins, even though they are likely not the target of proteolysis. From these findings it can be theorized that the loss of laminin observed in ARS may be the byproduct of a more general BM instability induced by Collagen IV loss.

To identify the substrate of ADAMTS-A, I can conceive of two critical experiments: (1) homogenizing ARS midguts, then using western blot to identify cleavage events; then (2) perform CO-IP on ADAMTS-A and its candidate substrate to identify protein-substrate interactions. Given the infrequency of tumours with invasive tumours, such experiments would be challenging to set up. However, if more thorough experimentation determines that ADAMTS-A definitively drives metastasis, and not merely delays it, such experiments may be worth exploring.

Does ADAMTS-A Become Secreted and if so, How?

Another outstanding question relates to whether or not ADAMTS-A becomes secreted at the invasive front. Even though this is reasonably inferred, I have no experimental data to support this. In the collectively migrating cells of the embryo salivary gland, ADAMTS-A has been found to overlap with the E.R and the Golgi and co-localize with the apical vesicle markers Rab11 and CSP2 [168]. These findings support a role for ADAMTS-A secretion during collective cell migration. Similar stains should be performed to investigate if the same thing could be occurring during ARS metastasis. Knockdown of some of these proteins could then be utilised to sort ADAMTS-A into a pathway by epistasis. Coupled with the identification of a substrate, these experiments should aid in providing a mechanistic explanation for the action of ADAMTS-A.

What is the Role of ADAMTS-A in Wild Type Guts?

Even if a mechanism could be provided for ADAMTS-A in driving metastatic outgrowth, it remains to be answered what the role of ADAMTS-A is in the nuclei of wild type guts. The occurrence of an extracellular protease being expressed in the nuclei is not unusual [216]. This includes ADAMTS proteases. For instance, the secreted mammalian protease ADAMTS-1—

which is in the same structural family as ADAMTS-A—has been identified to be expressed in the nuclei of the breast cancer cell lines MCF7 and MDA-MB-231, as well as the normal like breast cell line: MCF10-A. In these cells ADAMTS1 acts to cleave aggrecan filaments in the nucleus, demonstrating a non-canonical role distinct from its usual role of extracellular proteolysis [217].

Other nuclear roles for extracellular matrix proteases more broadly include activities related to such processes as transcription, proliferation, and chromatin remodelling [216]. Unfortunately, given this diversity it is difficult to infer the role of ADAMTS-A in the nuclei of WT guts. With more time an interesting experiment would be to knock down ADAMTS-A in WT ISCs then assess for changes in the self-renewal rate of ISCs. This can easily be assessed by quantifying the GFP% coverage of the guts and comparing them to WT. If a significant change is observed, ADAMTS-A is likely to be playing an important physiological role in the regenerative health of the gut. Unfortunately, obtaining a more exact answer to the role of ADAMTS-A in the gut remains outside of the scope of this project.

ADAMTS, EMT, and Drug Targeting

EMT-TFs are typically considered to be poor drug targets due to a lack of affinity for drugs and the presence of a great number of homeostatic life-sustaining genes that may be disturbed by inhibiting EMT. Downstream targets are therefore sought after for more selective, and clinically beneficial, inhibition of EMT outcomes. The relationship of EMT and proteases is well established, with some being directly transcribed by EMT-TFs [61, 64]. Moreover, proteases are notoriously good drug targets, with approximately 24% of all drug targets being proteases [206]. MMPs have thus far been the idealized proteases for the downstream therapeutic targeting of EMT. However, these proteases are highly pleiotropic, and homologs are often very structurally similar [82]. Therefore, many of the initial MMP inhibitors developed thus far have fallen through due to intolerable adverse effects, in particular bone and joint pathologies [207].

Despite facing somewhat similar challenges, ADAMTS proteins have been found to exert comparatively more focused roles, and are considered to be less subject to issues of non-selectivity [208, 209]. Although, the expression of ADAMTS-A in the nuclei of WT guts makes suggestion of the possibility that ADAMTS-A may also be exerting important physiological roles. If true this would suggest that, like the MMPs, ADAMTS proteases are limited as therapeutic targets due to the strong possibility of intolerable side effects. This possibility

makes it all the more important to assess flies for effects on survival and self-renewal following ADAMTS-A knockdown.

Project Limitations

As hypothesized, my research was able to relate cell polarity and ECM remodelling to metastatic progression, with loss of E-Cadherin and BM appearing to be particularly critical changes. Nonetheless, I was challenged with two reoccurring experimental problems that impeded or hindered results. Firstly, the infrequency of ARS flies exhibiting invasive phenotypes presented itself as a challenge for obtaining high-enough sample sizes, by which the most interesting changes could be studied. It is possible that this may be attributable to flies dying before most secondary tumours have time to form; although if this is the case, the metastasis model is subject to much of the same challenges as murine models of metastasis. A second issue related to staining of the gut being a challenging ordeal: with most antibodies resulting in poor and non-robust stains, as well as diverse fixation protocols all exhibiting unreliable results. By refining protocols many stains could be improved with time, however a far from trivial proportion continued to exhibit difficulties. The combination of these two challenges resulted in a large amount of time and samples being required in order to perform needed experiments.

Another non-experimental challenge relates to cancer heterogeneity. Although all the important changes leading up to metastasis could be reasoned to occur prior to Day 6 PCI, there was nonetheless a remarkable degree of heterogeneity in terms of tumour progression occurring within the confines of those preceding days. This presented itself as a significant impediment in terms of inferring when cell biological changes in gut tumours occur as a sequence of events, because any given identifiable change could be seen to occur at different days for different tumours at varying levels of development. Especially, changes that occur within the rare subset of tumours that undergo metastasis: loss of E-Cadherin and Laminin, for example, were found to be novel changes coinciding in space, however I was unable to sort out which change occur first.

Future Directions

Although, the heterogeneity of flies and infrequency of metastasis makes sorting events into a timeline a considerable challenge, it is not an unresolvable one. By co-staining markers, I can screen for tumours where the one marker is expressed, and not the other, and use that to infer

an order of events; even though the succession of events may fall under diverging days for different flies. However, given the infrequency of metastatic flies, a very large sample will likely be required for co-staining to capture which changes come first in that particular subset. Although, by taking care to prioritize the most pertinent stains, this should be a feasible endeavour by rearing high enough sample sizes. In particular, as E-Cadherin, ADAMTS-A, and Laminin, appear to be novel changes occurring in metastatic tumours; it would be of interest to determine how they occur in a sequence of events.

A reoccurring problem that is in need of an answer, is the question of whether macrometastasis is a function of CTC quantity or CTC quality. The failure of secondary tumours to form in later days when CTCs are higher. As well as the discrepancy between the frequency of high-scale dissemination and invasive phenotypes of the gut, suggest that high CTC quantities are insufficient, and maybe even unnecessary, for macrometastasis. However, it is possible that these challenges can be explained away by flies dying before secondary tumours can form, and the low frequency of invasive gut phenotypes being due to unobservable microtears by single migrating CTCs. Unfortunately, many invasive behaviours may result in rapid dissemination of cells from the gut. Therefore, as soon as cells loss their adhesions and are exposed to the haemolymph; there is a strong possibility that they will be washed off. This may make some of the most potentially interesting phenotypes unavailable for analysis by histology of the gut, including: complete versus partial loss of E-Cadherin, the potential loss of protrusions, and delocalization of protease activity.

To begin to answer many of these outstanding questions, I believe attention will need to be redirected from the guts to CTCs isolated from the haemolymph. These cells can then be stained for E-Cadherin, Proteases, Apoptosis, and CSC markers, to tease apart important details that can’t be captured from tumours of the gut. Moreover, it might delineate if there is a difference in CTC subtypes in terms of metastatic potential. Moreover, coupling immunohistochemistry to live-imaging protocols should aid in providing answers to the ratio of single vs collective CTCs and whether there is a possibility of microtearing resulting in no visible BM loss: and thus, the possibility that there are invasive phenotypes I may have missed.

Conclusion

Given the alarming increase in cancer, there is a pressing need to develop new therapies. Especially, for the treatment of metastasis, which is responsible for 90% of cancer deaths. This in turn requires a deeper understanding of its underlying mechanisms, which currently remain poorly understood. My project set forth to identify mechanisms by which EMT drives metastatic progression in a *Drosophila* model of colorectal cancer that was recently developed. Through my efforts, I identified numerous changes coinciding with EMT induced metastatic outgrowth, with ADAMTS-A appearing to play a particularly critical role. ADAMTS proteins have been established to be involved in human metastatic progression, with great potential as drug targets. However, there is little experimental evidence demonstrating a causal role for ADAMTS in driving metastasis in-vivo. By evidencing that loss of ADAMTS-A disrupts metastasis in ARS flies, I have made an important contribution to our understanding of the metastatic potential of ADAMTS. A number of shortcomings and lingering discrepancies remain, including more work to establish the mechanisms of ADAMTS-A and if its repression results in a durable loss of metastasis. Nonetheless, I contend that I have demonstrated that the *Drosophila* midgut is a relevant system for modelling metastatic progression, with proven worth in identifying relevant targets with clinical potential in the targeting of metastasis: one of our number one killers.

Summary of Research Findings

1. A standard ARS cancer progression scheme occurs, whereby the whole-body tumour burden and dissemination of CTCs increase up until Day 10, after which an exponential decrease can be observed, as flies begin to die in large numbers.
2. The entire metastatic cascade is completed within Day 6 and coincides with an enrichment of CTCs in the haemolymph, which contains single and collective cell entities. Whether CTC quantity or the properties of CTC subtypes have a bearing on the likelihood of macrometastasis remains undetermined.
3. Large-scale dissemination occurs at a higher frequency than macrometastasis and does not correlate with whole body-tumour burden, which encompasses more than just primary tumour growth.
4. Invasion through the midgut features BM deterioration and tracheal mediated outgrowth, is regionalized to specific sites, and occurs at a similar frequency to macrometastasis, but not large-scale dissemination. The possibility of invasion through BM microtears, unvisible by confocal, cannot be ruled out.
5. ADAMTS-A is upregulated in ARS, becomes dysregulated at the site of BM breaks, and following genetic ablation results, at minimum, in a temporary elimination of metastasis.
6. Numerous alterations to primary tumour cell polarity can be observed, such as delocalization of DLG and F-Actin. However, only loss of E-Cadherin is unique to metastatic tumours of ARS and co-localizes at the site of BM breaks and dysregulation of ADAMTS-A. Experimental knockdown of E-Cadherin in AR fails to phenocopy ARS but has conflicting results on tumour size.

Acknowledgements

I owe many my thanks. Id like to extend my gratitude to my supervisor, Kyra Campbell, whose support and guidance, allowed me to explore my interests in basic biology and grow as a junior scientist. I have learnt a great deal having Kyra as a supervisor and role-model. I would like to thank my colleagues for fostering an intellectual, jovial, and encouraging lab environment. Our senior postdoc, Andrew Plygawko, for setting a good example, encouraging my ideas, and providing thoughtful advice on my project. Joanne Sharpe, who taught me a lot about *Drosophila* husbandry, encouraged my interests in writing, and whose thesis gave clues for my own writeup. Jamie Adams, who showed me the ropes around the lab, and whose gregarious nature contributed to a light-hearted working environment. Eddie Shohei Kan, for teaching me important skills on using the confocal, and for providing me wonderful company during the lonely out-of-hours. Jason Morgan, whose instinct for diligence and precision, taught me a lot about good science. Our lab technician, Rachid, for his friendly demeanour and assistance around the lab.

I would also like to thank our collaborator, Andreu Casali, for providing sage advice and sending needed fly lines. My scientific adviser, Emily Noel, for giving important feedback from a non-*Drosophila* perspective. My pastoral adviser, Elena Rainerio, for thoughtful comments on the ADAMTS-A phenotypes. Natalia Bulgakova, for providing valuable feedback during lab meetings. Like all research, this thesis stands on the shoulders of others: O'Martorell et al, *Conserved Mechanisms of Tumorigenesis in the Drosophila Adult Midgut*, which established the APC-Ras model. Campbell et.al, *Collective cell migration and metastases induced by an epithelial-to-mesenchymal transition in Drosophila intestinal tumours*, which developed the APC-Ras-Snail model. I must also acknowledge the work of Jason Morgan and Jamie Adams, which made up most of the first results chapter. Finally, I must extend my sincere gratitude to my friends and family, whose unwavering love, patience, and support, sustained this thesis.

References

1. American Cancer Society. Global Cancer Facts & Figures 4th Edition. Atlanta: American Cancer Society; 2018.
2. Ahmad AS, Ormiston-Smith N, Sasieni PD. Trends in the lifetime risk of developing cancer in Great Britain: comparison of risk for those born from 1930 to 1960. British Journal of Cancer. 2015 Feb 3;112(5):943–7.
3. Kelland L. The resurgence of platinum-based cancer chemotherapy. Nature Reviews Cancer. 2007 Jul 12;7(8):573–84.
4. Devilli L, Chiara Garonzi, Balter R, Bonetti E, Matteo Chinello, Zaccaron A, et al. Long-Term and Quality of Survival in Patients Treated for Acute Lymphoblastic Leukemia during the Pediatric Age. 2021 Mar 5;13(2):8847–7.
5. Mehlen P, Puisieux A. Metastasis: a question of life or death. Nature Reviews Cancer. 2006;6(6):449-458.
6. Weiss F, Lauffenburger D, Friedl P. Towards targeting of shared mechanisms of cancer metastasis and therapy resistance. Nature Reviews Cancer. 2022 Jan 10;22(3):157–73.
7. Drasin DJ, Robin TP, Ford HL. Breast cancer epithelial-to-mesenchymal transition: examining the functional consequences of plasticity. Breast Cancer Research. 2011 Nov 1;13(6).
8. Berger NA, Savvides P, Koroukian SM, Kahana EF, Deimling GT, Rose JH, et al. Cancer in the Elderly. Transactions of the American Clinical and Climatological Association. 2006;117:147–56.
9. Shackleton M, Quintana E, Fearon ER, Morrison SJ. Heterogeneity in cancer: cancer stem cells versus clonal evolution. Cell. 2009;138(5):822–9.
10. D'Arcangelo E, Wu NC, Cadavid JL, McGuigan AP. The life cycle of cancer-associated fibroblasts within the tumour stroma and its importance in disease outcome. British Journal of Cancer. 2020 Jan 29;122(7):931–42.
11. Datta R, Sivanand S, Lau AN, Florek LV, Barbeau AM, Wyckoff J, et al. Interactions with stromal cells promote a more oxidized cancer cell redox state in pancreatic tumors. Science Advances.;8(3):eabg6383.
12. Krontiris TG, Cooper GM. Transforming activity of human tumor DNAs. Proceedings of the National Academy of Sciences. 1981 Feb;78(2):1181–4.
13. Taparowsky E, Suard Y, Fasano O, Shimizu K, Goldfarb M, Wigler M. Activation of the T24 bladder carcinoma transforming gene is linked to a single amino acid change. Nature. 1982 Dec 1;300(5894):762–5.

14. Zhang L, Vijg J. Somatic Mutagenesis in Mammals and Its Implications for Human Disease and Aging. Annual Review of Genetics. 2018 Nov 23;52:397–419.
15. Land H, Parada LF, Weinberg RA. Tumorigenic conversion of primary embryo fibroblasts requires at least two cooperating oncogenes. Nature. 1983 Aug;304(5927):596–602.
16. Sinn E, Muller W, Pattengale P, Tepler I, Wallace R, Leder P. Coexpression of MMTV/v-Ha-ras and MMTV/c-myc genes in transgenic mice: Synergistic action of oncogenes in vivo. Cell. 1987 May;49(4):465–75.
17. Vogelstein B, Papadopoulos N, Velculescu VE, Zhou S, Diaz LA, Kinzler KW. Cancer Genome Landscapes. Science. 2013 Mar 28;339(6127):1546–58.
18. Wood LD, Parsons DW, Jones S, Lin J, Sjöblom T, Leary RJ, et al. The genomic landscapes of human breast and colorectal cancers. Science (New York, NY). 2007;318(5853):1108–13.
19. Hannahan D, Weinberg RA. The Hallmarks of Cancer. Cell. 2000.
20. Zhou X, Chen Y, Cui L, Shi Y, Guo C. Advances in the pathogenesis of psoriasis: from keratinocyte perspective. Cell Death & Disease. 2022 Jan;13(1).
21. MACDONALD TT. Epithelial Proliferation in Response to Gastrointestinal Inflammation. Annals of the New York Academy of Sciences. 1992 Oct;664(1 Neuro-immuno-):202–9.
22. Hanahan D, Weinberg RA. Hallmarks of cancer: the next Generation. Cell. 2011 Mar;144(5):646–74.
23. Prior IA, Hood FE, Hartley JL. The Frequency of Ras Mutations in Cancer. Cancer Research. 2020 Jul 15;80(14):2969–74.
24. Rajaraman R, Guernsey DL, Rajaraman MM, Rajaraman SR. Stem cells, senescence, neosis, and self-renewal in cancer. Cancer Cell International. 2006;6(1):25.
25. Weinberg RA. The retinoblastoma protein and cell cycle control. Cell. 1995 May;81(3):323–30.
26. Zhao M, Mishra L, Deng CX. The role of TGF-β/SMAD4 signaling in cancer. International Journal of Biological Sciences. 2018;14(2):111–23.
27. Jögi A, Vaapil M, Johansson M, Påhlman S. Cancer cell differentiation heterogeneity and aggressive behavior in solid tumors. Upsala Journal of Medical Sciences. 2012 May 1;117(2):217–24.

28. Enane FO, Saunthararajah Y, Korc M. Differentiation therapy and the mechanisms that terminate cancer cell proliferation without harming normal cells. Cell Death & Disease. 2018 Sep;9(9).
29. Kinzler KW, Vogelstein B. Lessons from Hereditary Colorectal Cancer. Cell. 1996 Oct;87(2):159–70.
30. Sjölund J, Manetopoulos C, Stockhausen MT, Axelson H. The Notch pathway in cancer: Differentiation gone awry. European Journal of Cancer. 2005 Nov;41(17):2620–9.
31. Aunan JR, Cho WC, Søreide K. The Biology of Aging and Cancer: A Brief Overview of Shared and Divergent Molecular Hallmarks. Aging and Disease. 2017;8(5):628.
32. Blackburn EH, Epel ES, Lin J. Human telomere biology: A contributory and interactive factor in aging, disease risks, and protection. Science. 2015 Dec 3;350(6265):1193–8.
33. Mohammad RM, Muqbil I, Lowe L, Yedjou C, Hsu HY, Lin LT, et al. Broad targeting of resistance to apoptosis in cancer. Seminars in Cancer Biology. 2015 Dec;35:S78–103.
34. Wong RS. Apoptosis in cancer: from pathogenesis to treatment. Journal of Experimental & Clinical Cancer Research. 2011 Sep 26;30(1).
35. O'Brien MA, Kirby R. Apoptosis: A review of pro-apoptotic and anti-apoptotic pathways and dysregulation in disease. Journal of Veterinary Emergency and Critical Care. 2008 Dec;18(6):572–85.
36. Aubrey BJ, Kelly GL, Janic A, Herold MJ, Strasser A. How does p53 induce apoptosis and how does this relate to p53-mediated tumour suppression? Cell Death & Differentiation. 2017 Nov 17;25(1):104–13.
37. Baugh EH, Ke H, Levine AJ, Bonneau RA, Chan CS. Why are there hotspot mutations in the TP53 gene in human cancers? Cell Death & Differentiation. 2017 Nov 3;25(1):154–60.
38. Carmeliet P, Jain RK. Molecular mechanisms and clinical applications of angiogenesis. Nature. 2011 May;473(7347):298–307.
39. Djonov V, Andres AC, Ziemiecki A. Vascular remodelling during the normal and malignant life cycle of the mammary gland. Microscopy Research and Technique. 2001 Jan 15;52(2):182–9.
40. Donnem T, Hu J, Ferguson M, Adighibe O, Snell C, Harris AL, et al. Vessel co-option in primary human tumors and metastases: an obstacle to effective anti-angiogenic treatment? Cancer Medicine. 2013 Jul 8;2(4):427–36.

41. Paulis YWJ, Soetekouw PMMB, Verheul HMW, Tjan-Heijnen VCG, Griffioen AW. Signalling pathways in vasculogenic mimicry. Biochimica Et Biophysica Acta. 2010 Aug 1;1806(1):18–28.
42. Chen HF, Wu KJ. Endothelial Transdifferentiation of Tumor Cells Triggered by the Twist1-Jagged1-KLF4 Axis: Relationship between Cancer Stemness and Angiogenesis. Stem Cells International. 2016; 2016:1–10.
43. Krock BL, Skuli N, Simon MC. Hypoxia-Induced Angiogenesis: Good and Evil. Genes & Cancer. 2011 Sep 27;2(12):1117–33.
44. Fares J, Fares MY, Khachfe HH, Salhab HA, Fares Y. Molecular principles of metastasis: a hallmark of cancer revisited. Signal Transduction and Targeted Therapy. 2020 Mar 12;5(1).
45. Luzzi KJ, MacDonald IC, Schmidt EE, Kerkvliet N, Morris VL, Chambers AF, et al. Multistep Nature of Metastatic Inefficiency. The American Journal of Pathology. 1998 Sep 1;153(3):865–73.
46. Wiedswang G. Isolated Tumor Cells in Bone Marrow Three Years after Diagnosis in Disease-Free Breast Cancer Patients Predict Unfavorable Clinical Outcome. Clinical Cancer Research. 2004 Aug 15;10(16):5342–8.
47. Fabisiewicz A, Szostakowska-Rodzos M, Zaczek AJ, Grzybowska EA. Circulating Tumor Cells in Early and Advanced Breast Cancer; Biology and Prognostic Value. International Journal of Molecular Sciences. 2020 Feb 29;21(5):1671.
48. Krebs MG, Sloane R, Priest L, Lancashire L, Hou JM, Greystoke A, et al. Evaluation and Prognostic Significance of Circulating Tumor Cells in Patients With Non–Small-Cell Lung Cancer. Journal of Clinical Oncology. 2011 Apr 20;29(12):1556–63.
49. Franken B, de Groot MR, Mastboom WJ, Vermes I, van der Palen J, Tibbe AG, et al. Circulating tumor cells, disease recurrence and survival in newly diagnosed breast cancer. Breast Cancer Research. 2012 Oct;14(5).
50. Yang J, Antin P, Berx G, Blanpain C, Brabletz T, Bronner M et al. Guidelines and definitions for research on epithelial–mesenchymal transition. Nature Reviews Molecular Cell Biology. 2020;21(6):341-352.
51. Imani S, Hosseinifard H, Cheng J, Wei C, Fu J. Prognostic Value of EMT-inducing Transcription Factors (EMT-TFs) in Metastatic Breast Cancer: A Systematic Review and Meta-analysis. Scientific Reports. 2016 Jun;6(1).

52. Bai F, Chan HL, Scott A, Smith MD, Fan C, Herschkowitz JI, et al. BRCA1 Suppresses Epithelial-to-Mesenchymal Transition and Stem Cell Dedifferentiation during Mammary and Tumor Development. Cancer Research. 2014 Nov 1
53. Fenizia C, Bottino C, Corbetta S, Fittipaldi R, Floris P, Gaudenzi G, et al. SMYD3 promotes the epithelial-mesenchymal transition in breast cancer. Nucleic Acids Research. 2019 Feb 20;47(3):1278–93.
54. Thiery JP, Acloque H, Huang RYJ, Nieto MA. Epithelial-Mesenchymal Transitions in Development and Disease. Cell. 2009 Nov;139(5):871–90.
55. Debnath P, Huirem R, Dutta P, Palchaudhuri S. Epithelial–mesenchymal transition and its transcription factors. Bioscience Reports. 2021 Dec 23;42(1).
56. Gonzalez DM, Medici D. Signaling mechanisms of the epithelial-mesenchymal transition. Science Signaling. 2014 Sep 23;7(344):re8–8.
57. Loh CY, Chai JY, Tang TF, Wong WF, Sethi G, Shanmugam MK, et al. The E-Cadherin and N-Cadherin Switch in Epithelial-to-Mesenchymal Transition: Signaling, Therapeutic Implications, and Challenges. Cells. 2019 Sep 20;8(10):1118.
58. Dudás J, Ladányi A, Ingruber J, Steinbichler TB, Riechelmann H. Epithelial to Mesenchymal Transition: A Mechanism that Fuels Cancer Radio/Chemoresistance. Cells. 2020 Feb 12;9(2):428.
59. Aban CE, Lombardi A, Neiman G, Biani MC, La Greca A, Waisman A, et al. Downregulation of E-cadherin in pluripotent stem cells triggers partial EMT. Scientific Reports. 2021 Jan 21;11(1).
60. Sharma A, Kaur H, De R, Srinivasan R, Pal A, Bhattacharyya S. Knockdown of E-cadherin induces cancer stem-cell-like phenotype and drug resistance in cervical cancer cells. Biochemistry and Cell Biology. 2021 Oct;99(5):587–95.
61. Weiss MB, Abel EV, Mayberry MM, Basile KJ, Berger AC, Aplin AE. TWIST1 is an ERK1/2 effector that promotes invasion and regulates MMP-1 expression in human melanoma cells. Cancer research. 2012 Dec 15;72(24):6382–92.
62. Debnath P, Huirem R, Dutta P, Palchaudhuri S. Epithelial–mesenchymal transition and its transcription factors. Bioscience Reports. 2021 Dec 23;42(1).
63. Zeng Y, Que T, Lin J, Zhan Z, Xu A, Wu ZY, et al. Oncogenic ZEB2/miR-637/HMGA1 signaling axis targeting vimentin promotes the malignant phenotype of glioma. 2021 Jan 5;23:769–82.

64. Wu WS, You RI, Cheng CC, Lee MC, Lin TY, Hu CT. Snail collaborates with EGR-1 and SP-1 to directly activate transcription of MMP 9 and ZEB1. Scientific Reports. 2017 Dec 19;7(1):17753.
65. Adhikary A, Chakraborty S, Mazumdar M, Ghosh S, Mukherjee S, Manna A, et al. Inhibition of Epithelial to Mesenchymal Transition by E-cadherin Up-regulation via Repression of Slug Transcription and Inhibition of E-cadherin Degradation. Journal of Biological Chemistry. 2014 Sep;289(37):25431–44.
66. Yang L, Shi P, Zhao G, Xu J, Peng W, Zhang J, et al. Targeting cancer stem cell pathways for cancer therapy. Signal Transduction and Targeted Therapy. 2020 Feb 7;5.
67. Dave B, Mittal V, Tan NM, Chang JC. Epithelial-mesenchymal transition, cancer stem cells and treatment resistance. Breast Cancer Research. 2012 Jan 19;14(1).
68. Peyre L, Meyer M, Hofman P, Roux J. TRAIL receptor-induced features of epithelial-to-mesenchymal transition increase tumour phenotypic heterogeneity: potential cell survival mechanisms. British Journal of Cancer. 2020;124(1):91-101.
69. Buckley CE, St Johnston D. Apical–basal polarity and the control of epithelial form and function. Nature Reviews Molecular Cell Biology. 2022 Aug 1;23(8):559–77.
70. Lamouille S, Xu J, Derynck R. Molecular mechanisms of epithelial–mesenchymal transition. Nature Reviews Molecular Cell Biology. 2014 Mar;15(3):178–96.
71. Cavallaro U, Christofori G. Cell adhesion and signalling by cadherins and Ig-CAMs in cancer. Nature Reviews Cancer. 2004;4(2):118-132.
72. Friedl P, Alexander S. Cancer Invasion and the Microenvironment: Plasticity and Reciprocity. Cell. 2011 Nov;147(5):992–1009.
73. Parsons J, Horwitz A, Schwartz M. Cell adhesion: integrating cytoskeletal dynamics and cellular tension. Nature Reviews Molecular Cell Biology. 2010;11(9):633-643.
74. Brabletz T, Kalluri R, Nieto MA, Weinberg RA. EMT in cancer. Nature Reviews Cancer. 2018 Jan 12;18(2):128–34.
75. Saxena K, Jolly MK, Balamurugan K. Hypoxia, partial EMT and collective migration: Emerging culprits in metastasis. Translational Oncology. 2020 Aug 8;13(11).
76. Campanale JP, Mondo JA, Montell DJ. A Scribble/Cdep/Rac pathway controls follower-cell crawling and cluster cohesion during collective border-cell migration. Developmental Cell. 2022 Nov;57(21):2483-2496.e4.
77. Pozzi A, Yurchenco PD, Iozzo RV. The nature and biology of basement membranes. Matrix biology : journal of the International Society for Matrix Biology. 2017 Jan 1;57-58:1–11.

78. Glentis A, Gurchenkov V, Vignjevic DM. Assembly, heterogeneity, and breaching of the basement membranes. Cell Adhesion & Migration. 2014 Apr 8;8(3):236–45.
79. Spaderna S, Schmalhofer O, Hlubek F, Berx G, Eger A, Merkel S et al. A Transient, EMT-Linked Loss of Basement Membranes Indicates Metastasis and Poor Survival in Colorectal Cancer. Gastroenterology. 2006;131(3):830-840.
80. d'Ardenne A. Use of basement membrane markers in tumour diagnosis. Journal of Clinical Pathology. 1989;42(5):449-457.
81. Page-McCaw A, Ewald AJ, Werb Z. Matrix metalloproteinases and the regulation of tissue remodelling. Nature Reviews Molecular Cell Biology. 2007 Mar;8(3):221–33.
82. Robertson JG. Enzymes as a special class of therapeutic target: clinical drugs and modes of action. Current Opinion in Structural Biology. 2007 Dec;17(6):674–9.
83. Kim SK. Enzymes as Targets for Drug Development II. International Journal of Molecular Sciences. 2023 Jan 1;24(4):3258.
84. Henley MJ, Koehler AN. Advances in targeting “undruggable” transcription factors with small molecules. Nature Reviews Drug Discovery. 2021 May 18;20(9):669–88.
85. Taube J, Herschkowitz J, Komurov K, Zhou A, Gupta S, Yang J et al. Core epithelial-to-mesenchymal transition interactome gene-expression signature is associated with claudin-low and metaplastic breast cancer subtypes. Proceedings of the National Academy of Sciences. 2010;107(35):15449-15454.
86. Barriere G, Fici P, Gallerani G, Fabbri F, Rigaud M. Epithelial Mesenchymal Transition: a double-edged sword. Clinical and Translational Medicine. 2015 Apr 14;4(1).
87. Kalluri R, Weinberg RA. The basics of epithelial-mesenchymal transition. Journal of Clinical Investigation. 2009 Jun 1;119(6):1420–8.
88. Banyard J, Bielenberg DR. The role of EMT and MET in cancer dissemination. Connective Tissue Research. 2015 Aug 20;56(5):403–13.
89. Ocaña Oscar H, Córcoles R, Fabra Á, Moreno-Bueno G, Acloque H, Vega S, et al. Metastatic Colonization Requires the Repression of the Epithelial-Mesenchymal Transition Inducer Prrx1. Cancer Cell. 2012 Dec;22(6):709–24.
90. Tsai Jeff H, Donaher J, Murphy Danielle A, Chau S, Yang J. Spatiotemporal Regulation of Epithelial-Mesenchymal Transition Is Essential for Squamous Cell Carcinoma Metastasis. Cancer Cell. 2012 Dec;22(6):725–36.
91. Sanae El Harane, Bochra Zidi, Nadia El Harane, Krause KH, Matthes T, Olivier Preynat-Seauve. Cancer Spheroids and Organoids as Novel Tools for Research and

Therapy: State of the Art and Challenges to Guide Precision Medicine. Cells. 2023 Mar 24;12(7):1001–1.

92. Devarasetty M, Forsythe SD, Shelkey E, Soker S. In Vitro Modeling of the Tumor Microenvironment in Tumor Organoids. Tissue Engineering and Regenerative Medicine. 2020 May 12.
93. Al Ameri W, Ahmed I, Al-Dasim FM, Ali Mohamoud Y, Al-Azwani IK, Malek JA, et al. Cell Type-Specific TGF-β Mediated EMT in 3D and 2D Models and Its Reversal by TGF-β Receptor Kinase Inhibitor in Ovarian Cancer Cell Lines. International Journal of Molecular Sciences. 2019 Jul 22;20(14):3568.
94. Bankert R, Egilmez N, Hess S. Human–SCID mouse chimeric models for the evaluation of anti-cancer therapies. Trends in Immunology. 2001;22(7):386-393.
95. Martin E, Belmont P, Sinnamon M, Richard L, Yuan J, Coffee E et al. Development of a Colon Cancer GEMM-Derived Orthotopic Transplant Model for Drug Discovery and Validation. Clinical Cancer Research. 2013;19(11):2929-2940
96. Gateff E. Malignant Neoplasms of Genetic Origin in Drosophila melanogaster. Science. 1978 Jun 30;200(4349):1448–59.
97. St Johnston D, Ahringer J. Cell Polarity in Eggs and Epithelia: Parallels and Diversity. Cell. 2010 May;141(5):757–74
98. Jennings BH. Drosophila – a versatile model in biology & medicine. Materials Today. 2011 May;14(5):190–5.
99. Flores-Benitez D, Knust E. Dynamics of epithelial cell polarity in Drosophila: how to regulate the regulators? Current Opinion in Cell Biology. 2016 Oct;42:13–21.
100. Pagliarini RA. A Genetic Screen in Drosophila for Metastatic Behavior. Science. 2003 Nov 14;302(5648):1227–31.
101. Su TT. Drug screening in Drosophila; why, when, and when not? WIREs Developmental Biology. 2019 May 5;8(6).
102. Sharpe JL, Morgan J, Nisbet N, Campbell K, Casali A. Modelling Cancer Metastasis in Drosophila melanogaster. Cells. 2023 Feb 21;12(5):677.
103. Lee T, Luo L. Mosaic Analysis with a Repressible Cell Marker for Studies of Gene Function in Neuronal Morphogenesis. Neuron. 1999 Mar;22(3):451–61.
104. Eichenlaub T, Cohen SM, Herranz H. Cell Competition Drives the Formation of Metastatic Tumors in a Drosophila Model of Epithelial Tumor Formation. Current Biology. 2016 Feb;26(4):419–27.

105. Calleja M, Morata G, Casanova J. Tumorigenic Properties of Drosophila Epithelial Cells Mutant for lethal giant larvae. Developmental Dynamics. 2016 Jul 15;245(8):834–43.
106. Micchelli CA, Perrimon N. Evidence that stem cells reside in the adult Drosophila midgut epithelium. Nature. 2005 Dec 7;439(7075):475–9.
107. Capo F, Wilson A, Di Cara F. The Intestine of Drosophila melanogaster: An Emerging Versatile Model System to Study Intestinal Epithelial Homeostasis and Host-Microbial Interactions in Humans. Microorganisms. 2019 Sep 9;7(9):336.
108. Xi Y, Xu P. Global colorectal cancer burden in 2020 and projections to 2040. Translational Oncology. 2021 Oct 1;14(10):101174.
109. Alzahrani S, Al Doghaither H, Al-Ghafari A. General insight into cancer: An overview of colorectal cancer (Review). Molecular and Clinical Oncology. 2021 Nov 1;15(6).
110. Markowitz AJ, Winawer SJ. Management of colorectal polyps. CA: A Cancer Journal for Clinicians. 1997 Mar 1;47(2):93–112.
111. SILVA SM e, ROSA VF, SANTOS ACN dos, ALMEIDA RM de, OLIVEIRA PG de, SOUSA JB de. Influence of patient age and colorectal polyp size on histopathology findings. ABCD Arquivos Brasileiros de Cirurgia Digestiva (São Paulo). 2014 Jun;27(2):109–13.
112. Bailey CE, Hu CY, You YN, Bednarski BK, Rodriguez-Bigas MA, Skibber JM, et al. Increasing disparities in the age-related incidences of colon and rectal cancers in the United States, 1975-2010. JAMA surgery. 2015;150(1):17–22.
113. Xu J, Gordon JI. Honor thy symbionts. Proceedings of the National Academy of Sciences. 2003 Aug 15;100(18):10452–9.
114. Annunziata R, Andrikou C, Perillo M, Cuomo C, Arnone MI. Development and evolution of gut structures: from molecules to function. Cell and Tissue Research. 2019 Aug 24;377(3):445–58.
115. Casali A, Batlle E. Intestinal Stem Cells in Mammals and Drosophila. Cell Stem Cell. 2009 Feb;4(2):124–7.
116. Symons R, Daly D, Gandy R, Goldstein D, Aghmesheh M. Progress in the Treatment of Small Intestine Cancer. Current Treatment Options in Oncology. 2023 Apr 1;24(4):241–61.
117. Kiela PR, Ghishan FK. Physiology of Intestinal Absorption and Secretion. Best Practice & Research Clinical Gastroenterology. 2016 Apr;30(2):145–59.

118. Rao JN, Wang JY. Intestinal Architecture and Development. Morgan & Claypool Life Sciences; 2010.
119. Miguel-Aliaga I, Jasper H, Lemaitre B. Anatomy and Physiology of the Digestive Tract of Drosophila melanogaster. Genetics. 2018 Oct;210(2):357–96.
120. Du H, Wang Y, Haensel D, Lee B, Dai X, Nie Q. Multiscale modelling of layer formation in epidermis. Maini PK, editor. PLOS Computational Biology. 2018 Feb 26;14(2):e1006006.
121. Blanpain C, Fuchs E. Epidermal homeostasis: a balancing act of stem cells in the skin. Nature Reviews Molecular Cell Biology. 2009 Feb 11;10(3):207–17.
122. Booth C, Potten CS. Gut instincts: thoughts on intestinal epithelial stem cells. Journal of Clinical Investigation. 2000 Jun 1;105(11):1493–9.
123. Yeung TM, Chia LA, Kosinski CM, Kuo CJ. Regulation of self-renewal and differentiation by the intestinal stem cell niche. Cellular and Molecular Life Sciences. 2011 Apr 21;68(15):2513–23.
124. K.I. Mamis, Zhang R, Bozic I. A simple stochastic model for cell population dynamics in colonic crypts. bioRxiv (Cold Spring Harbor Laboratory). 2023 Mar 23;
125. Radtke F. Self-Renewal and Cancer of the Gut: Two Sides of a Coin. Science. 2005 Mar 25;307(5717):1904–9.
126. Chen J, St Johnston D. Epithelial Cell Polarity During Drosophila Midgut Development. Frontiers in Cell and Developmental Biology. 2022 Jun 30;10.
127. Lucchetta EM, Ohlstein B. The Drosophila midgut: a model for stem cell driven tissue regeneration. Wiley Interdisciplinary Reviews: Developmental Biology. 2012 Apr 9;1(5):781–8.
128. Ohlstein B, Spradling A. Multipotent Drosophila Intestinal Stem Cells Specify Daughter Cell Fates by Differential Notch Signaling. Science. 2007 Feb 16;315(5814):988–92.
129. Guo X, Huang H, Yang Z, Cai T, Xi R. Division of Labor: Roles of Groucho and CtBP in Notch-Mediated Lateral Inhibition that Controls Intestinal Stem Cell Differentiation in Drosophila. Stem cell reports. 2019 May 1;12(5):1007–23.
130. Chen J, Xu N, Wang C, Huang P, Huang H, Jin Z, et al. Transient Scute activation via a self-stimulatory loop directs enteroendocrine cell pair specification from self-renewing intestinal stem cells. Nature Cell Biology. 2018 Feb 1;20(2):152–61.
131. Kuraishi T, Binggeli O, Opota O, Buchon N, Lemaitre B. Genetic evidence for a protective role of the peritrophic matrix against intestinal bacterial infection in

Drosophila melanogaster. Proceedings of the National Academy of Sciences. 2011 Sep 6;108(38):15966–71.

132. Van Neerven SM, Vermeulen L. The interplay between intrinsic and extrinsic Wnt signaling in controlling intestinal transformation. Differentiation. 2019 Jul 1;108:17–23.

133. Mah AT, Yan KS, Kuo CJ. Wnt pathway regulation of intestinal stem cells. The Journal of physiology. 2016;594(17):4837–47.

134. Parker TW, Neufeld KL. APC Controls Wnt-induced β-catenin Destruction Complex Recruitment in Human Colonocytes. Scientific Reports. 2020 Feb 19;10(1).

135. Korinek V, Barker N, Moerer P, van Donselaar E, Huls G, Peters PJ, et al. Depletion of epithelial stem-cell compartments in the small intestine of mice lacking Tcf-4. Nature Genetics. 1998 Aug;19(4):379–83.

136. Pinto D. Canonical Wnt signals are essential for homeostasis of the intestinal epithelium. Genes & Development. 2003 Jul 15;17(14):1709–13.

137. Munemitsu S, Albert I, Souza B, Rubinfeld B, Polakis P. Regulation of intracellular beta-catenin levels by the adenomatous polyposis coli (APC) tumor-suppressor protein. Proceedings of the National Academy of Sciences. 1995 Mar 28;92(7):3046–50.

138. Lin G, Xu N, Xi R. Paracrine Wingless signalling controls self-renewal of Drosophila intestinal stem cells. Nature. 2008 Sep 21;455(7216):1119–23.

139. Cordero JB, Stefanatos RK, Scopelliti A, Vidal M, Sansom OJ. Inducible progenitor-derived Wingless regulates adult midgut regeneration in Drosophila. The EMBO Journal. 2012 Oct 3;31(19):3901–17.

140. Tian A, Benchabane, H, and Ahmed Y. Wingless/Wnt Signaling in Intestinal Development, Homeostasis, Regeneration and Tumorigenesis: A Drosophila Perspective. Journal of Developmental Biology. 2018 Mar 28;6(2):8.

141. Cancedda R, Mastrogiacomo M. Transit Amplifying Cells (TACs): a still not fully understood cell population. Frontiers in Bioengineering and Biotechnology. 2023;11:1189225.

142. Jensen J, Pedersen EE, Galante P, Hald J, Heller RS, Ishibashi M, et al. Control of endodermal endocrine development by Hes-1. Nature Genetics. 2000 Jan 1;24(1):36–44.

143. Korzelius J, Naumann SK, Loza-Coll MA, Chan JS, Dutta D, Oberheim J, et al. Escargot maintains stemness and suppresses differentiation in Drosophila intestinal stem cells. The EMBO Journal. 2014 Oct 8;33(24):2967–82.

144. Brosens LA. Juvenile polyposis syndrome. World Journal of Gastroenterology. 2011;17(44):4839.
145. Haramis AP. G. De Novo Crypt Formation and Juvenile Polyposis on BMP Inhibition in Mouse Intestine. Science. 2004 Mar 12;303(5664):1684–6.
146. MacFarland SP, Ebrahimzadeh JE, Zelley K, Begum L, Bass LM, Brand RE, et al. Phenotypic Differences in Juvenile Polyposis Syndrome With or Without a Disease-causing SMAD4/BMPR1A Variant. Cancer Prevention Research (Philadelphia, Pa). 2021 Feb 1;14(2):215–22.
147. He XC, Zhang J, Tong WG, Tawfik O, Ross J, Scoville DH, et al. BMP signaling inhibits intestinal stem cell self-renewal through suppression of Wnt–β-catenin signaling. Nature Genetics. 2004 Sep 19;36(10):1117–21.
148. Guo Z, Driver I, Ohlstein B. Injury-induced BMP signaling negatively regulates Drosophila midgut homeostasis. The Journal of Cell Biology. 2013 Jun 10;201(6):945–61.
149. Zhou J, Boutros M. JNK-dependent intestinal barrier failure disrupts host–microbe homeostasis during tumorigenesis. Proceedings of the National Academy of Sciences. 2020 Apr 10;117(17):9401–12.
150. Tian A, Jiang J. Intestinal epithelium-derived BMP controls stem cell self-renewal in Drosophila adult midgut. eLife. 2014 Mar 11;3.
151. Jiang H, Patel PH, Kohlmaier A, Grenley MO, McEwen DG, Edgar BA. Cytokine/Jak/Stat Signaling Mediates Regeneration and Homeostasis in the Drosophila Midgut. Cell. 2009 Jun;137(7):1343–55.
152. Buchon N, Broderick NA, Kuraishi T, Lemaitre B. Drosophila EGFR pathway coordinates stem cell proliferation and gut remodeling following infection. BMC Biology. 2010 Dec;8(1).
153. Jiang H, Grenley MO, Bravo MJ, Blumhagen RZ, Edgar BA. EGFR/Ras/MAPK Signaling Mediates Adult Midgut Epithelial Homeostasis and Regeneration in Drosophila. Cell Stem Cell. 2011 Jan;8(1):84–95.
154. Lee J, Cabrera AJH, Nguyen CMT, Kwon YV. Dissemination of RasV12-transformed cells requires the mechanosensitive channel Piezo. Nature Communications. 2020 Jul 16;11(1).
155. Vogelstein B, Fearon ER, Hamilton SR, Kern SE, Preisinger AC, Leppert M, et al. Genetic alterations during colorectal-tumor development. The New England Journal of Medicine. 1988 Sep 1;319(9):525–32.

156. Malki A, El Ruz RA, Gupta I, Allouch A, Vranic S, Al Moustafa AE. Molecular Mechanisms of Colon Cancer Progression and Metastasis: Recent Insights and Advancements. International Journal of Molecular Sciences. 2020 Dec 24;22(1).
157. Kwong LN, Dove WF. APC and its modifiers in colon cancer. Advances in experimental medicine and biology. 2009;656:85–106.
158. Porru M, Pompili L, Caruso C, Biroccio A, Leonetti C. Targeting KRAS in metastatic colorectal cancer: current strategies and emerging opportunities. Journal of Experimental & Clinical Cancer Research. 2018 Mar 13;37(1).
159. Frey P, Devisme A, Rose K, Schrempp M, Freihen V, Andrieux G, et al. SMAD4 mutations do not preclude epithelial–mesenchymal transition in colorectal cancer. Oncogene. 2021 Dec 3;41(6):824–37.
160. Li XL. p53 mutations in colorectal cancer- molecular pathogenesis and pharmacological reactivation. World Journal of Gastroenterology. 2015;21(1):84.
161. Haggar F, Boushey R. Colorectal Cancer Epidemiology: Incidence, Mortality, Survival, and Risk Factors. Clinics in Colon and Rectal Surgery. 2009 Nov;22(04):191–7.
162. Francí C, Takkunen MJ, Dave N, Alameda F, S. Gómez, Rodríguez RL, et al. Expression of Snail protein in tumor–stroma interface. Oncogene. 2006 Mar 27;25(37):5134–44.
163. Fan F, Samuel S, Evans KW, Lu J, Xia L, Zhou Y, et al. Overexpression of Snail induces epithelial-mesenchymal transition and a cancer stem cell-like phenotype in human colorectal cancer cells. Cancer Medicine. 2012 Jun 8;1(1):5–16.
164. Feride Kroepil, Georg Fluegen, Vallböhmer D, Baldus S, Dizdar L, Raffel A, et al. Snail1 expression in colorectal cancer and its correlation with clinical and pathological parameters. BMC Cancer. 2013 Mar 22;13(1).
165. Martorell Ò, Merlos-Suárez A, Campbell K, Barriga FM, Christov CP, Miguel-Aliaga I, et al. Conserved Mechanisms of Tumorigenesis in the Drosophila Adult Midgut. Leulier F, editor. PLoS ONE. 2014 Feb 6;9(2):e88413.
166. Campbell K, Rossi F, Adams J, Pitsidianaki I, Barriga FM, Garcia-Gerique L, et al. Collective cell migration and metastases induced by an epithelial-to-mesenchymal transition in Drosophila intestinal tumors. Nature Communications. 2019 May 24;10(1).

167. Hayes SA, Miller JM, Hoshizaki DK. serpent, a GATA-like transcription factor gene, induces fat-cell development in Drosophila melanogaster. Development. 2001 Apr 1;128(7):1193–200.
168. Ismat A, Cheshire AM, Andrew DJ. The secreted AdamTS-A metalloprotease is required for collective cell migration. Development. 2013 Mar 27;140(9):1981–93.
169. Izumi Y, Yanagihashi Y, Furuse M. A novel protein complex, Mesh-Ssk, is required for septate junction formation in the Drosophila midgut. Journal of Cell Science. 2012 Aug 1;125(20):4923–33.
170. Chambers AF, Naumov GN, Vantyghem SA, Tuck AB. Molecular biology of breast cancer metastasis Clinical implications of experimental studies on metastatic inefficiency. Breast Cancer Research. 2000 Dec;2(6).
171. Luzzi KJ, MacDonald IC, Schmidt EE, Kerkvliet N, Morris VL, Chambers AF, et al. Multistep Nature of Metastatic Inefficiency. The American Journal of Pathology. 1998 Sep;153(3):865–73.
172. Cameron MD, Schmidt EE, Kerkvliet N, Nadkarni KV, Morris VL, Groom AC, et al. Temporal progression of metastasis in lung: cell survival, dormancy, and location dependence of metastatic inefficiency. Cancer Research. 2000 May 1.
173. Ilie M, Hofman V, Long-Mira E, Selva E, Vignaud JM, Padovani B, et al. “Sentinel” Circulating Tumor Cells Allow Early Diagnosis of Lung Cancer in Patients with Chronic Obstructive Pulmonary Disease. Kalinichenko VV, editor. PLoS ONE. 2014 Oct 31;9(10):e111597.
174. Wrenn E, Huang Y, Cheung K. Collective metastasis: coordinating the multicellular voyage. Clinical & Experimental Metastasis. 2021 Jul 12;38(4):373–99.
175. Pereira-Veiga T, Schneegans S, Pantel K, Wikman H. Circulating tumor cell-blood cell crosstalk: Biology and clinical relevance. Cell Reports. 2022 Aug;40(9):111298.
176. Yamamoto A, Doak AE, Cheung KJ. Orchestration of Collective Migration and Metastasis by Tumor Cell Clusters. Annual Review of Pathology: Mechanisms of Disease. 2023 Jan 24;18(1):231–56.
177. Amintas S, Bedel A, Moreau-Gaudry F, Boutin J, Buscail L, Merlio JP, et al. Circulating Tumor Cell Clusters: United We Stand Divided We Fall. International Journal of Molecular Sciences. 2020 Jan 1;21(7):2653.
178. Quan Q, Wang X, Lu C, Ma W, Wang Y, Xia G, et al. Cancer stem-like cells with hybrid epithelial/mesenchymal phenotype leading the collective invasion. Cancer Science. 2020 Jan 17;111(2):467–76.

179. Chen J, Sayadian AC, Lowe N, Lovegrove HE, St Johnston D. An alternative mode of epithelial polarity in the Drosophila midgut. Tapon N, editor. PLOS Biology. 2018 Oct 19;16(10):e3000041.
180. Galenza A, Moreno-Roman P, Su YH, Acosta-Alvarez L, Debec A, Guichet A, et al. Basal stem cell progeny establish their apical surface in a junctional niche during turnover of an adult barrier epithelium. Nature Cell Biology. 2023 May;25(5):658–71.
181. Chen J, St Johnston D. De novo apical domain formation inside the Drosophila adult midgut epithelium. eLife. 2022 Sep 28;11.
182. Hinck L, Näthke I. Changes in cell and tissue organization in cancer of the breast and colon. Current Opinion in Cell Biology. 2014 Feb;26:87–95.
183. Comber K, Huelsmann S, Evans I, Sanchez-Sanchez BJ, Chalmers A, Reuter R, et al. A dual role for the PS integrin myospheroid in mediating Drosophila embryonic macrophage migration. Journal of Cell Science. 2013 May 23;126(15):3475–84.
184. Jonusaite S, Beyenbach KW, Meyer H, Paululat A, Izumi Y, Furuse M, et al. The septate junction protein Mesh is required for epithelial morphogenesis, ion transport, and paracellular permeability in the Drosophila Malpighian tubule. American Journal of Physiology-Cell Physiology. 2020 Mar 1;318(3):C675–94.
185. Ngo S, Liang J, Su YH, O'Brien LE. Disruption of EGF Feedback by Intestinal Tumors and Neighboring Cells in Drosophila. Current biology: CB. 2020 Apr 20;30(8):1537-1546.e3.
186. Cabrera AJH, Gumbiner BM, Kwon YV. Remodeling of E-cadherin subcellular localization during cell dissemination. Molecular Biology of the Cell. 2023 May 1;34(5):ar46.
187. Edwards DR, Handsley MM, Pennington CJ. The ADAM metalloproteinases. Molecular Aspects of Medicine. 2008 Oct 1;29(5):258–89.
188. Mead TJ, Apte SS. ADAMTS proteins in human disorders. Matrix Biology. 2018 Oct;71-72:225–39.
189. Kelwick R, Desanlis I, Wheeler GN, Edwards DR. The ADAMTS (A Disintegrin and Metalloproteinase with Thrombospondin motifs) family. Genome Biology. 2015 May 30;16(1).
190. Cal S, López-Otín C. ADAMTS proteases and cancer. Matrix Biology. 2015 May;44-46:77–85.

191. Duffy MJ, Mullooly M, O'Donovan N, Sukor S, Crown J, Pierce A, et al. The ADAMs family of proteases: new biomarkers and therapeutic targets for cancer? Clinical Proteomics. 2011 Jun 9;8(1).
192. Ricciardelli C, Frewin K, de I, Williams ED, Opeskin K, Melanie April Pritchard, et al. The ADAMTS1 Protease Gene Is Required for Mammary Tumor Growth and Metastasis. American Journal of Pathology. 2011 Dec 1;179(6):3075–85.
193. Frolova AS, Petushkova AI, Makarov VA, Soond SM, Zamyatnin AA. Unravelling the Network of Nuclear Matrix Metalloproteinases for Targeted Drug Design. Biology. 2020 Dec 19;9(12):480.
194. Thapa R, Wilson GD. The Importance of CD44 as a Stem Cell Biomarker and Therapeutic Target in Cancer. Stem Cells International. 2016;2016:1–15.
195. Jeter CR, Yang T, Wang J, Chao HP, Tang DG. NANOG in cancer stem cells and tumor development: An update and outstanding questions. Stem cells. 2015 Aug 1;33(8):2381–90.
196. Koyama L, Aranda-Díaz A, Su Y, Balachandra S, Martin J, Ludington W et al. Bellymount enables longitudinal, intravital imaging of abdominal organs and the gut microbiota in adult Drosophila. PLOS Biology. 2020;18(1):e3000567.
197. Martin J, Sanders E, Moreno-Roman P, Jaramillo Koyama L, Balachandra S, Du X et al. Long-term live imaging of the Drosophila adult midgut reveals real-time dynamics of division, differentiation, and loss. eLife. 2018;7.
198. Tang R, Qin P, Liu XQ, Wu S, Yao R, Cai Guangjun, et al. Intravital imaging strategy FlyVAB reveals the dependence of Drosophila enteroblast differentiation on the local physiology. Communications biology. 2021 Oct 25;4(1).
199. Ohkubo T, Ozawa M. The transcription factor Snail downregulates the tight junction components independently of E-cadherin downregulation. Journal of Cell Science. 2004 Apr 1;117(9):1675–85.
200. Villarejo A, Cortés-Cabrera Á, Molina-Ortíz P, Portillo F, Cano A. Differential Role of Snail1 and Snail2 Zinc Fingers in E-cadherin Repression and Epithelial to Mesenchymal Transition. Journal of Biological Chemistry. 2013 Dec 1;289(2):930–41.
201. Mustafa S, Koran S, AlOmair L. Insights Into the Role of Matrix Metalloproteinases in Cancer and its Various Therapeutic Aspects: A Review. Frontiers in Molecular Biosciences. 2022 Sep 29;9.

202. Schulz B, Pruessmeyer J, Maretzky T, Ludwig A, Blobel CP, Saftig P, et al. ADAM10 Regulates Endothelial Permeability and T-Cell Transmigration by Proteolysis of Vascular Endothelial Cadherin. Circulation Research. 2008 May 23;102(10):1192–201.
203. Kohutek ZA, diPierro CG, Redpath GT, Hussaini IM. ADAM-10-Mediated N-Cadherin Cleavage Is Protein Kinase C-α Dependent and Promotes Glioblastoma Cell Migration. Journal of Neuroscience. 2009 Apr 8
204. Cain SA, Mularczyk EJ, Singh M, Massam-Wu T, Kielty CM. ADAMTS-10 and -6 differentially regulate cell-cell junctions and focal adhesions. Scientific Reports. 2016 Oct 25;6(1).
205. Lee SH, Park JS, Kim YS, Chung HY, Yoo MA. Requirement of matrix metalloproteinase-1 for intestinal homeostasis in the adult Drosophila midgut. Experimental Cell Research. 2012 Mar;318(5):670–81.
206. Cudic M, Fields G. Extracellular Proteases as Targets for Drug Development. Current Protein & Peptide Science. 2009 Aug 1;10(4):297–307.
207. Coussens L, Fingleton B, Matrisian L. Matrix Metalloproteinase Inhibitors and Cancer—Trials and Tribulations. Science. 2002;295(5564):2387-2392.
208. Tortorella M, Malfait F, Barve R, Shieh HS, Malfait AM. A Review of the ADAMTS Family, Pharmaceutical Targets of the Future. Current Pharmaceutical Design. 2009 Jul 1;15(20):2359–74.
209. Dubail J, Apte SS. Insights on ADAMTS proteases and ADAMTS-like proteins from mammalian genetics. Matrix Biology. 2015 May;44-46:24–37.
210. Weinberg R. The Biology of Cancer, 2nd edition. 2013
211. Hampel S, Chung P, McKellar CE, Hall D, Looger LL, Simpson JH. Drosophila Brainbow: a recombinase-based fluorescence labeling technique to subdivide neural expression patterns. Nature Methods. 2011 Feb 6;8(3):253–9.
212. Padmanaban V, Krol I, Suhail Y, Szczerba BM, Aceto N, Bader JS, et al. E-cadherin is required for metastasis in multiple models of breast cancer. Nature. 2019 Sep;573(7774):439–44.
213. Stockinger A, Eger A, Wolf J, Beug H, Foisner R. E-cadherin regulates cell growth by modulating proliferation-dependent β-catenin transcriptional activity. Journal of Cell Biology. 2001 Sep 17;154(6):1185–96.
214. Menéndez J, Pérez-Garijo A, Calleja M, Morata G. A tumor-suppressing mechanism in Drosophila involving cell competition and the Hippo pathway. Proceedings of the National Academy of Sciences. 2010 Aug 2;107(33):14651–6.

215. Skeath JB, Wilson BA, Romero SE, Snee MJ, Zhu Y, Lacin H. The extracellular metalloprotease AdamTS-A anchors neural lineages in place within and preserves the architecture of the central nervous system. Development. 2017 Jan 1.
216. Mannello F, Medda V. Nuclear localization of Matrix metalloproteinases. Progress in Histochemistry and Cytochemistry. 2012 Mar;47(1):27–58.
217. Silva SV, Lima MA, Cella N, Jaeger RG, Freitas VM. ADAMTS-1 Is Found in the Nuclei of Normal and Tumoral Breast Cells. Baek KH, editor. PLOS ONE. 2016 Oct 20;11(10):e0165061.